Exploring Fungal Diversity and Interactions with *Lecanosticta acicola* in Brown Spot Needle Blight

by

Emmanuel Duodu Nyarko

A thesis submitted to the Graduate Faculty of
Auburn University
In partial fulfillment of the Degree of
Master of Science

Auburn, Alabama
August 9, 2025

Approved by
Dr. Lori Eckhardt, Chair, Professor of Forestry, Wildlife and Environment
Dr. Brian Via, Professor of Forestry, Wildlife and Environment
Dr. Rabiu Olatinwo, Research Plant Pathologist

Abstract

Brown spot needle blight is a foliar disease that affects loblolly pines. It is characterized by small, necrotic spots on the needles that expand into brown lesions surrounded by a yellowish halo, often culminating in defoliation when conditions are favorable. Loblolly pine is the most abundant pine found in the southeast U.S. It is of a high economic value, however in recent years it has been threatened by brown spot needle blight disease, thereby impacting the region's forest economy. In this study morphological and molecular techniques were used to identify co-occurring foliar pathogens with *Lecanosticta acicola,* the causative pathogen of the disease. Twenty-one different fungi genera were recovered from these methods of which *Pestalotiopsis, Cladosporium, Hendersonia*, and *Trichoderma* were found to be the predominant fungi associated with *L. acicola*. The study further tested the susceptibility of seventeen different loblolly pine families to *L. acicola.* We ranked the best three families that had better tolerance to the pathogen, based on growth parameters such as mean height, disease rating root collar diameter and relative water content. Finally, we investigated how spore traps could be used to assess *L. acicola* spore loads in BSNB-infected plots. We found that climatic variables such as rainfall, relative humidity and temperature affected spore release throughout the sampling period, with rainfall having the best association with spore release.

Keywords: Loblolly pine, foliar pathogens, Brown spot needle blight

Acknowledgements

I wish to express my profound gratitude to my major advisor, Dr. Lori G. Eckhardt, for giving me the opportunity and the assistance during this project. I am grateful to my committee members Dr. Bian Via and Dr. Rabiu Olatinwo for their guidance and support throughout this project.

I am very thankful to the United States Forest Service for the grant provided for me to perform this research. I would like to thank all past and present members (lab managers, graduate students, undergraduates) of the Forest Health Dynamics Lab, especially Jessica Baldwin, Patricia Gordon, Laura Nieto, Jaden King, Temitope Folorunso, Andrew Howard, Drew Conway, Sharmin S. Toa, Maddox Golden, Angel Cagle, Gracey Goldsby, Alexandra Foreman, Joseph Anglin, Solana Hendrickson, Skyler Alvarez, Caleb McCrory, Garrett Gaar, Julianna Garrett, Ty Ennen, William Heaster, Logan Schatz and Ben VanDerlyke, for their invaluable help during the field and lab work.

Special thanks to Drs. John Mensah, Annakay Newell, Emily Carter, Lita, Glenn Glover (Glover Property) for their support to me. Also, to the Forest Health Cooperative, Longleaf Timber Company, Stallworth Property, William Family, and Kris Bradley, I am most grateful for your diverse contributions to my work.

Finally, I say a big thank you to my family and friends, CSIR-FORIG Director and Staff, for their unwavering support and encouragement during the entire period.

Table of Contents

List of tables

List of figures

Chapter One

Introduction and Literature Review

1.1 Forestry in the southeastern U.S.

The state of forestry in the southeastern U.S. has been a topic of interest for researchers over the years as it is considered the "Wood Basket of the World." A study by Badger & Stephenson, (1989) highlighted the significant use of wood for energy in the U.S., with 10% of residential energy and 8% of industrial energy coming from wood. Forestry in the southeast supports a robust economy, contributing billions of dollars annually and providing significant employment opportunities in timber production, wood processing, and related industries. The region's forests cover 23.03 million acres which include hardwood, pine, and mixed species stands, with southern pine plantations being particularly prominent (AFC, 2023). Nearly 93% of the forestland is held by private industrial owners who prefer timber production. Approximately 11% of U.S. timberland is planted forest, and these planted stands represent roughly 7% of the total U.S. forestland (FAO, 2001). The southeastern U.S. is characterized by warm, moist soils and a climate that enable exceptionally fast forest development, with stands often reaching financial maturity within 30-50 years. Timber yields are heavily shifted toward the Coastal Plain from Virginia through Alabama where about 60-69% of regional productivity occurs (Wear, 1996b). Softwood dominates this landscape and accounts for roughly 58% of the growing stock on industry lands. Within that category, loblolly pine (*Pinus taeda* L.) and shortleaf pine (*P. echinata* Mill.) comprise approximately 71% of the softwood inventory, emphasizing their central role in the region's forest economy (Smith et al., 2001). From an industrial perspective, these intensively managed pine plantations hold the U.S. wood products sector. However, the

characteristics that make plantations commercially attractive; species uniformity, high density, and a humid microclimate do also favor the epidemic development of diseases (Smith et al., 2001). Therefore, factors that affect the sustainability and growth of southern forests could impact on the wood resources of the country.

1.2 Loblolly pine (*Pinus taeda* L.)

1.2.1 Ecology and biology

Loblolly pine is a pine species native to the southeastern U.S., and it is widely distributed throughout the region (Baker et al., 1990). While historically found in low, wet, and muddy areas, it is not limited to such environments. Loblolly pine demonstrates resilience in poor surface conditions, slightly acidic clay soils, and various terrains, from flatlands to mountains (Wahlenberg, 1960). The southern U.S. accounts for 24% of the nation's land area, with forests covering 40% of the country's timberland (Wear, 1996a). This region's forests are among the most productive in the U.S., with loblolly pine standing out as the primary commercial timber species (Brender et al., 1981).

Over the past two centuries, human activities have significantly impacted the landscape of the southern U.S., benefiting the growth of loblolly pine. The early settlers cleared extensive forest areas for farmland as they migrated west into Piedmont, leading to the removal of hardwood forests and longleaf pine. As the farmland lost its fertility, the settlers continued clearing more forests which resulted in depleted topsoil and severe erosion. These degraded farmlands created favorable conditions for the expansion of loblolly pine plantations, as the species can thrive in such environments (Fisher, 2022). Management strategies, particularly those involving uneven-aged stand management, are noted to have implications for the genetic composition of loblolly pine. For instance, practices that favor certain growth characteristics,

such as higher wood density, could lead to selective pressures that reduce genetic variability, especially if resistant or less susceptible genotypes are preferentially retained or propagated. Such selective management could diminish the overall genetic pool, potentially impacting the resilience of loblolly pine to future pathogen pressures (Sykes et al., 2003).

1.2.2 Pine foliar diseases

Pine foliar diseases are of much concern in coniferous forests in the southeastern U.S. (Hansen et al., 2000). Pine foliar diseases refer to a range of pathological conditions affecting the needles of pine trees, primarily caused by various fungal, bacterial, and viral pathogens. These diseases can lead to significant declines in tree health, impacting growth, photosynthesis, and overall vitality (Dobbertin, 2006). The importance of understanding and managing pine foliar diseases lies in their potential to cause extensive economic losses in forestry and timber industries, as well as their ecological implications for forest ecosystems (Cherubini et al., 2021).

Healthy pine forests play a crucial role in carbon sequestration, biodiversity conservation, and providing habitat for numerous species. Therefore, effective management of foliar diseases is essential to maintain the health and productivity of pine forests (Nottingham et al., 2023). According to Lhotka et al., (2008), numerous pine species are susceptible to foliar diseases, with varying degrees of vulnerability depending on the specific pathogens involved. Commonly affected species include eastern white pine (*Pinus strobus* L.), loblolly pine (*P. taeda*), slash pine (*Pinus elliottii* Engelm), and scots pine (*Pinus sylvestris* L.). Each of these species exhibits unique responses to foliar pathogens, influenced by factors such as genetic predisposition, environmental conditions, and management practices. Pandit et al., (2020) noted that southern pines are increasingly being damaged by foliar diseases, so an early detection after

observation of changes in foliar characteristics and assessment of potential risks would be useful in effectively utilizing resources and sustainably managing forests.

Climate and weather play a crucial role in the development and severity of pine foliar diseases (Wyka et al., 2018). Temperature, humidity, and precipitation patterns directly influence the life cycles of pathogens and the susceptibility of pine trees. Warmer temperatures can accelerate pathogen reproduction and increase the likelihood of disease outbreaks (Demidko et al., 2021). High humidity and prolonged wet conditions create favorable environments for fungal pathogens, leading to increased infection rates (Brown et al., 2021). Additionally, extreme weather events, such as storms and droughts, can weaken trees, making them more vulnerable to diseases. Understanding these climatic factors is essential for predicting disease outbreaks and implementing timely management strategies (Gao et al., 2019).

Soil health and nutrient availability are critical determinants of pine health and their ability to resist foliar diseases (Prasolova et al., 2005). Nutrient deficiencies, particularly in nitrogen, phosphorus, and potassium, can impair tree vigor and increase susceptibility to pathogens. Healthy soils support robust root systems, which are vital for nutrient uptake and overall tree resilience. Soil pH, organic matter content, and microbial activity also influence nutrient availability and tree health. Practices that enhance soil health, such as organic amendments and proper fertilization, can improve tree resistance to foliar diseases and promote overall forest health (Liechty et al., 2005).

Human activities and land use significantly influence the prevalence and severity of pine foliar diseases. Deforestation, urbanization, and agricultural practices can drastically alter natural ecosystems, placing additional stress on pine populations (Smith et al., 2010; Wingfield

et al., 2015). Monoculture plantations often create conditions conducive to disease spread, as pathogens thrive in uniform stands with limited genetic diversity (Desprez-Loustau et al., 2007). Furthermore, the introduction of non-native species and pathogens through trade and international movement can exacerbate existing disease problems (Wingfield et al., 2009). Mitigation of these risks can be conducted through sustainable land management practices such as mixed-species planting, maintaining biodiversity, and reducing disturbances which are essential for preserving the resilience of pine ecosystems (FAO, 2016).

1.3 Common Needle Casts, Needle Blights and Needle Rusts Diseases

Needle cast diseases are caused by fungal pathogens that infect the current year's needles of pines, spruces, Douglas-fir, and true firs. Infected needles often turn yellow to brown and develop dark fruiting bodies before being shed prematurely, leaving trees with a sparse crown (Pscheidt, 1992). Needle blight diseases can infect needles of multiple ages, causing extensive necrosis and dieback. Needle rust diseases produce orange-to-brown pustules on needles and require alternate hosts to complete their life cycles (Cech & Klepzig, 2001; Gibson 1995).

1.3.1 Brown Spot Needle Blight

Brown spot needle blight (BSNB) is a significant foliar disease predominantly affecting pine species, with *Lecanosticta acicola* recognized as the primary causal agent (Barnes et al., 2008). The disease is historically found throughout the southeastern U.S. from Virginia through Alabama, Florida and west to Louisiana where warm, humid summers sustain multiple infection cycles (Barnes et al., 2019). In recent decades, BSNB has spread into mid-Atlantic and northeastern states, and it has been recorded in Europe (e.g., Spain, France, the UK) and parts of Asia on both native and exotic pines, driven by global trade and increasingly suitable climates

(U.S. Forest Service & Alabama Forestry Commission, 2022). The disease is of considerable concern in regions where longleaf pine is grown, particularly in the southeastern U.S., where the disease can severely hinder natural regeneration, reduce growth rates, and cause premature needle drop (Barnard, 1991). Typical symptoms include small, necrotic spots on needles that expand into brown lesions surrounded by a yellowish halo, often culminating in defoliation when conditions are favorable (Jankovský & Palovčíková, 2003).

Environmental factors such as warm temperatures, high humidity, and frequent rainfall events promote spore germination and dispersal, enhancing disease incidence and severity (Barnes et al., 2008). Dense canopy conditions, limited air circulation, and extended needle wetness further facilitate pathogen development (Barnard & Blakeslee, 1980). Management strategies for BSNB typically focus on cultural and silvicultural interventions, including thinning to improve airflow, prescribed burning to reduce infectious needle litter, and the use of resistant or more tolerant pine genotypes where available (Kelley & Williams, 2019). Current research aims to refine disease forecasts, improve diagnostic tools, and develop integrated management approaches that balance economic, ecological, and silvicultural objectives (Barnes et al., 2016).

1.3.2 Sydowia Needle Cast

Sydowia needle cast is a foliar disease primarily affecting conifers, most notably spruces and pines, caused by the ascomycete fungus *Sydowia polyspora* (Bref. & Tavel) E. Müll. Often considered a common endophyte in healthy conifer needles, *S. polyspora* can shift to a pathogenic role when the host tree is under stress or environmental conditions favor fungal proliferation (Johannesson, 2000; Kehr & Wulf, 1993). *Sydowia polyspora* has a broad geographical distribution across the Northern Hemisphere. It is common throughout Europe,

including Italy, Spain, Poland, Lithuania, and the Balkan region, where it infects a wide range of conifer hosts (Lazarević & Menkis, 2020). In North America, *S. polyspora* has been reported on species such as *Pinus ponderosa* (P.& C. Lawson) and *Thuja* spp., often in association with bark-beetle-infested plantations (Muñoz-Adalia et al., 2017). The pathogen also occurs in Asia, having been detected on pines in China (Lazarević & Menkis, 2020). Its presence in both high-altitude Mediterranean stands and temperate coastal forests highlights its adaptability to diverse climates, although outbreaks are typically linked to warm, humid conditions that stress hosts (Lazarević & Menkis, 2020; Muñoz-Adalia et al., 2017).The disease is characterized by necrotic lesions on needles, ultimately leading to defoliation and a reduction in growth if infections are severe and persist over multiple growing seasons (Butin, 2011; Schnabel et al., 2018).

Cool and moist environmental conditions typically promote spore germination and infection (Kehr & Wulf, 1993). The symptoms often begin as small, discolored spots that expand over time, causing needle browning and premature abscission (Schnabel et al., 2018). Cultural and silvicultural management strategies, such as thinning to improve airflow and reduce humidity within the canopy, can help mitigate the risk of infection (Butin, 2011). In outbreak situations, ongoing research has explored the potential utility of fungicidal treatments, though efficacy varies, and prevention through proper site selection and tree vigor maintenance remains a cornerstone of disease management (Johannesson, 2000).

1.3.3 Rhizosphaera Needle Cast

Rhizosphaera needle cast is a common foliar disease primarily affecting spruce species, most notably Colorado blue spruce (*Picea pungens* Engelm.), but it can also infect Norway spruce (*Picea abies* L. Karst.) and other conifers (Jacobi & Tisserat, 2011; Worf, 2002).

The disease is caused by the fungus *Rhizosphaera kalkhoffii* Bubak, which infects needles through their stomata under prolonged wet or humid conditions (Hansen & Lewis, 1997; Jacobi & Tisserat, 2011). *Rhizosphaera kalkhoffii* is widespread across the Northern Hemisphere, especially in cool, moist spruce forests. In North America, it occurs from Alaska and British Columbia eastward through the Pacific Northwest, the Rocky Mountains, and across to the northeastern U.S. and eastern Canada (Sinclair & Lyon, 2005). In Europe, infections are reported from Scandinavia south through the Alps and Carpathians into the Mediterranean mountains (Stone & Roberts, 2002). The pathogen also inhabits parts of Asia, including Japan, Korea, and the Russian Far East, wherever spruce species such as *P. abies* grow under humid, temperate conditions (Sinclair & Lyon, 2005).

Early symptoms typically manifest as yellowish or purplish discoloration of older needles, progressing to browning and eventual defoliation (Worf, 2002). Because *Rhizosphaera* overwinters in infected needles, the disease often recurs season after season, gradually weakening the host tree and reducing aesthetic quality (Hartman, 2018). Environmental factors, such as extended periods of needle wetness and poor air circulation, can exacerbate disease severity (Hartman, 2018; Jacobi & Tisserat, 2011). Effective management strategies focus on reducing moisture around susceptible trees via proper spacing, pruning of lower branches, and improved site drainage (Hansen & Lewis, 1997). Fungicidal applications, typically containing chlorothalonil or copper-based formulations can help protect new growth when applied preventatively in spring and early summer (Jacobi & Tisserat, 2011).

1.3.4 Dothistroma Needle Blight

Dothistroma needle blight (DNB), also commonly referred to as red band needle blight, is a significant foliar disease of numerous conifer species worldwide, particularly pines. It is

primarily caused by two closely related fungal pathogens, *Dothistroma septosporum* (Dorog.) M. Morelet and *Dothistroma pini* (Hulbary), which infect host needles, creating characteristic red transverse bands and leading to premature needle drop (Barnes et al., 2004; Woods et al., 2005). The disease can drastically reduce photosynthetic areas, resulting in growth losses and, in severe cases, tree mortality (Barnes et al., 2014).

The rapid spread of DNB is influenced by a combination of favorable environmental conditions such as high humidity, prolonged leaf wetness, moderate temperatures and anthropogenic factors that facilitate pathogen movement, including global trade and transport of infected plant material (Woods et al., 2005; Mullett et al., 2017). Outbreaks have been reported across Europe, North America, and parts of the Southern Hemisphere, with notable epidemics in commercial pine plantations, leading to significant economic losses in the forestry sector (Mullett et al., 2017). Integrated disease management strategies emphasize regular monitoring, implementation of quarantine measures to prevent pathogen spread, and the application of fungicides where feasible (Kabir et al., 2015). Additionally, breeding and selection programs aim to develop and deploy resistant or tolerant pine genotypes, offering a sustainable long-term solution to the challenges posed by DNB (Barnes et al., 2004). Future research efforts are increasingly focused on understanding the genetic diversity of Dothistroma populations and the potential impacts of climate change, which may further alter disease dynamics and distribution patterns (Woods et al., 2005; Barnes et al., 2014).

1.3.5 Lophodermium Needle Cast

Lophodermium needle cast, chiefly caused by *Lophodermium seditiosum* Minter, Staley & Millar (teleomorph: *Scytalidum seditiosum*) and *Lophodermium pinastri* (Schrad.) Chevall., is a widespread defoliator in pine stands (Sinclair & Lyon, 2005). Its geographic range is nearly

cosmopolitan, affecting pines on every continent except Antarctica. In North America, epidemics occur from coastal British Columbia through the Rocky Mountains and across the northeastern U.S. to the Atlantic coast, especially on young pine plantations (Sinclair & Lyon, 2005). Europe has seen extensive damage in commercial Scots pine forests from Scandinavia south to the Mediterranean Basin (Stone & Roberts, 2002). In the Southern Hemisphere, severe outbreaks have devastated radiata pine (*Pinus radiata* D. Don) plantations in New Zealand, Chile, and South Africa under warm, wet summers (Webber & Flentje, 2008). More recently, *Dothistroma* has emerged in Asia including China and Japan on both native and exotic pine species. The pathogen's broad distribution reflects its ability to infect over 75 pine species and thrive wherever the mean summer rainfall exceeds 300 mm coupled with moderate temperatures (15-25 °C). The pathogen overwinters in fallen needles and litter as mycelium, producing pseudothecia in early spring that releases ascospores during cool (10-15 °C), wet periods (Stone & Roberts, 2002). Infection is symptomless until late winter when needles rapidly brown and drop, often in a synchronous "needle-flush" event that can defoliate 30-70% of foliage (Harrington, McNew, & Vidaver, 2010). Conidia produced in flank pycnidia contribute to secondary spread under humid summers (Harrington et al., 2010). Management relies on thinning to improve airflow, timely raking of litter to reduce inoculum, and judicious copper or strobilurin-based sprays timed to ascend spore release forecasts from degree-day models (Sinclair & Lyon, 2005; Stone & Roberts, 2002). Recent genetic studies using microsatellite markers reveal high population structure among geographically isolated epidemics, suggesting limited long-distance dispersal but marked local adaptation (Harrington et al., 2010). With warmer, wet winters predicted under climate change, modeling efforts suggest *Lophodermium* outbreaks will intensify and extend northward by 2050 (Stone & Roberts, 2002).

1.3.6 Coleosporium Needle Rust

Coleosporium needle rust is a foliar disease primarily affecting pine species (*Pinus* spp.). It is caused by rust fungi in the genus *Coleosporium*, most notably *Coleosporium asterum* (Dietel) Syd. & P. Syd., *Coleosporium solidaginis* (Schwein.) Thüm., and *Coleosporium ipomoeae* (Schwein) Burill. These pathogens are heteroecious, requiring two unrelated hosts: commonly a pine and a member of the Asteraceae family, especially Goldenrods (*Solidago* spp.), Asters (*Symphyotrichum* spp.), Fleabanes (*Eigeron* spp.) and Wild sunflowers (*Helianthus* spp.) to complete their life cycle (Sinclair & Lyon, 2005). On pines, the disease manifests as yellow to orange pustules (uredinia) on needles, which later produces powdery spores. Severe infections can result in premature needle drop, stunted growth, and even mortality in young trees or seedlings (Cech & Klepzig, 2001).

One of the most widely studied species is *Coleosporium asterum*, which infects several pine species including loblolly pine (*Pinus taeda*), slash pine (*Pinus elliottii*), and shortleaf pine (*Pinus echinata*) and ponderosa pine (*Pinus ponderosa* P. Lawson & C. Lawson). The disease is widespread across North America, particularly in the eastern U.S., southeast U.S., and parts of Mexico and Canada (Cech & Klepzig, 2001; Hennon et al., 2007). The disease cycle begins in late summer or early fall, when urediniospores infect pine needles. These spores can spread rapidly under humid conditions, and epidemics are often associated with periods of extended leaf wetness (Sinclair & Lyon, 2005). The impact of *Coleosporium* spp. is generally more significant in nurseries or young plantations, where high tree density and overhead irrigation create ideal conditions for spore dispersal and infection (Goswami & Pereira, 2011). While older trees tend to tolerate infections better, repeated defoliation can still weaken trees and predispose them to other stresses and pathogens (Cech & Klepzig, 2001). Control measures

include reducing humidity through proper spacing, avoiding overhead watering, avoiding planting of pines near alternate hosts, and in severe cases, applying fungicides (feasible in nursery settings or high value ornamentals) (Hennon et al., 2007).

1.3.7 Phytophthora Needle Blight

Phytophthora needle blight (PNB) is relatively rare, but it has increasingly been recognized as a disease affecting various pine species, primarily in nursery and plantation settings. It is caused by water molds in the genus *Phytophthora*, a group of oomycetes known for their devastating impact on forest and agricultural ecosystems. Among the species that exhibit needle blight symptoms are *Phytophthora pluvialis* Resser, Sutton & E. Hansen and *Phytophthora pinifolia* Alv. Durán, Gryzenh. & M. J. Wingf., both of which have caused notable outbreaks in pine forests of New Zealand, the Pacific Northwest of the U.S., and Chile (Durán et al., 2008; Reeser et al., 2013).

Phytophthora needle blight typically manifests as necrotic needle lesions, browning from the tip backward, premature needle cast, and in severe cases, twig dieback. The disease is often associated with periods of prolonged leaf wetness, high humidity, and poor drainage conditions that favor the production and spread of motile zoospores (Hansen et al., 2012). These symptoms can significantly reduce the photosynthetic capacity of trees, affecting overall vigor, especially in young trees and seedlings (Reeser et al., 2013). *Phytophthora pluvialis*, has been confirmed as the causal agent of red needle cast in radiata pine (*Pinus radiata*) in New Zealand and later in Douglas-fir and ponderosa pine (*Pinus ponderosa*) in Oregon. The pathogen has been detected in forest plantations and managed nurseries, which suggests a broader range of susceptible hosts and increasing concerns about its spread (Reeser et al., 2013; Hansen et al., 2012).

Phytophthora pinifolia was first identified in Chile, where it caused widespread foliar blight and needle cast in *Pinus radiata* plantations, leading to significant economic losses in the timber industry (Durán et al., 2008). This was the first known case of a *Phytophthora* species causing a foliar blight in pines, challenging previous assumptions that *Phytophthora* species primarily cause root or collar rot in conifers (Erwin et al., 1996). Management of PNB is complex due to the soil and water-borne nature of the pathogen. Some best management practices include improving site drainage, reducing overhead irrigation, using pathogen-free planting stock, and applying phosphite-based fungicides when necessary (Hansen et al., 2012).

1.3.8 White Pine Blister Rusts

White pine blister rust (WPBR) is a devastating disease of five-needle pines, particularly affecting eastern white pine (*Pinus strobus*), western white pine (*P. monticola*), sugar pine (*Pinus lambertiana*), and limber pine (*Pinus flexilis*). The disease is caused by the heteroecious rust fungus *Cronartium ribicola* J.C. Fisch. in Rabenh., which requires an alternate host in the genus Ribes (currants and gooseberries) to complete its life cycle (Geils et al., 2010; Zambino & Kinloch, 2007). The disease was introduced to North America from Europe in the early 1900s via infected nursery stock (Spaulding, 1922). Since then, it has spread throughout the native range of susceptible white pines in both the eastern and western parts of the continent. The disease has a widespread range across the northeastern U.S., the Appalachian Mountains, and the Pacific Northwest, and it has expanded into Canada (British Columbia and Alberta), and parts of the Rocky Mountains (Geils et al., 2010; Maloy, 1997).

The disease begins when basidiospores produced on infected Ribes plants infect pine needles. The fungus grows into the bark and vascular tissues, eventually forming cankers that girdle branches or stems, leading to branch dieback or tree death. Symptoms include chlorotic

needle spots, cankers with resin exudation, and the development of blister-like aecia that release infectious spores (Zambino & Kinloch, 2007). White pine blister rust is lethal to young trees and seedlings, and it has caused substantial mortality in natural forests and plantations. Management strategies include breeding and deployment of WPBR-resistant pine genotypes and silvicultural practices such as pruning infected branches can be used as an integrated management approach to control the disease (Kinloch et al., 2003).

1.3.9 White Pine Needle Damage (WPND)

White Pine Needle Damage (WPND) is an emerging disease complex that primarily affects eastern white pine (*Pinus strobus*), although symptoms have also been observed in other five-needle pine species. First widely recognized in the early 2000s, WPND has since been documented across much of the northeastern and central U.S., particularly in states like New Hampshire, Pennsylvania, New York, and as far west as Minnesota, and parts of southeastern Canada (Ostry et al., 2012; Munck et al., 2016).

White pine needle damage is characterized by chlorosis, needle tip necrosis, premature needle shed, and overall thinning of foliage, which can reduce tree vigor and growth. The symptoms are most observed in early summer, and affected trees often display a gradient of damage from lower to upper crown depending on environmental exposure (Ostry et al., 2012). The damage is primarily attributed to a complex of fungal pathogens, including *Lecanosticta acicola*, *Bifusella linearis* Höhn and *Septorioides strobi* Wyka & Broders, often acting synergistically under favorable environmental conditions (Munck et al., 2016; Lavallée et al., 2019). Fungal infection is typically preceded or worsened by environmental stressors, particularly warm, wet springs followed by cool, moist summer conditions which create ideal conditions for spore germination and infection (Munck et al., 2016). Research also suggests that

air pollution, particularly ozone and sulfur dioxide, may contribute to needle stress and increased susceptibility (Lavallée et al., 2019).

Diagnosis of WPND is complicated by the presence of multiple co-infecting organisms and overlapping symptomatology with other needle diseases such as brown spot needle blight and Dothistroma needle blight. Some management strategies include improving air circulation and sunlight exposure, avoiding overcrowding, and pruning infected branches. Fungicide applications may be effective, particularly when applied early in the growing season, although chemical management is not always feasible in forest settings (Ostry et al., 2012). The expanding geographic range and increasing severity of WPND emphasizes the need for continued surveillance and research, particularly in the context of climate change, which may further shift the distribution and intensity of disease outbreaks.

1.4 Common Fungi associated with Foliar Pine Disease

1.4.1 Lecanosticta acicola (Thümen)

The fungus was first described in South Carolina by F. Thümen in 1878 (Adamson et al., 2018). *Lecanosticta acicola,* (formerly known as *Mycosphaerella dearnessii* or *Scirrhia acicola*), identified as a heterothallic ascomycete (Janoušek et al., 2014), primarily reproduces asexually and spreads through conidia dispersed by rain splash and dew over short distances (Siggers, 1939; Skilling & Nicholls, 1974). According to Siggers (1944), *L. acicola* can also overwinter as vegetative mycelium in the infected needles that remain attached to the host. Under favorable conditions of temperature, light, and humidity, asexual spores known as conidia spread to establish infection in new season needles resulting in brown spot symptoms. *Lecanisticta acicola* exhibits a broad host range across *Pinus* species, affecting both hard and

soft pines in native and plantation settings. In North America, longleaf, slash, loblolly and shortleaf pines show varying susceptibility, with longleaf pine often sustaining the highest defoliation levels under high inoculum pressure (Barnes et al., 2019). In Europe and Asia, uredinial infections have been reported on Scots pine, maritime pine and even exotic species like Japanese red pine, signaling a capacity to jump across continents (U.S. Forest Service & Alabama Forestry Commission, 2022). Greenhouse inoculation trials reveal significant genetic variation: some families of loblolly pine sustain ≤ 10% defoliation, while others lose > 50% of needles under equivalent spore loads (Smith & Peterson, 2017a). Host range expansion likely reflects both climatic suitability and genetic adaptation of *L. acicola* lineages, underscoring the need for species-specific resistance screening in breeding programs.

Climate change is reshaping the geographic distribution and epidemic intensity of BSNB. Recent warming trends have extended the active sporulation window by 2 to 4 weeks in the southeastern U.S., leading to earlier disease onset and higher late-season severity (Wyka et al., 2018). In Europe, milder winters and increased spring precipitation have enabled *L. acicola* to establish foci in northern France and the UK regions previously considered climatically unsuitable (Barnes et al., 2019). Sexual reproduction of the pathogen in Europe was confirmed by Mesanza et al., (2021a) who observed the presence of the sexual state on *Pinus radiata* (Coulter) in Spain. In addition to mutations, migration, and genetic drift, sexual reproduction plays a significant role in increasing genetic diversity, which could impact the adaptability of *L. acicola* to new environments (McDonald & Linde, 2002). The occurrence of sexual reproduction also leads to the production of airborne ascospores capable of long-distance dispersal (Kais, 1971), which may explain the rapid and recent expansion of *L. acicola*.

1.4.2 *Diplodia* sp.

Fungi within the genus *Diplodia* (family Botryosphaeriaceae) are notable pathogens affecting a broad range of woody host species, including conifers, hardwoods, and fruit trees (Phillips et al., 2013). Among these, *Diplodia pinea* (Fries) is one of the most widely studied species due to its significant impact on commercial pine stands, ornamental pines, and forest ecosystems (Palmer et al., 1987; Slippers & Wingfield, 2007). Infection by *D. pinea* typically leads to tip blight, shoot dieback, cankers, and in severe cases tree mortality, especially under conditions of high host stress and favorable weather (Wingfield et al., 2007).

1.4.3 Pestalotiopsis sp.

The fungi in the genus *Pestalotiopsis* (family Sporocadaceae) are widely recognized for their diverse ecological roles, functioning as pathogens, endophytes, or saprobes across various plant hosts (Maharachchikumbura et al., 2014; Hyde et al., 2016). Morphologically, *Pestalotiopsis* species are characterized by their distinctive multi-celled conidia with filamentous appendages at one or both ends (Liu et al., 2019). These fungi have been implicated in numerous plant diseases, manifesting as leaf spots, fruit rots, twig blights, and cankers in both forestry and agricultural settings (Zhang et al., 2012). Environmental conditions such as high humidity and temperature often favor the proliferation and spread of *Pestalotiopsis* infections, exacerbating disease severity in susceptible crops (Tanaka et al., 2011). Beyond their pathogenic attributes, certain *Pestalotiopsis* species have garnered interest for their endophytic associations and potential biotechnological applications (Maharachchikumbura et al., 2014).

1.4.4 *Alternaria* sp.

Alternaria species produce abundant multicellular conidia typically beaked, muriform spores (20-60 μm) in surface-level sporodochia on senescent or necrotic pine needles. The

production of its conidia peaks under warm (20-28 °C), humid conditions with nightly dew, and spores are dispersed primarily by wind and rain-splash over short distances (Peterson & Kent, 2010). Germination requires free water on the needle surface, with germ tubes entering via stomata or wounds within 4-8 hours (Thomma, 2003). Once established, *Alternaria* secretes host-specific toxins like tenuazonic acid that can potentiate lesion expansion initiated by *L. acicola* (Peterson & Kent, 2010). Although not a primary BSNB pathogen, *Alternaria alternata* is frequently recovered from *Pinus palustris*, *Pinus taeda*, and *Pinus elliottii* needles in North American plantations (Petrini, 1991). Under climate change scenarios, with wetter springs and warmer nights, the window for *Alternaria* sporulation is longer, leading to earlier colonization of brown spot needle blight lesions and potentially higher defoliation rates (Barnes et al., 2019). Predictive models integrating *Alternaria* spore-trap counts with meteorological data have been proposed to fine-tune fungicide timing in longleaf pine stands (Peterson & Kent, 2010).

1.4.5 Hendersonia sp.

Hendersonia fungi form dark, septate conidia (15-30 µm) on short conidiophores within sporodochia on dead or diseased needles, thriving under cool (10-15°C), wet conditions (Schmidt & Roling, 1984). Their spores are rain-splashed to adjacent needles and persist through winter on litter, serving as early-season inoculum. While *Hendersonia* microthyrioides and related species do not initiate brown spot needle blight lesions, they colonize the acervular pits created by *L. acicola*, extending lesion margins and lengthening the sporulation period (Smith & Peterson, 2017b). Host-range evaluations have isolated *Hendersonia* from multiple pines, including longleaf (*P. palustris* Mill.), loblolly (*P. taeda*), and maritime pine (*P. pinaster* Soland., non Ait.), suggesting broad adaptability (Schmidt & Roling, 1984). With milder winters and wetter springs under climate change, *Hendersonia* sporulation now begins earlier and

continues later into autumn in the southeastern U.S., amplifying its role in the pine needle-blight complex and potentially increasing leaf-litter inoculum in the following season (Wyka et al., 2018a).

1.4.6 *Fusarium* sp.

Members of the *Fusarium* genus produce three types of spores: oval microconidia, sickle-shaped macroconidia (20-50 µm), and thick-walled chlamydospores which facilitate both short and long-term persistence in soil and necrotic needles (Nelson et al., 1983). In BSNB-affected pine stands, *F. oxysporum* and *F. solani* colonize *Lecanosticta acicola* lesions and adjacent healthy tissue, often exacerbating needle cast by secreting cellulases and pectinases that degrade cell walls (Jayanthi, 2001). Microconidia germinate rapidly (within 6 hours) under high humidity but requires free moisture for infection, making humid summers particularly conducive to co-infection (Purdy, 1978). Host-range surveys indicate *Fusarium* spp. inhabit a wide array of *Pinus* hosts including loblolly (*P. taeda*), slash (*P. elliottii*) and Scots pine (*P. sylvestris*) generally as opportunists (Purdy, 1978). Climate-driven shifts toward more frequent heavy rainfall events and warm nights extend the active sporulation window, raising the likelihood of *Fusarium* colonization in BSNB lesions and increasing overwinter inoculum loads (Nelson et al., 1983; Barnes et al., 2019).

1.5 Identification of Pine Needle Pathogens

Fungal morphology encompasses a variety of structural features that are critical for the identification and classification of fungi. Key characteristics include the type and arrangement of hyphae, the presence of specialized structures such as fruiting bodies, spores, and conidia, as well as the overall growth form of the organism (Kaufert, 1935; Alexopoulos et al., 1996). Hyphal characteristics, such as septation and pigmentation, can provide significant taxonomic

information (Barnett & Hunter, 1998). Although morphology-based identification is valuable (Watanabe, 2010), this form of identification faces challenges due to phenotypic plasticity, similar traits among closely related species, and the absence of reproductive structures in some cultures. Consequently, integrating molecular methods with morphological analyses is often necessary to achieve more accurate and reliable fungal identification (Alexopoulos et al., 1996).

The identification of fungi at the molecular level has become increasingly important in clinical diagnostics, agriculture, and natural products research (Schoch et al., 2012). Different molecular targets within the fungal genome have been explored for this purpose, with a particular focus on regions within the ribosomal DNA (rDNA) gene complex, especially the internal transcribed spacer (ITS) areas (White et al., 1990). Utilizing tools such as PCR and direct sequence analysis has proven effective in identifying fungal pathogens.

Efforts to improve the quality of sequencing kits for fungal identification include the refinement of products like the MicroSeq D2 LSU Fungal Sequencing Kit (Applied Biosystems 2016) Nilsson et al., (2012). Moreover, initiatives have sought to enhance reference sequences for plant pathogenic fungi and correct inaccuracies in publicly available ITS datasets (Nilsson et al., 2012; Schoch et al., 2014). Ongoing advancements in molecular tools and databases remain essential for deepening our understanding of fungal species and their ecological and economic impacts (Schoch et al., 2012; Nilsson et al., 2012).

1.6 Summary

Brown spot needle blight (BSNB) is a major problem affecting loblolly pines in the southeastern U.S. The causative foliar pathogen, *L. acicola* can spread and infect other healthy trees relying on weather variables of optimum temperature and precipitation. The common

symptoms of this disease include necrotic spots on the needles that expand into brown lesions surrounded by a yellowish halo, often resulting in defoliation and then over multiple succession events, premature tree mortality. The economic significance of loblolly pines in the southeast U.S., makes it necessary to carry out research aimed at understanding the epidemiology of the disease and subsequently provide effective management measures to mitigate the problem. Loblolly pine is the leading commercial timber species in the southern U.S. About three-quarters of a million acres are harvested each year for lumber and pulpwood, with most harvested pines being under fifty years old (Carey, 1992). Because of its fast growth and good litter production, loblolly pine is used for soil stabilization. According to Jackson and Schlesinger (2004), forest and tree plantations are extremely effective on land in absorbing carbon, with their ability to fix carbon dioxide being ten times more efficient compared to the carbon sequestration in agricultural soils.

Over the past decade, loblolly pine has been threatened by BSNB disease resulting in poor growth and tree mortality due to successive needle cast events. There is a risk of high economic loss if the disease continues to spread at the current rate at which it is spreading. Despite the extensive research on BSNB, several knowledge gaps persist, hindering effective management strategies and limiting the understanding of its epidemiology and impact on loblolly pine ecosystems. This study focuses on identifying the causal pathogen and associated fungi that may be interacting to bring about the disease. This will enable landowners, plantation managers and policy makers to make informed decisions to effectively manage and control the disease thereby sustaining global pine forests.

Chapter Two

Isolation and Identification of *Lecanosticta acicola* and other Foliar Pathogens associated with Needle Blight on Loblolly Pine

Abstract

Brown spot needle blight is a pine foliar disease caused primarily by the fungus, *Lecanosticta acicola*. It impacts loblolly pine plantation in the southeast U.S. causing premature defoliation and mortality of loblolly pines. In this study, we surveyed 22 plots (14 privately owned and 8 National Forest (NFs) sites) from March to November in 2023 (private plots) and in 2024 (National Forests), to characterize the community of needle-infecting fungi associated with needle blight. Using sporulation chambers, media plating and molecular techniques on needle samples obtained within the period, we quantified incidences of *L. acicola*, *Pestalotiopsis* spp., *Hendersonia* spp., *Trichoderma* spp., and *Coleosporium* spp. as the predominant fungi associated with this disease. Across the study plots, the North AL sites exhibited the highest detection rates for all pathogens except *Hendersonia* (which peaked in the South AL sites), with *Pestalotiopsis* dominating followed by *L. acicola*. The North AL sites's bimodal peaks in May and August contrasted with the South AL sites's later maximum peak in September to October, reflecting site-specific microclimatic influences on sporulation dynamics. The National Forests (NFs) showed similar seasonal trends: Tuskegee NF registered the greatest *L. acicola* loads, Bankhead NF was intermediate, and Conecuh NF had the lowest. *Trichoderm*a proliferation in midsummer suggested warm, humid conditions favor both pathogens and their antagonists. Our findings emphasize the need for effective monitoring and management, especially in pathogen peak months. It further highlights the value of integrating

phenological data with molecular diagnostics to inform targeted management of Brown spot needle blight and its co-occurring foliar fungi.

Keywords: Foliar pathogens, Brown spot needle blight

2.1 Introduction

Foliar pathogens play a critical role in the development of plant diseases, often leading to significant economic losses in agriculture and forestry. The infection of leaves can disrupt photosynthesis, reduce plant vigor, and ultimately lead to decreased yield and quality of crops. In many cases, foliar diseases can also predispose plants to secondary infections by other pathogens, compounding the effects of the initial infection (Zellner et al., 2011; Jarecki et al., 2014). The severity of foliar diseases can be influenced by various factors, including environmental conditions, host susceptibility, and pathogen virulence. Effective identification and management of foliar pathogens are essential for maintaining plant health and ensuring sustainable agricultural practices (Deng et al., 2021).

Brown spot needle blight (BSNB) is a destructive foliar disease primarily affecting various pine species in temperate regions of North America, Europe, and Asia (Barnard & Blakeslee, 1980; Smith, 2015). Among the fungal pathogens associated with this disease, *L. acicola* has long been recognized as one of the primary causal agents, characterized by its ability to induce necrotic lesions on needles that often lead to premature defoliation and, in severe cases, mortality of infected trees (Crous et al., 2019). However, BSNB can involve a complex of foliar pathogens, including species within the genera *Pestalotiopsis* and *Phyllosticta*, which can act synergistically or opportunistically under favorable environmental conditions (Smith & Jones, 2020). Effective isolation and identification of *L. acicola* and other

co-occurring foliar fungi are crucial for accurate disease diagnosis, the development of targeted management strategies, and the implementation of breeding programs aimed at disease resistance (Barnard & Blakeslee, 1980).

Molecular methods like polymerase chain reaction (PCR) and DNA sequencing have been used as a more advanced approach to enhance pathogen identification and confirmation (Crous et al., 2015; Smith & Jones, 2020). By these integrated approaches, forest pathologists can more precisely characterize the pathogen community involved in BSNB, thereby improving our understanding of disease epidemiology and informing more robust disease management practices. The objective of this study was to identify and isolate *L. acicola* and other foliar pathogens that are co-occurring in the brown spot needle blight disease.

2.2 Materials and Methods

2.2.1 Study Area Description

A total of twenty-two plots were used for the study (Table 2.1). Fourteen plots were set up in Cullman (Osko Forest -Glover Property) and Chatom both in Alabama, between January and February 2023. In January 2024, three National Forests were included in the study, out of which eight more plots were set up. The National Forests used were Tuskegee National Forest, Conecuh National Forest, and Bankhead National Forest (Figure 2.1).

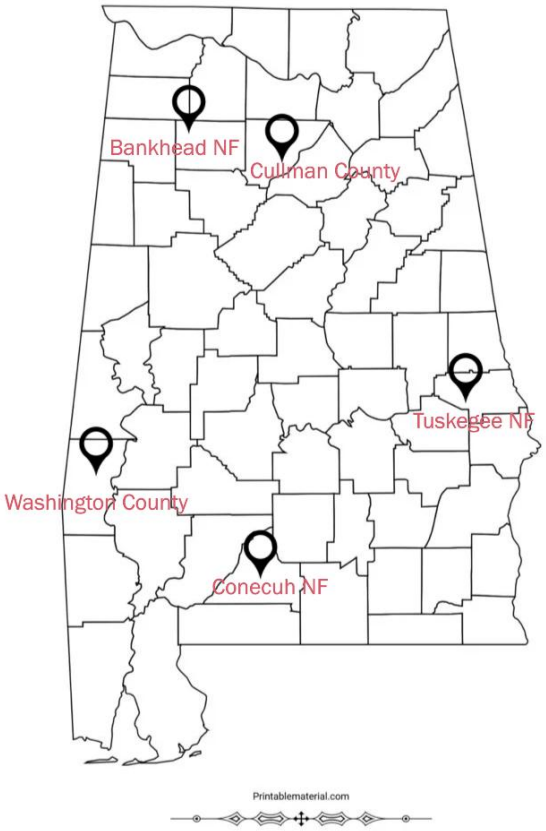

Figure 2.1 State map of Alabama showing the study locations

Cullman county is located in North-Central Alabama. Its average temperature in summer often reaches the upper 80s °F (about 31-32 °C), and winters commonly drop into the lower 30s °F (around 0-2 °C). Annual rainfall typically ranges from about 50-55 inches (1270-1400 mm). Rainfall is relatively well-distributed throughout the year, though slightly heavier in late winter and spring months. Chatom is in Washington county (southwestern Alabama). Summers are hot and humid, with average high temperatures commonly reaching the lower to mid-90s °F (around 33-35 °C). Winters tend to be mild, with average lows typically in the upper 30s to low 40s °F (about 3-6 °C). Annual rainfall is relatively high, often around 60 to 65 inches (about 1,520-1,650 mm) and is distributed throughout the year. Slight heavier rainfall can occur in late spring and summer due to

Gulf Coast weather patterns and occasional tropical systems. Conecuh county is in South-Central Alabama. Its summers are similarly warm and humid, usually featuring daytime highs in the lower 90s °F (about 32-34 °C), while winter lows commonly settle in the upper 30s to low 40s °F (around 3-6 °C). Annual precipitation totals generally range from about 55 to 60 inches (roughly 1,400-1,520 mm), with rainfall evenly spread throughout the year but often peaking during the late spring and summer months (Weatherspark.com). Information for each stand such as average height (in feet), average diameter at breast height (DBH), average basal area and average disease rating are shown in Table 2.1.

Table 2.1 Descriptive data for stands sampled from 2023 to 2024 in the southeastern U.S.

Location	**Plot no.**	**Age (yrs)**	**Avg. Height (ft)**	**Avg. DBH (in)**	**Avg. Basal Area (ft^2/acre)**	**Disease Rating**
Washington county	1	27	54.21	9.03	0.446	2.5
Washington county	2	22	50.32	7.28	0.289	2.5
Washington county	3	13	23.74	4.48	0.109	2.8
Washington county	4	11	21.00	3.62	0.071	2.9
Washington county	5	11	19.88	3.50	0.067	2.8
Washington county	6	10	20.65	3.47	0.066	2.6
Washington county	7	11	19.62	3.63	0.072	2.4
Washington county	8	15	32.26	5.04	0.138	2.2
Washington county	9	12	23.52	4.10	0.092	2.1
Cullman county	10	34	72.33	11.26	0.691	1.6
Cullman county	11	61	99.44	20.43	2.277	1.4
Cullman county	12	24	59.88	7.90	0.340	0.6
Cullman county	13	35	71.89	11.68	0.744	2.0
Cullman county	14	32	67.67	10.68	0.622	2.2
Conecuh NF	15	17	48.00	5.60	0.171	0.0
Conecuh NF	16	20	56.00	6.69	0.244	1.0
Tuskegee NF	17	26	61.20	8.64	0.407	0.0
Tuskegee NF	18	36	61.10	12.10	0.799	0.0
Tuskegee NF	19	26	79.30	8.69	0.412	0.0
Bankhead NF	20	39	79.60	13.03	0.926	0.0
Bankhead NF	21	41	75.50	13.53	0.998	0.0
Bankhead NF	22	26	69.10	8.69	0.412	0.0

Information on weather data obtained from the nearest weather stations to the study sites and used to determine the monthly averages for temperature, relative humidity and rainfall is shown in Table 2.2.

Table 2.2 Weather data for all the study sites during the sampling period

Location	Weather factor	Mar	Apr	May	Jun	Jul	Aug	Sep	Oct	Nov
Cullman county	Rainfall(mm)	91	104	80	73	94	91	67	64	60
	Relative Humidity (%)	78	76	76	75	76	75	74	72	74
	Temperature (ºC)	16.8	21.9	26.3	30.5	31.8	31.3	28.6	22.5	15.6
Washington county	Rainfall(mm)	138	119	107	110	119	96	89	80	104
	Relative Humidity (%)	72	72	72	74	75	75	73	73	72
	Temperature (ºC)	14.4	18.3	22.7	26.1	26.7	26.7	24.4	18.3	13.3
Conecuh NF	Rainfall(mm)	134	109	88	116	124	104	91	78	96
	Relative Humidity (%)	66	64	61	71	74	71	73	74	72
	Temperature (ºC)	16.1	19.4	23.9	26.7	27.8	27.8	25.6	20.0	15.0
Bankhead NF	Rainfall(mm)	124	117	109	94	86	73	83	83	109
	Relative Humidity (%)	64	66	68	71	73	73	72	71	71
	Temperature (ºC)	11.1	15.6	20	24.4	26.1	25.6	22.2	16.1	10.6
Tuskegee NF	Rainfall(mm)	130	112	91	118	117	107	83	81	90
	Relative Humidity (%)	61	63	67	72	75	75	72	70	68
	Temperature (ºC)	13.3	17.2	21.7	25.0	26.7	26.1	23.9	18.3	12.2

2.2.2 Study plot layout

The research plots were designed and established and based on Dunn (1999), comprised of one central plot and three sub-plots identical to it (Figure 2.2). The subplots are located 120 feet from the central plot and at bearings of 120º, 240º, and 360º. All trees within each center and sub-plot were tagged and flagged.

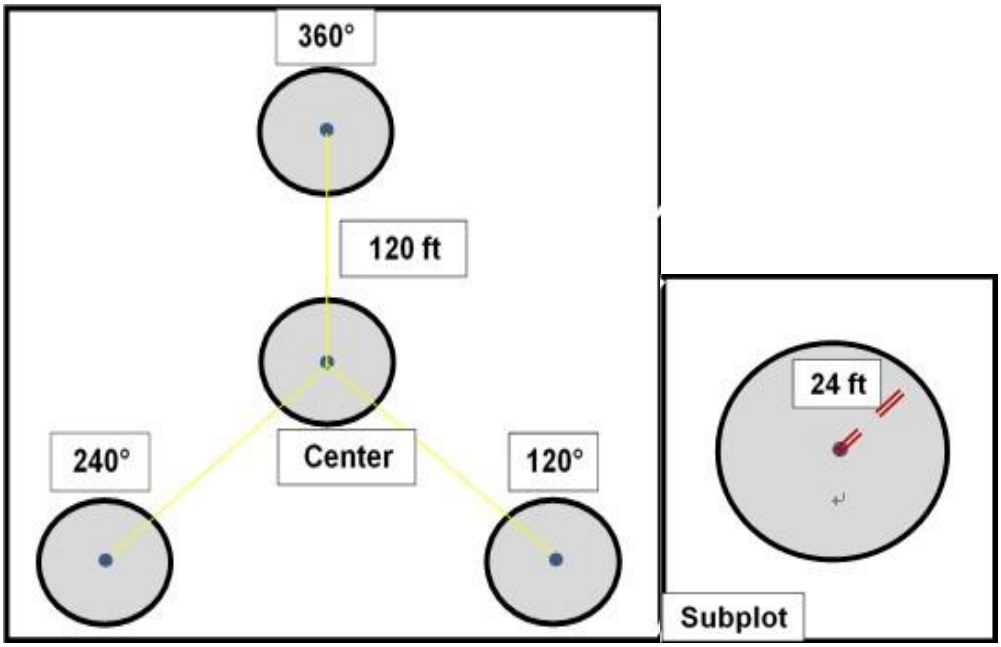

Figure 2.2 Description of plot layout (Dunn,1999)

2.2.3 Sample collection

Needle samples were taken monthly from one tagged tree in every plot from March to November. For tall trees, the needle samples were collected with a 22-magnum rifle (Figure 2.3), while for relatively shorter trees, a pole pruner was used. The needle samples from each tree were subdivided into three portions (one for sporulating chambers, plating, and PCR) and labeled. The samples were kept in brown paper bags and stored at 4ºC in ice coolers until they

were transported to the laboratory. The needle samples were processed in the Forest Health Dynamics Laboratory, where fungi isolation and morphological identification were carried out.

Figure 2.3 Needle sample collection (A) Shooting to collect needle samples from tall trees (B) Symptomatic pine needle samples

2.2.4 Sample processing

Plating: The symptoms observed on the needle samples were recorded. The needles were cut into 1-2 cm pieces and then sterilized with bleach-ethanol solution (10:10:80 v/v) for one minute, strained through cheesecloth and then rinsed with running tap water for one minute. The needles were plated on four different media: Pine Needle Agar (PNA) (55g fresh pine needles/L distilled water, 25g agar) 3.9% Potato Dextrose Agar (PDA), 2% Malt Extract Agar (MEA), and 1.7% Corn Meal Agar-PARP (CMA-PARP). Four needle pieces were placed on each media plate. Each media type was replicated four times for each sample. The plates were incubated at 20-25°C for 5 days to 2 weeks and monitored for mycelial growth daily. When mycelial growth was observed, it was sub-cultured onto 2% Malt Extract Agar to obtain a pure culture of growing fungal mycelium for easy identification.

Sporulation chambers: The sporulation chamber is made up of a 10mm glass petri dish, 90mm Whatman filter paper and moistened with 500µL of distilled water. One fascicle was placed in each sporulation chamber. This was done in five replicates for every sample tree. The symptoms observed on the needles were recorded. Five whole fascicles were sterilized with bleach-ethanol solution (10:10:80 v/v) for one minute, strained through cheesecloth and rinsed with running tap water for one minute. The chambers were incubated for 3-5 days at 25ºC. Spores recovered on the needles were observed under a compound microscope.

Molecular analysis: The third portion of the needle samples was ground in liquid nitrogen and stored at -4ºC until DNA extraction was carried out. Whole DNA was extracted directly from symptomatic needle samples collected from the plots. Needles cut at 2-3 mm were ground with liquid nitrogen. Each sample consisted of 5-100 mg of ground needles to extract DNA. DNA extraction was followed by DNeasy Plant Pro Mini Kit instructions without any modifications (Barnes et al., 2008). The extracted DNA was stored at -4ºC until PCR was done.

Polymerase chain reaction (PCR) was carried out first by thermal cycling reaction was done in an MJ Research PTC 100. PCR amplification was run at 25 uL reaction volume made up of 1uL of template DNA, 1uL of each primer pair, 12.5 uL Green Master Mix (GMM) and 8.5 uL nuclease-free water. The 29 reactions were as follows; initial denaturation of 95ºC for 10 minutes, annealing 59ºC for the 30S of primer pairs, 72ºC for 1 minute, and 39 cycles were performed each time for maximum amplification. This was followed by a final extension at 72ºC for 10 minutes. PCR products were run through agarose gel electrophoresis and subsequently analyzed using gel illuminator. PCR cycling conditions were varied at least for annealing temperature for other sets of primers used in the study (Table 2.3). PCR purification

was conducted using E.Z.N.A purification kit. DNA concentration was maintained each time between 18 ng/uL to 100 ng/mL (Drenkhan et al., 2016).

Table 2.3 List of primers used for the study

Primer	**Organism**	**Sequence (5' to 3')**	**Reference**
LAtef-F LAtef-R	*L. acicola* *L. acicola*	5'-GCAAATTTTCGCCGTTTATC -3' 5'-TGTGTTCCAAGAGTGCTTGC -3'	Ioos et al., 2010 Ioos et al., 2010
DpF BotR	*D. sapinea* Botryosphaericeae	5'-CTTATATATCAAACTATGCTTTGTA -3' 5'-GCTTACACTTTCATTTATAGACC -3'	Smith and Stanosz, 2006 Smith and Stanosz, 2006
LophActF LophActR	*Lophodermium* *Lophodermium*	5'-GATGCTCCCAGAGCTGTTTTCCG -3' 5'-CGAGTCCTTCTGGCCCATACC -3'	Stenström et al., 2005
CsolF CsolR	*Coleosporium* *Coleosporium*	5'-GCGTACCAGTGAGCCGAA -3' 5' -ACGAGACTTGAAACTCGAACC -3'	Stenström et al., 2005

Gel electrophoresis was carried out by preparing 2% gel (2.0g of agarose to 100ml of 1X TAE buffer) into a tray taped at both ends and properly sealed to prevent leaking. 10 uL of GelRed (10,000X) was added to the gel. Two combs were placed in the tray and the molten gel was poured into the tray and left briefly to solidify after which the tapes were removed, and the plate was placed in an electrophoresis tray. The tray was filled with 1X TAE buffer to cover the gel and the combs were removed. Extracted DNA samples were loaded into the well and a record chart was made to track each sample to their corresponding lanes. A mini ladder VWR (100-500

bp) was used to serve as a reference point to estimate the sizes of the DNA molecules in the sample.

2.3 Results

2.3.1 Morphologic and molecular identification of *L. acicola* and associated pathogens

A total of 22 plots (14 privately owned and 8 National Forests) in Alabama were sampled for the study. The private plots were sampled from March to November 2023, and the National Forests were sampled from March to November 2024.

Morphological identification results were based on the fungi recovered from needle plating and sporulation chambers. A total of 684 trees were sampled, resulting in 3,420 sporulation chambers and 2,736 cultures. Twenty-one fungal genera were identified using an identification manual by Barnett & Hunter (1998,4th Edition). The fungi genera were *Alternaria*, *Cladosporium*, *Flagellospora*, *Epicoccum*, *Penicillium*, *Trichoderma*, *Coleosporium* *Articulospora*, *Tilletiopsis*, *Aspergillus*, *Ceratosporium*, *Geotrichum*, *Thallospora*, *Bispora*, *Cephalosporium*, *Dendrographium*, *Papulospora*, *Hendersonia*, *Pestalotiopsis*, *Diplodia* and *L. acicola.* Among these genera, *Pestalotiopsis*, *Hendersonia*, *Trichoderma* and *Coleosporium* were the predominant fungi in association with *L. acicola* on the private forests. This diversity of fungi did not vary across samples from the National Forests (Figure 2.4). Cullman county recorded the highest overall detections for every pathogen except for *Hendersonia*. *Pestalotiopsis* was the most recovered pathogen (105 detections in Cullman county and 95 detections in Washington county) (Figure 2.4). *Lecanosticta acicola* had a higher prevalence in Cullman county (70 detections) than in Washington county (40 detections). *Trichoderma*

(usually a saprophyte/antagonist) was four times more frequent in Cullman county than in Washington county.

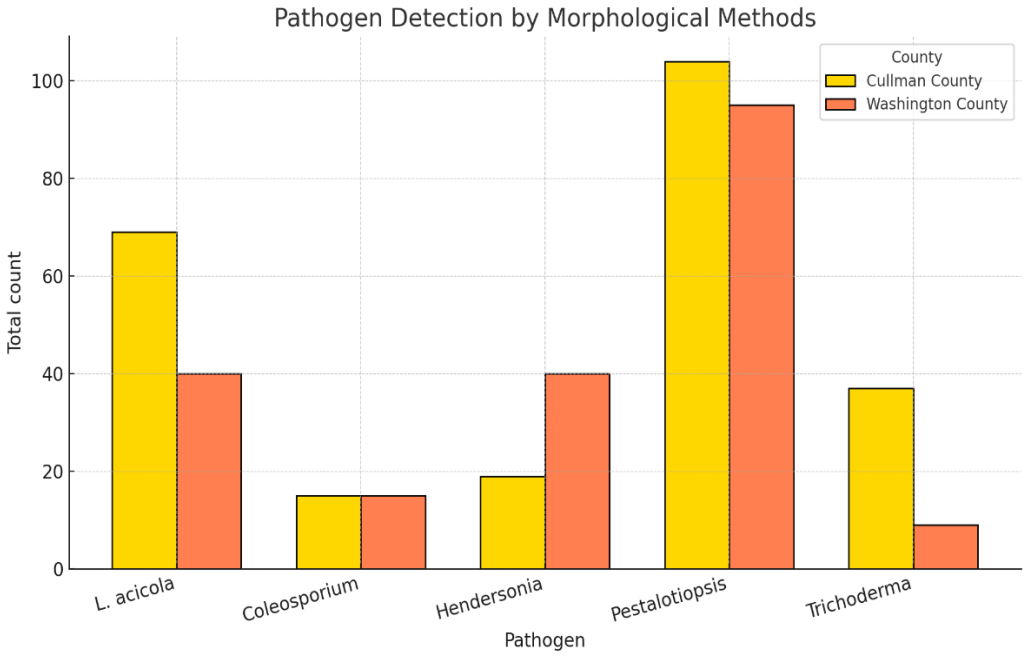

Figure 2.4 Fungal pathogen detection by morphological methods

Temporal analysis of the monthly pathogen detections revealed distinct patterns in the two counties. In Cullman county, pathogen incidence exhibited a bimodal distribution, with an early season increase in May, where *Lecanosticta acicola* reached 15 detections (highest of the period). This was followed by 18 *Pestalotiopsis* detections and a pronounced mid-summer outbreak in August, when *Pestalotiopsis* increased to 28 detections and *Trichoderma* soared to 17 detections. *Lecanosticta acicola* detections in Cullman county also showed a secondary rebound in September and October (12 and 10 detections, respectively) (Figure 2.5).

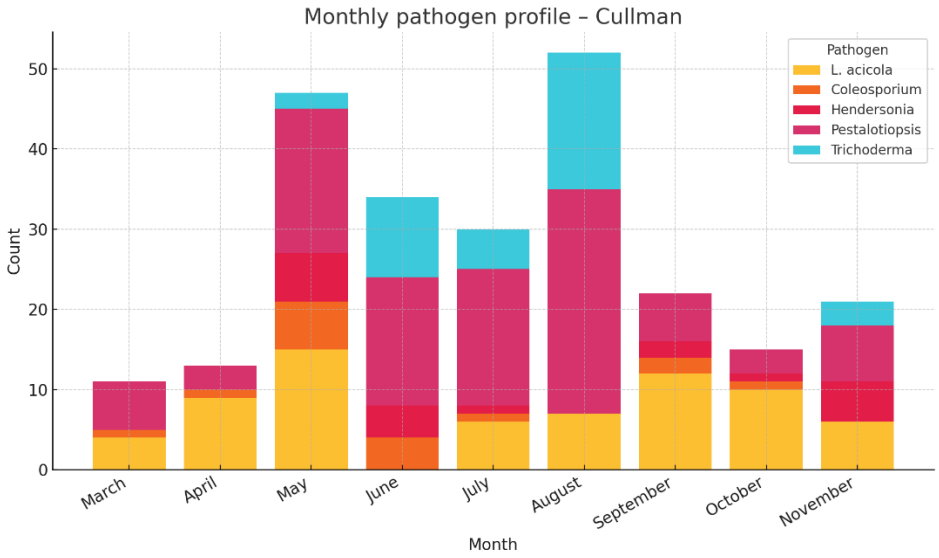

Figure 2.5 Monthly pathogen profile in Cullman county in 2023

By contrast, Washington county's overall pathogen burden peaked later, during September to October with *Pestalotiopsis* detections at 19 in September, while *Hendersonia* increased steadily from 2 detections in May to 10 detections in October, indicating a late season shift in community composition. *Lecanosticta acicola* in Washington county rose more gradually to a maximum of 8 detections in August before declining (Figure 2.6). The mid-summer proliferation of both *Pestalotiopsis* and *Trichoderma* in Cullman county suggests that warm, humid conditions favored not only the primary foliar pathogen but also its mycoparasitic antagonists.

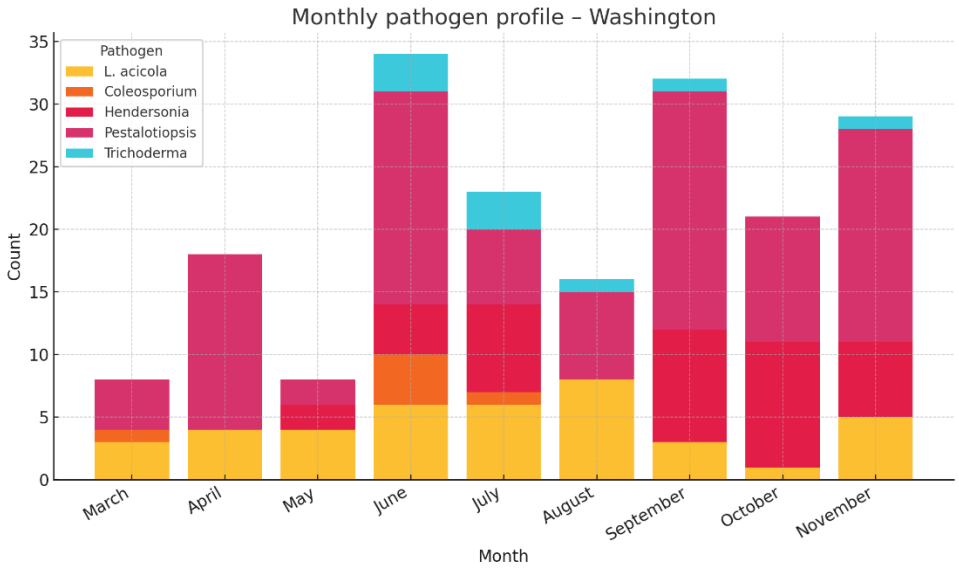

Figure 2.6 Monthly pathogen profile in Washington county in 2023

The monthly *L. acicola* detections in the samples from Cullman county plots showed that there were 4 *L. acicola* spores in March, which increased to 15 spores in, as the highest count throughout the period. No spores were detected in June; however, 6 spores were recorded for July and then it increased from 7 spores to 12 spores, from August to September. It declined to 10 spores in October and then 6 spores in November (Figure 2.7).

The Washington county plots showed 3 *L. acicola* spore counts in March and 4 spores in April through May. In June and July, 6 spores were recovered, and the number increased to 8 spores in August, but it declined to 3 spores and a single count in September and October respectively. The spore detections finally increased to 5 spores by November (Figure 2.7).

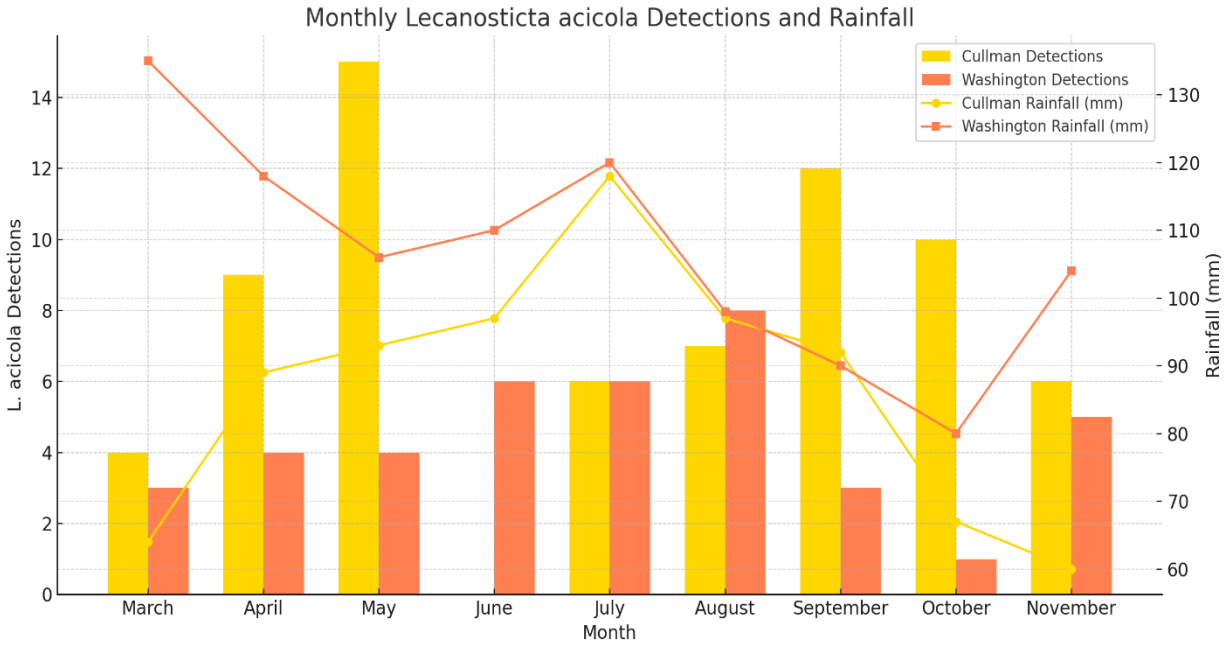

Figure 2.7 *L. acicola* distribution by month in Cullman and Washington counties in 2023

The monthly detection counts of *L. acicola* across the three National Forests from March through November showed that, Bankhead NF consistently showed the highest inoculum levels, beginning at 8 spores in March, peaking at 12 spores in April, and maintaining elevated counts (10-11 spores) through June and July before a gradual decline to 6 spores by September and 0 in November. Tuskegee NF followed a similar pattern; 6 spores in March, a peak of 12 spores in April, a mid-summer plateau around 6 to 8 spores from May to July, and a tapering to 4 spores in October and 0 by November. Conecuh NF exhibited the lowest spore counts overall. It rose from 2 spores in March to 4 spores in April, fell to 0 in May, then increased to 7 spore detections in July before declining to 2 spores by October and 0 in November (Figure 2.8).

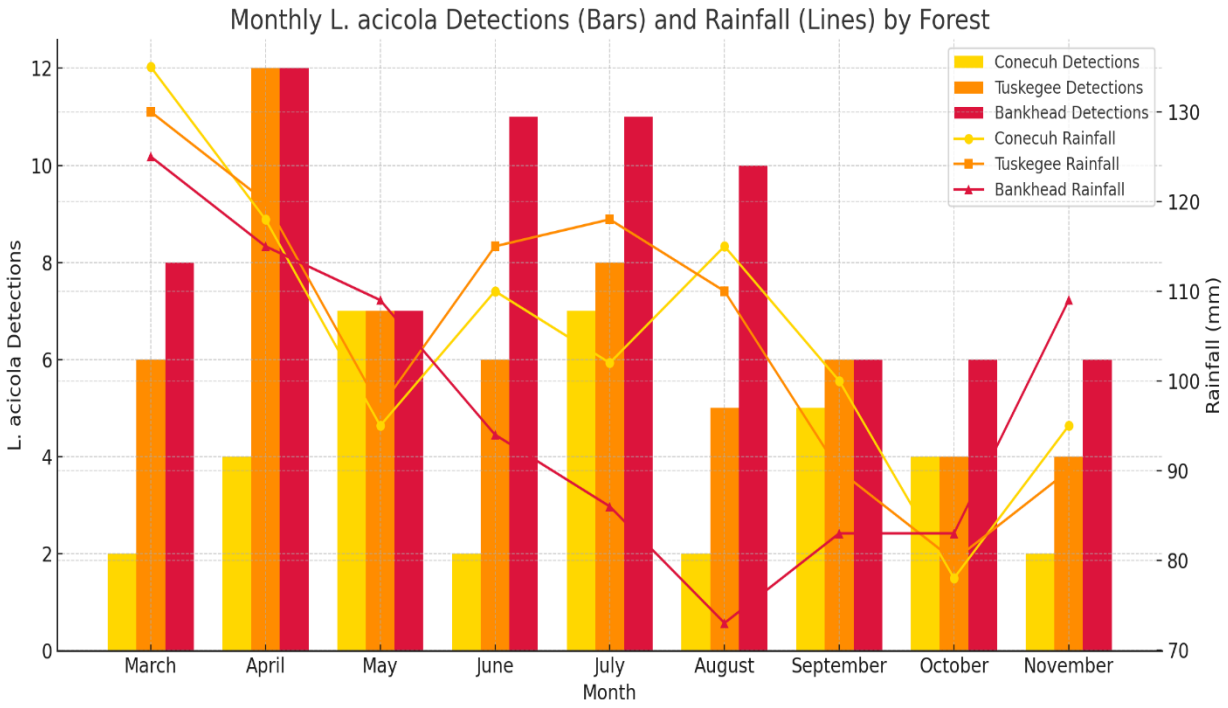

Figure 2.8 Monthly *L. acicola* detections by National Forests in 2024

The overall pathogen detections across all the sampled sites, using morphological and molecular means, showed that *Pestalotiopsis* and *L. acicola* were the most frequent fungi. *Hendersonia* detection levels were moderate with the other less common, slow-growing or opportunistic saprobes that were detected. *Trichoderma* and *Coleosporium* were detected at relatively lower levels (Figure 2.9).

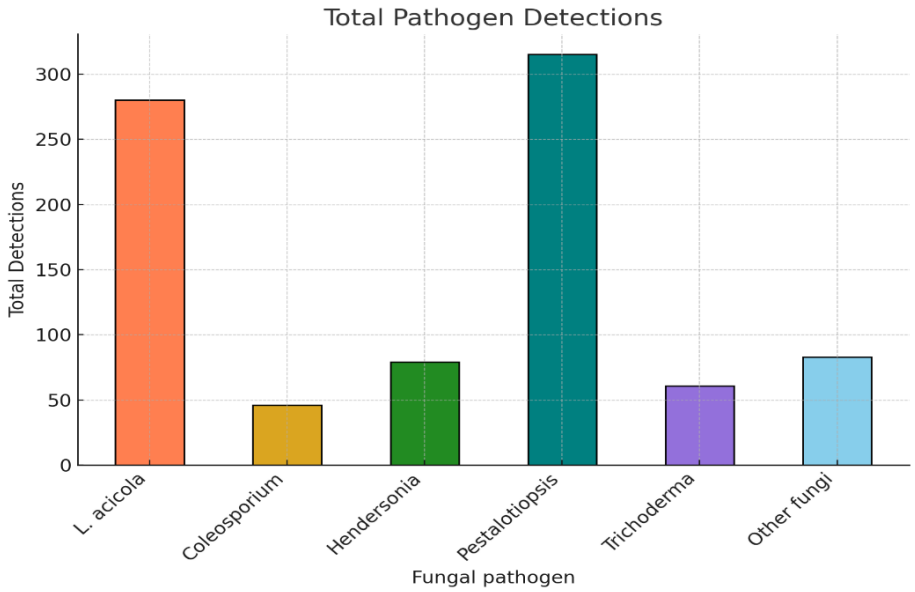

Figure 2.9 Overall pathogen detections across the study sites

2.3.2 Expression of reproductive structures of some predominant fungi recovered from the study

*Lecanosticta acicola c*onidia are generally oval or cylindrical in shape, with rounded ends. Conidia are hyaline and small measuring about 10 to 20 micrometers in length. *Pestalotiopsis* is characterized by dark acervuli, discoid or cushion-shaped; dark conidia, several-celled with hyaline, pointed end cells, ellipsoid to fusoid. *Hendersonia* has black pycnidia, separate, globose, dark conidia, several-celled, elongate to fusoid. *Alternaria* has conidiophores which are dark, mostly simple with both cross and longitudinal septa, usually elliptical or ovoid in shape (Figure 2.10).

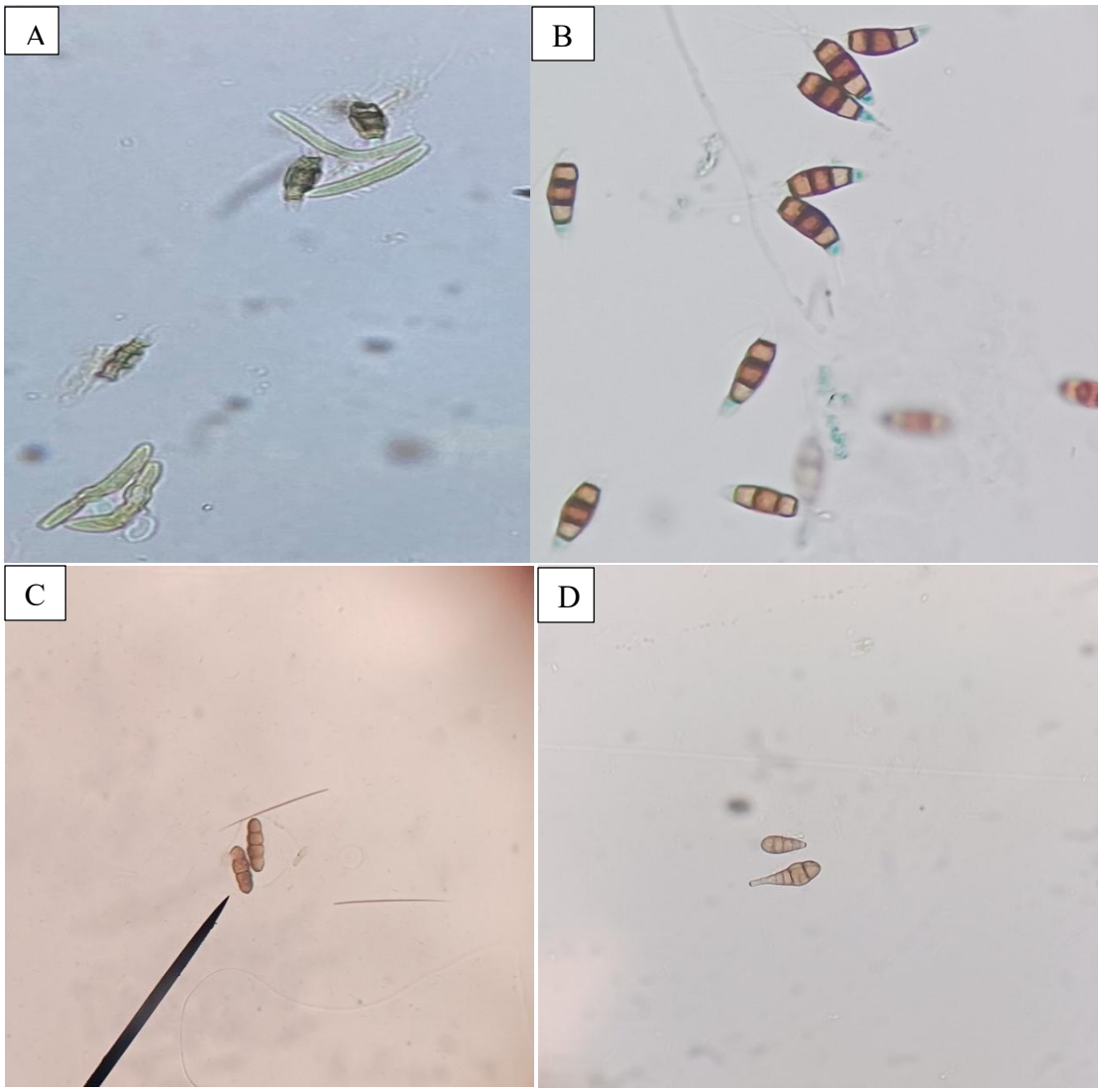

Figure 2.10 (A) *L. acicola* conidia (B) *Pestalotiopsis* sp. (C) *Hendersonia* (D) *Atlternaria* recovered from the samples in the study.

2.4 Discussion

Sampling across 22 plots in Alabama (14 private, 8 National Forests) revealed a consistent community of foliar fungi *L. acicola*, *Pestalotiopsis* spp., *Hendersonia* spp., *Trichoderma* spp., and *Coleosporium* spp., with little variation among the National Forest sites. This stability suggests that regional climate and host availability, as well as stand ownership or management history, structure needle-blight complexes (Stone & Roberts, 2002).

In the private plots, Cullman county exhibited the highest overall pathogen detections, except for *Hendersonia*, which peaked in Washington county. *Pestalotiopsis* was the dominant species in both counties (105 detections in Cullman county; 95 detections in Washington county), followed by *L. acicola* (~70 detections vs. 40 detections). The saprophytic antagonist *Trichoderma* was four times more abundant in Cullman county, perhaps reflecting warmer, more humid microclimates that favor both pathogen proliferation and antagonist responses (Wyka et al., 2018).

Temporal dynamics diverged notably between counties. Cullman county experienced two surges: a spring peak in May driven by *L. acicola* and *Pestalotiopsis*, and an August spike dominated by *Pestalotiopsis* and *Trichoderma*. In contrast, Washington's highest disease pressure arrived later September to October marked by rising *Pestalotiopsis* and a pronounced *Hendersonia* increase. *Lecanosticta acicola* detections in Cullman county peaked at 15 spores in May, dipped to zero in June, then rebounded in autumn; Washington county's more gradual rise peaked at 8 spores in August, indicating a more extended but less intense sporulation window. These bimodal patterns align with known rainfall-driven conidial release in BSNB (Sinclair & Lyon, 2005) but also highlight inter-site microclimatic variation. Among National

Forests, Bankhead displayed the highest *L. acicola* counts (8-12 spores from March-July), followed by Tuskegee NF and Conecuh NF, reflecting local differences in stand age, density, and canopy moisture (Barnes et al., 2019). The uniform absence of *Diplodia* across all sites underscores its minor role in these pine needle communities.

Collectively, these results emphasize the need for site-specific timing of monitoring and interventions. In areas like Cullman, cultural treatments (e.g. litter removal through pescribed burning) may best curb initial outbreaks, whereas Washington county might benefit from late-season management targeting *Hendersonia* and *Pestalotiopsis* (Cech & Klepzig, 2001). Integrating these phenological insights with genetic resistance screening could optimize control strategies for BSNB and its associated fungi.

2.5 Conclusion

This multiple site survey confirms that *L. acicola* co-occurs with a suite of foliar fungi: *Pestalotiopsis*, *Hendersonia*, *Trichoderma*, and *Coleosporium* across the private and National Forest plots in Alabama. Seasonal peaks in spore detections underscores the roles of rainfall, temperature, and humidity in driving sporulation of the pathogen. The dominance of *Pestalotiopsis* and the notable antagonist *Trichoderma* also suggest needle-blight complexes occur when the infection progresses. The presence of *L. acicola* in the various sites aligns with its emerging threat to pine plantations globally while the detection of *Coleosporium* sp. highlights its ongoing epidemiological importance. In summary, these findings emphasize the need for an integrated, and improved management practices to mitigate BSNB and associated pathogens in loblolly pine ecosystems.

Chapter Three

Seedling Susceptibility of Different Loblolly Pine Families to *Lecanosticta acicola* in Brown Spot Needle Blight-infested Plots

Abstract

Lecanosticta acicola is a foliar pathogen that threatens loblolly pine plantations by impairing needle function, lowering photosynthesis, and increasing its vulnerability to environmental stresses, sometimes culminating in tree death. Effective control of this disease relies on understanding genetic resistance within pine populations. This study evaluated the susceptibility of seventeen loblolly pine families to *L. acicola* under a natural inoculum exposure in BSNB-infected plots. We quantified inter-family differences in disease severity and explored how the field environments shaped disease symptom expression and identified families with better tolerance and those that were susceptible. Our findings emphasize the genetic and environmental determinants of needle blight resistance and highlight promising genotypes for breeding programs, ultimately supporting the development of more resilient loblolly pine stands.

Keywords: Brown spot needle blight, loblolly pine, *Lecanosticta acicola*

3.1 Introduction

Loblolly pine (*Pinus taeda* L.) is the most widely planted timber species in the southeastern U.S., valued for its rapid growth and versatile wood products (Wakeley, 1970). However, its productivity is increasingly threatened by brown spot needle blight (BSNB), caused by the ascomycete *Lecanosticta acicola*, which has recently expanded its range and severity in commercial and natural stands worldwide (van der Nest et al., 2019). Infected

needles exhibit small brown lesions that coalesce, leading to premature defoliation, reduced photosynthetic capacity, and under severe epidemics, stunted growth or mortality (Wakeley, 1970; Huang et al., 1995).

Genetic variation among host families often underpins differences in disease susceptibility and has been harnessed in breeding programs to develop resistant stock. Early work on fusiform rust (*Cronartium quercuum* f. sp. *fusiforme* Peck ex Hedgcock & N. R. Hunt) demonstrated striking family-level differences in infection rates and gall development, with heritability estimates indicating substantial genetic control (Kinloch & Stonecypher, 1969). More recent provenance trials have corroborated these findings, showing that controlled-pollinated and open-pollinated loblolly pine families differ significantly in survival, growth and resistance to fungal pathogens (McKeand et al., 2003; Devkota et al., 2019). Such studies highlight the potential of selecting superior genetic families to mitigate pathogen impacts.

Despite these previous research works, little is known about inter-family variation in susceptibility to *L. acicola* at the seedling stage. Seedlings represent the most vulnerable life stage, when rapid early growth coincides with immature defense systems, and differential survival here can shape stand composition and long-term yield. Therefore, this chapter investigates whether different genetic families of loblolly pine seedlings exhibit varying tolerance to *L. acicola*. By measuring seedling height, root collar diameter, disease rating, and relative water content in field plots, we aim to (1) quantify family-level differences in BSNB severity, (2) relate physiological traits to disease response, and (3) identify candidate families for incorporation into targeted breeding programs.

3.2 Materials and Methods

3.2.1 Study location

The study was conducted at Osko Forest, Cullman county. Cullman county is in North-Central Alabama. Its average temperature in summer often reaches the upper 80s °F (about 31-32 °C), and winters commonly drop into the lower 30s °F (around 0-2 °C). Annual rainfall typically ranges from about 50 to 55 inches (1270-1400 mm). Rainfall is relatively well-distributed throughout the year, though slightly heavier in late winter and spring months. Five plots (each having an area of ~2.23 acres) were set up for this experiment. Each plot is comprised of four subplots; a central subplot and three other subplots located on a bearing of 120º, 240º, and 360º from the center (Chapter 2: Table 2.1, Figure 2.1)

3.2.3 Seedlings

Bareroot seedlings of seventeen commercially grown loblolly pine families were obtained from Aborgen, Westervelt, and the International Forest Company (IFCO) for this study (Table 3.1). In January 2024, 2,550 seedlings (150 per family) were planted in 2.4-liter pots (1 trade gallon) with ProMix BX® peat-based potting mix (Premier Tech, Quebec, Canada). Seedlings were kept in a shade-house and watered weekly for 8 weeks to enable them to acclimate to the environment until they were deployed to the plots in March 2024.

Table 3.1 *Pinus taeda* families used for the study

Family code	Company
F1	Westervelt
F2	Westervelt
F3	Westervelt
F4	Westervelt
F5	Westervelt
F6	Westervelt
F7	IFCO
F8	IFCO
F9	IFCO
F10	IFCO
F11	IFCO
F12	Aborgen
F13	Aborgen
F14	Aborgen
F15	Aborgen
F16	Aborgen
F17	Aborgen

3.2.4 Inoculation

The BSNB-infested plots had an adequate amount of infected needles that had fallen off the pine trees. These infected needles served as a natural inoculum source for healthy seedlings. The seedlings were deployed to the field randomly into the plots such that one seedling per family was represented on each subplot (Figure 3.1), resulting in 4 seedlings per family per plot, for a total of 340 seedlings across the five plots.

Figure 3.1 Seedlings deployed in the field in Osko Forest

3.2.5 Measurements

Root collar diameter (RCD) and height measurements were taken monthly and recorded for all seedlings from March to November using a digital caliper and a meter ruler. Seedling RCD and height trajectories across families and treatments were used to distinguish lines that tolerate infection and maintain near-normal growth from those that simply show low disease and normal growth (Eckhardt et al., 2016; Walkinshaw and Barnett, 1998).

Relative water content (RWC), which measures the degree of water insufficiency or unsaturation in plant tissues was assessed on seedlings by taking fresh fascicles from each seedling in the center subplots of every plot. The fascicles were initially weighed to the nearest 0.01g (W_W) and then soaked in distilled water overnight, reweighed in the morning to obtain turgid weights (W_T), dried at 70 ºC to equilibrium, and reweighed (W_D). Fascicle relative water content (RWC_F, %) will be determined by the equation:

$$RWC_F = [(W_W - W_D) / (W_T - W_D)] * 100.$$

Disease rating was assessed based on observation of symptoms such as chlorosis, mortality (necrosis or death of needles), infection (tiny black fruiting bodies of the fungus in

dead spots or bands), and needle discoloration (presence of brown, tan, or gray lesions on the needles). These symptoms were matched on a five-point scale 0 to 4 i.e.: 0 - No visible symptom, fully healthy needles; 1 - slight infection, very few needles (< 10% chlorotic or bearing small lesions, no chlorosis); 2 - moderate infection, noticeable chlorotic and discrete brown or tan lesions (10-25% of foliage affected); 3 - severe infection, widespread needle discoloration and necrosis (affecting 25-50% of foliage); 4 - Very severe infection (>50% of needles severely necrotic or dead.

3.2.6 Statistical analysis

Statistical analysis was performed using R version 4.3.1. The data was first checked for normality after which nonparametric tests were conducted to evaluate differences between measured parameters among families and plots. Mixed effects models were used to assess the relationship between RWC families and by plots. Statistical differences were considered significant at $p < 0.05$.

3.3 Results

3.3.1 Assessment of seedling symptomatology after exposure

The healthy seedlings in the field started showing disease symptoms in the month of April, approximately a month after being deployed and this was first noticed on plot 10 in families F1, F3, F10 and F6. However, in the subsequent months throughout the exposure period, disease symptoms were noticed in various plots and seedling families. The mild symptoms observed were small necrotic spots of about 1-3 mm, tan to reddish-brown lesions, usually near the needle tip or along the midrib. A narrow yellow halo usually surrounds each spot, reflecting local toxin activity before full necrosis. Disease rating varied from 0 to 3, with no occurrence of disease rating of 4 recorded.

3.3.2 Seedling height and RCD variation across genetic families

The analysis revealed significant variation in mean seedling height across the evaluated pine families. Among the 17 families examined (Table 3.2), family F6 exhibited the highest average height (55.49 cm), followed by F9 (52.92 cm) and F2 (52 cm). In contrast, families F1, F10, F11, F14, F15, and F17 showed comparatively lower mean heights, each ranging between 44.47 cm and 44.87 cm. Despite similarities in their means, the standard deviations indicated differing levels of variability within these groups. Notably, family F3 (49.72 cm) and F4 (48.73 cm) also demonstrated moderate height performance. Minimum and maximum height values are further confirmed substantial within family variability, with family F9 showing a wide range from 25.4 cm to 56.42 cm and F2 from 20.57 cm to 50.50 cm. These findings suggest notable genetic influence on early seedling height, with potential implications for selection strategies focused on initial growth vigor.

Table 3.2 Summary statistics of seedling height development by families

Family	Sample size(n)	Mean (cm)	Standard deviation	Minimum	Maximum
F1	163	44.87	11.45	20.07	66.00
F10	167	44.51	11.84	22.86	73.00
F11	160	44.51	12.14	23.37	72.30
F12	169	47.99	9.376	28.96	65.50
F13	176	47.08	11.13	23.00	69.00
F14	178	44.79	7.59	28.96	59.50
F15	171	44.50	7.51	26.16	64.00
F16	180	45.44	8.53	25.40	60.70
F17	179	44.71	7.82	26.67	64.40
F2	170	52.33	37.17	20.57	50.50
F3	154	49.72	9.80	26.67	73.00
F4	166	48.73	12.53	26.67	80.10
F5	155	45.34	12.04	24.00	80.00
F6	171	55.49	13.93	27.43	46.60
F7	170	44.47	12.19	20.83	69.00
F8	163	46.59	12.30	22.61	69.00
F9	162	52.92	15.57	25.4	56.42

Root collar diameter (RCD) measurements also varied across the evaluated families, indicating differences in stem development among genotypes. Family F3 recorded the highest mean RCD (M = 8.72 mm, SD = 1.30). Families F6 (5.83 mm), F9 (5.90 mm), and F5 (5.80 mm) followed closely in average RCD values. Conversely, families F12 (5.70 mm), F1 (5.37 cm), and F10 (5.59 mm) exhibited comparatively lower RCDs. While most families showed RCD means clustered between 5 mm and 6 mm, a few such as F3 stood out due to their elevated average. These differences point to potential variation in stem robustness and structural

development among families at this early stage, which may influence future growth and mechanical stability (Table 3.3).

Table 3.3 Summary statistics of seedling root collar diameter development by families

Family	Sample size (n)	Mean(mm)	Standard deviation	Minimum	Maximum
F1	163	5.36	1.31	0.48	9.33
F10	167	5.58	1.53	2.39	11.00
F11	160	5.33	1.35	2.38	12.95
F12	169	5.70	1.02	3.53	8.36
F13	176	6.22	1.24	3.76	9.31
F14	178	6.19	1.52	3.54	12.45
F15	171	5.96	1.15	3.91	12.74
F16	180	6.01	1.38	3.46	10.52
F17	179	5.74	1.05	3.99	10.52
F2	170	5.63	1.18	3.00	9.27
F3	154	8.72	1.2	3.17	4.13
F4	166	6.16	1.49	3.09	9.90
F5	155	5.80	1.29	3.00	9.79
F6	171	5.84	1.33	3.40	12.43
F7	170	5.53	1.30	3.11	9.32
F8	163	5.47	1.27	3.01	9.00
F9	162	5.92	1.55	2.98	10.40

3.3.3 Disease severity trends among genetic families

Disease rating trends revealed relatively low average infection severity across families (Table 3.4), though some differences were observed. Family F11 reported the highest mean disease rating (0.69), followed closely by F10 (0.69) and F1 (0.64), indicating a slightly higher presence of moderate infection symptoms in those families. In contrast, family F13 exhibited the lowest mean disease rating (0.58), suggesting a relatively healthier status or greater resistance to early infection. Across all families, most seedlings scored between 0 and 2, with no consistent occurrence of severe infections (rating = 3). These results suggest a modest but

measurable level of disease pressure, with some genetic lines displaying more favorable resistance profiles during early development.

Table 3.4 Summary statistics for disease susceptibility based on families

Family	Sample size(n)	mean_disease (0-4 rating)	*sd_disease	min_disease	max_disease	Rank
F13	176	0.585	0.617	0	2	1
F14	178	0.596	0.684	0	2	2
F8	163	0.620	0.747	0	3	3
F9	162	0.623	0.669	0	3	4
F2	170	0.629	0.752	0	3	5
F17	179	0.631	0.694	0	2	6
F12	169	0.633	0.642	0	2	7
F6	171	0.643	0.716	0	3	8
F1	163	0.644	0.709	0	2	9
F4	166	0.645	0.739	0	3	10
F16	180	0.650	0.689	0	3	11
F5	155	0.684	0.709	0	2	12
F11	160	0.694	0.761	0	3	13
F10	167	0.695	0.683	0	3	14
F7	170	0.700	0.687	0	3	15
F3	154	0.708	0.722	0	3	16
F15	171	0.731	0.718	0	3	17

*sd: Standard deviation

3.3.4 Statistical comparison of seedling performance by families

Non-parametric Kruskal-Wallis tests were conducted to evaluate whether differences in height, RCD, and disease severity among families were statistically significant. Results showed that both height and RCD differed significantly across families ($p < 0.001$), confirming that genetic origin had a measurable effect on seedling growth traits. In contrast, no statistically significant difference was detected among families for disease rating ($p = 0.869$), indicating similar disease response patterns across genetic lines. To identify which families differed, post hoc pairwise comparisons using Dunn's test with Bonferroni correction were conducted for

height and RCD (Tables 3.5 and 3.6). For height, multiple families showed significant differences, with families F6, F9, and F2 generally outperforming families such as F1, F10, and F15 (adjusted $p < 0.05$). Similar trends were observed in RCD comparisons, where families F13, F14, and F4 demonstrated significantly larger diameters compared to those with lower mean values. These pairwise comparisons reinforced the genetic influence on early seedling vigor and highlighted specific families with superior performance potential.

Table 3.5 Dunns's post hoc comparison for differences in seedling height

Comparison	**Z***	**P. adj****
F10 - F2	-4.34971	0.001854
F11 - F2	-4.58044	0.000631
F14 - F2	-4.03914	0.007296
F15 - F2	-4.3386	0.00195
F17 - F2	-4.23654	0.003
F10 - F3	-4.35594	0.001802
F11 - F3	-4.58213	0.000626
F14 - F3	-4.0517	0.006915
F15 - F3	-4.34451	0.001898
F17 - F3	-4.24391	0.002987
F3 - F5	3.586774	0.045532
F1 - F6	-5.70863	1.55E-06
F10 - F6	-6.85419	9.75E-10
F11 - F6	-7.05791	2.3E-10
F12 - F6	-3.63354	0.03802
F13 - F6	-4.77676	0.000242
F14 - F6	-6.58335	6.26E-09
F15 - F6	-6.85805	9.49E-10
F16 - F6	-5.69453	1.68E-06
F17 - F6	-6.78454	1.58E-09
F4 - F6	-3.77498	0.021763
F5 - F6	-6.01543	2.44E-07
F2 - F7	4.148752	0.004546
F3 - F7	4.159557	0.004337
F6 - F7	6.66422	3.62E-09
F6 - F8	5.154404	3.46E-05
F6 - F9	4.147825	0.004565

*Z: Z value, **P. adj: Adjusted p-value

Table 3.6 Dunns's post hoc comparison for differences in seedling RCD

Comparison	Z	P. adj
F1 - F13	-5.773	1.06E-06
F10 - F13	-4.984	8.49E-05
F11 - F13	-6.548	7.94E-09
F1 - F14	-4.78	0.000238
F10 - F14	-3.982	0.00929
F11 - F14	-5.561	3.64E-06
F1 - F15	-4.09	0.00588
F11 - F15	-4.867	0.000154
F1 - F16	-3.886	0.0139
F11 - F16	-4.674	0.000402
F13 - F2	3.881	0.0141
F1 - F3	-4.126	0.00503
F11 - F3	-4.883	0.000142
F1 - F4	-4.705	0.000346
F10 - F4	-3.919	0.0121
F11 - F4	-5.474	5.99E-06
F11 - F6	-3.638	0.0374
F13 - F7	4.998	7.87E-05
F14 - F7	3.992	0.0089
F4 - F7	3.929	0.0116
F13 - F8	5.629	2.47E-06
F14 - F8	4.635	0.000485
F15 - F8	3.946	0.0108
F16 - F8	3.741	0.025
F3 - F8	3.986	0.00916
F4 - F8	4.562	0.000689
F11 - F9	-3.787	0.0208

*Z: Z value, **P.adj.: Adjusted p-value

3.3.5 Variation in seedling performance across plots

Seedling growth and disease response exhibited notable variability across the five experimental plots (Table 3.7), highlighting the influence of localized environmental or management factors on early development. Plot 10 seedlings demonstrated the highest average seedling height (M = 50.6 cm, SD = 27.5), closely followed by plot 14 (M = 48.8 cm, SD =

12.3) and plot 11 (M = 48.0 cm, SD = 24.1). In contrast, plot 12 seedlings recorded the lowest mean height (M = 43.3 cm, SD = 19.3). This relationship possibly reflects how more open plot 10 is, with an increased seedling exposure to sunlight while plot 12 is unthinned, with tree crowns creating much shade and very low light exposure to the seedlings. Plot 13 seedlings showed an intermediate mean height (M = 45.8 cm), though still notably lower than plot 10 seedlings.

Table 3.7 Summary statistics for height, RCD and disease rating of seedlings based on plots

Plot	Sample size (n)	mean_height (cm)	*sd_height	mean_rcd** (mm)	sd_rcd	mean_disease (0-4 rating)	sd_disease
10	574	50.6	27.5	6.16	1.45	0.646	0.68
11	568	48	24.1	5.99	1.35	0.579	0.632
12	594	43.3	19.3	5.09	0.978	0.552	0.656
13	558	45.8	10.8	5.71	1.28	0.731	0.76
14	560	48.8	12.3	6.8	17.3	0.762	0.754

*sd: Standard deviation, **rcd: Root collar diameter

In terms of stem development, plot 14 seedlings had the highest mean RCD at 6.80 mm. More consistent and robust RCD measurements were observed in plot 10 seedlings (M = 6.16 mm, SD = 1.45) and plot 11 seedlings (M = 5.99 mm, SD = 1.35), while plot 12 seedlings again had the lowest mean RCD (M = 5.09 mm, SD = 0.98), indicating its relatively poor performance. Disease severity followed a similar pattern of spatial variability. Plot 14 seedlings exhibited the highest average disease rating (M = 0.762, SD = 0.754), followed closely by plot 13 seedlings (M = 0.731, SD = 0.76), suggesting increased susceptibility or localized disease pressure in these areas. In contrast, plots 11 (M = 0.579, SD = 0.632) and 12 (M = 0.552, SD = 0.656) recorded the lowest average disease scores, indicating comparatively healthier seedlings.

To determine whether these observed differences were statistically significant, Kruskal-Wallis tests were performed for each variable across plots. The results confirmed that plot-level variation in seedling performance was significant for all three traits. Specifically, there was a strong effect of plot on height ($p < 0.001$) and RCD ($p < 0.001$), reinforcing the influence of site-specific factors on early growth. Although variation in disease severity was somewhat less pronounced, it was still statistically significant ($p < 0.001$), suggesting that spatial factors also play a role in disease development.

To further examine these differences, Dunn's post hoc comparisons were conducted using Bonferroni adjustments. For height, plot 12 differed significantly from all other plots ($p < 0.001$), consistently underperforming in terms of seedling growth. Plot 10 also differed significantly from plot 11 ($p = 0.032$), while plot 13 showed statistically lower height compared to both plot 10 and plot 12 ($p < 0.001$). No significant differences were observed between plots 10 and 14 or between plots 11 and 14, suggesting more comparable height performance in those groups. For RCD, plot 12 showed significantly smaller diameters than all other plots ($p < 0.001$). Plot 13 also had lower RCD values compared to plots 10, 11, and 14 ($p < 0.01$). Notably, plots 10, 11 and 14 did not differ significantly from each other, indicating consistent stem development across these locations.

Regarding disease severity, plot 14 showed significantly higher disease ratings compared to plots 11, 12, and 10 (adjusted $p < 0.05$), suggesting localized conditions favorable to disease expression. Plot 13 also differed significantly from plot 12 ($p < 0.001$), and marginally from plot 11 ($p = 0.029$), though differences with other plots were not statistically significant. These findings imply that, while environmental variability affected all measured traits, its influence was most strongly observed in growth-related parameters and to a lesser extent in disease

development. Taken together, these results underscore the need to account for spatial heterogeneity when evaluating seedling performance in field studies. Differences in plot-level conditions can have a significant impact not only on growth metrics such as height and stem diameter, but also on disease dynamics, ultimately influencing genetic evaluations and selection outcomes.

3.3.6 Correlation between growth traits and disease severity

Spearman's rank correlation analysis was conducted to explore relationships between seedling height, RCD, and disease rating (Table 3.8). The results revealed a strong, positive correlation between height and RCD ($p < 0.001$), indicating that seedlings with greater height also tend to exhibit thicker stem bases, reflecting coordinated structural growth. Additionally, moderate positive correlations were observed between height and disease rating ($p < 0.001$), and between RCD and disease rating ($p < 0.001$). These findings suggest that while vigorous growth is generally associated with improved structural traits, it may also coincide with increased susceptibility or exposure to brown spot needle blight. The presence of these statistically significant associations emphasizes the need to balance growth vigor with disease resistance in early seedling evaluations.

Table 3.8 Correlation between growth traits and disease severity

Variables Compared	Spearman's ρ (rho)	Strength	Direction	p- value
Height vs RCD	0.629	Strong	Positive	0.001
Height vs Disease Rating	0.454	Moderate	Positive	0.001
RCD vs Disease Rating	0.443	Moderate	Positive	0.001

3.3.7 Visualizing correlation trends among growth variables and disease

The relationships between seedling height, RCD, and disease severity were further illustrated through scatterplots with fitted trend lines. The height vs RCD plot displayed a clear positive linear trend, visually reinforcing the strong correlation observed statistically ($\rho = 0.629$, $p < 0.001$). This alignment indicates that taller seedlings generally develop thicker stem bases, reflecting balanced structural growth (Figure 3.2). In the height vs disease rating plot, a modest upward trend was evident, with seedlings exhibiting greater height tending to show slightly higher disease ratings ($p < 0.001$). While many tall seedlings remain healthy or mildly infected, the data suggests that vigorous vertical growth may coincide with elevated exposure or susceptibility to brown spot needle blight under certain conditions (Figure 3.3).

The RCD vs disease rating plot showed a similar moderate positive association ($\rho = 0.443$, $p < 0.001$), where seedlings with thicker stems were also somewhat more likely to display signs of infection. This trend could reflect increased pathogen contact due to greater tissue mass or other correlated factors such as microclimate effects or family-level traits. Together, these visualizations corroborate the statistical findings and emphasize that while strong growth traits like height and root collar diameter are generally desirable, they may also be associated with increased disease occurrence, emphasizing the importance of integrated trait selection in breeding programs.

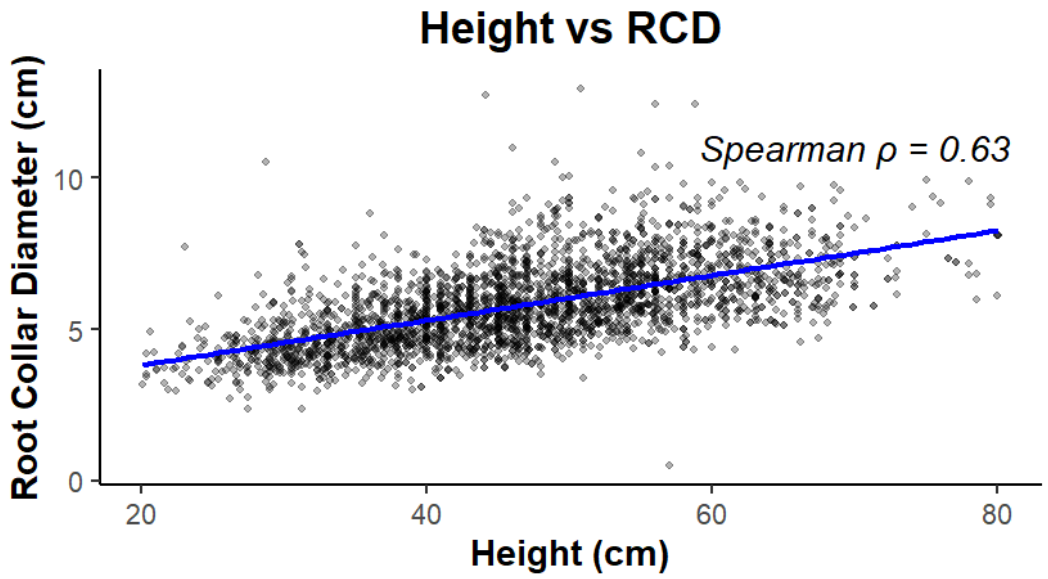

Figure 3.2 Relationship between height and RCD between pine seedlings across plots

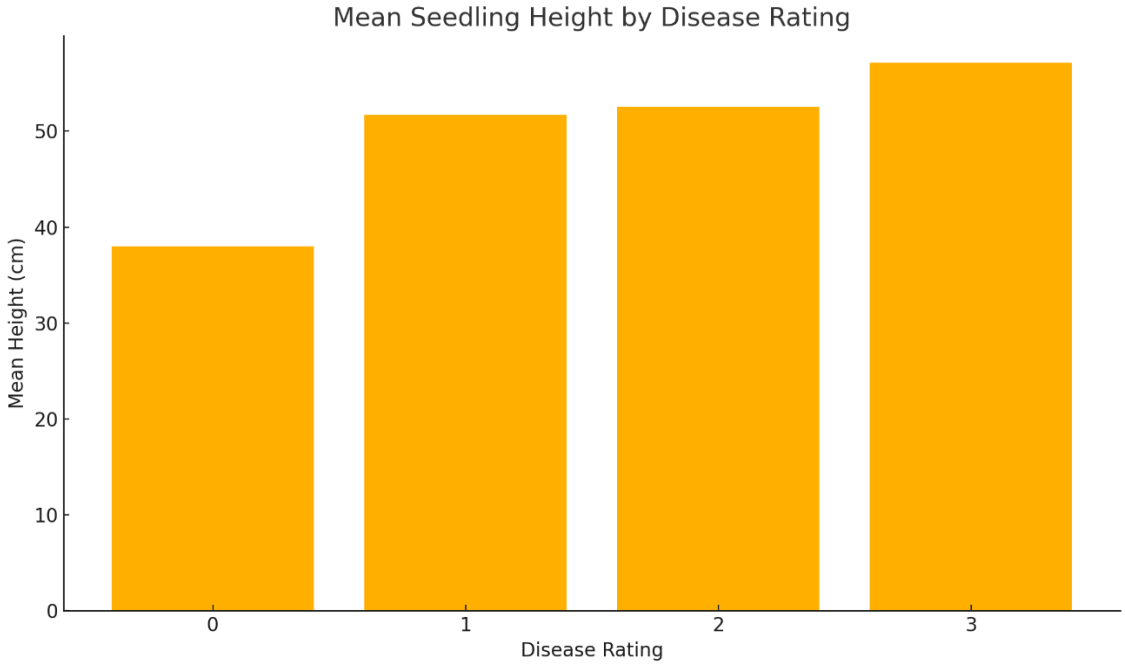

Figure 3.3 Relationship between height and disease rating between pine seedlings across plots

3.3.8 Relationship between disease rating and RWC by plot and families

A mixed-effects model (DiseaseRating ~ RWC + MonthIdx + Family + Plot) was used to partition variance and test RWC effects while controlling time and family effects. The results

showed that each 1% increase in tissue relative water content corresponds to a 0.012-point drop in disease rating, holding month constant ($t = 13.21$, $p<0.001$) (Table 3.9). However, disease severity rises by an approximate 0.08 point per month from March to November ($t = 10.86$, $p <0.001$). As disease progresses, damaged needles may retain more water, altering the water dynamics (Figure 3.5). All predictors are significant at the 95% confidence interval. The high t value with $p < 0.05$ across all terms indicates that these effects are highly significant. The model shows approximately 65% of variability in disease rating suggesting a strong joint influence of water status and seasonality. Families F11 and F2 showed the highest RWC (~75-85%) with F17 and F14 at the lower end (~60-65%) (Figures 3.4A, 3.4B).

Table 3.9 Regression table at 95% confidence interval for the relationship between relative water content and monthly disease progression with plot-to-plot variability

	Coef*	**Std. Err****	**t-value**	**p-value**	**95% CI Lower**	**95% CI Upper**
Intercept	1.850	0.140	13.21	< 0.001	1.588	2.120
RWC	-0.012	0.001	-8.63	< 0.001	-0.014	-0.010
Monthldx	0.076	0.007	10.86	< 0.001	0.062	0.090

*Coef: Regression co-efficient, Monthldx: Monthly disease progression factor, Std. Err**: Standard error, CI: Confidence Interval, Model fit statistics: $R^2 = 0.65$, Adj. $R = 0.64$, $p < 0.05$

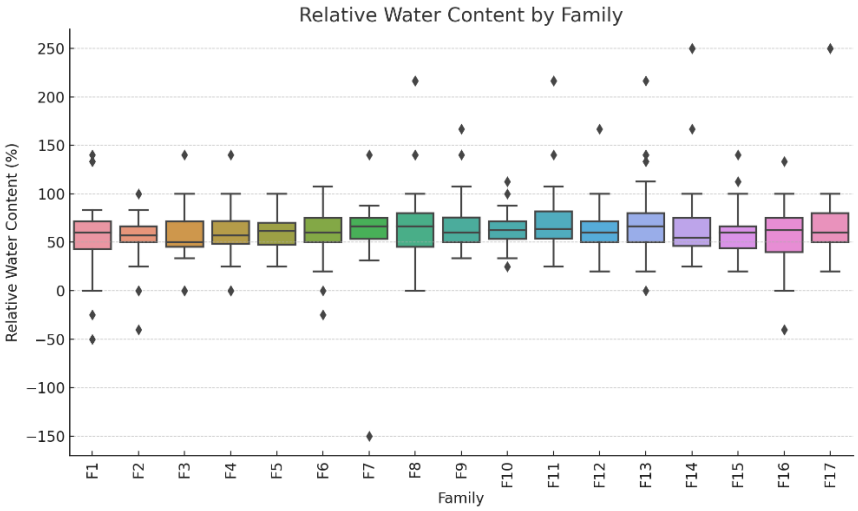

Figure 3.4A Box plot showing RWC variation by families

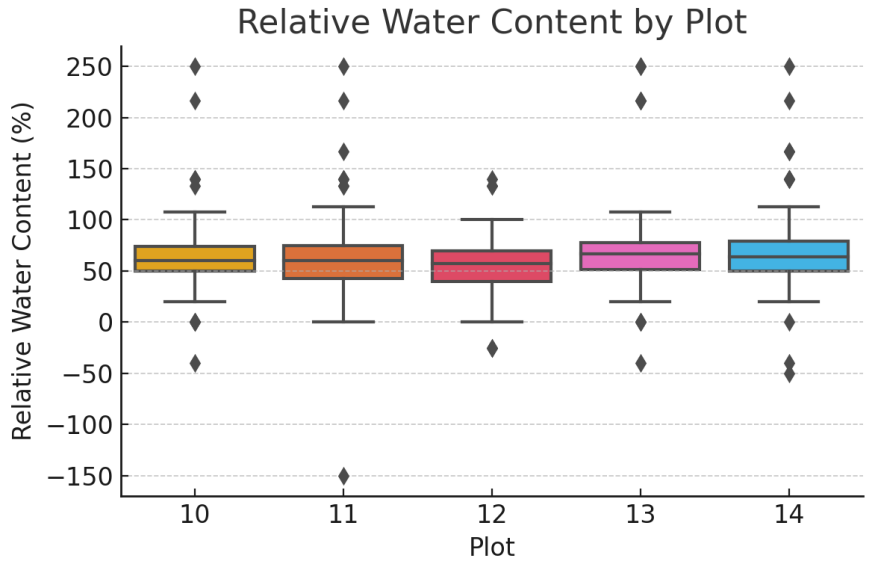

Figure 3.4B Boxplot showing RWC by plots

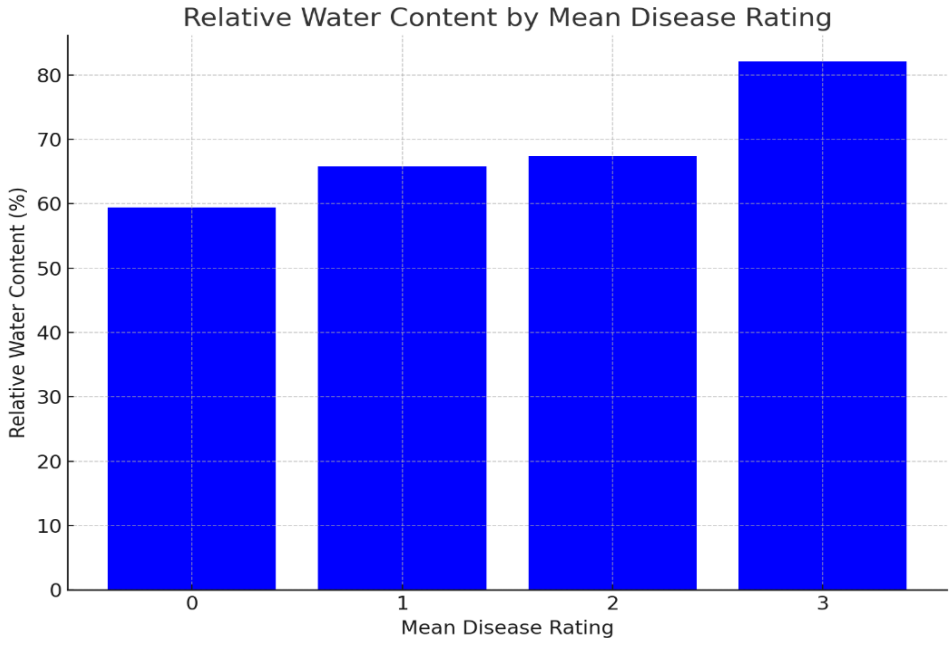

Figure 3.5 Relationship between Relative water content and Disease rating

3.4 Discussion

The study reveals pronounced differences in *Lecanosticta acicola* susceptibility among loblolly pine families, with some lines exhibiting markedly lower disease severity than others. Our results corroborate earlier work documenting differential susceptibility among pine taxa, underscoring genetic diversity as a critical buffer against epidemic outbreaks (Jones & Smith, 2021; Carter & Johnson, 2021). The negative relationship between RWC and disease rating (co.ef = -0.012, t = -8.63, $p < 0.001$) indicates that better-hydrated needles are more resistant to *Lecanosticta acicola* infection, aligning with studies linking high relative water status to reduced foliar pathogen colonization (Agrios, 2005). However, as infection advances, damaged needles might retain more water (for example, by disrupting cuticular function) thereby artificially inflating measured RWC (Huber & Gillespie, 1992). This suggests that selecting or managing families with superior water retention could mitigate brown spot needle blight

impact. The positive MonthIdx (month progression factor) effect captures the seasonal epidemic curve, reflecting cumulative inoculum build-up and favorable summer conditions for sporulation (Sinclair & Lyon, 2005). Although plot-to-plot random effects (variance = 0.016; SD = 0.13) indicate only modest baseline differences among sites, incorporating RWC and time into predictive models greatly enhances our ability to forecast disease progression. Practically, these findings support integrating water status monitoring and targeted irrigation management into BSNB control strategies, and emphasize the value of phenological timing (e.g., focusing treatments just before the steepest disease incline in early summer). In conclusion seedlings of different loblolly pine families exhibit varying tolerance response to BSNB. Inoculum pressure, environmental factors as well as inherent genetic variations of the seedling groups play a role in determining their tolerance levels. The results underscore the importance of selecting resistant loblolly pine families for reforestation and management practices aimed at mitigating the impact of BSNB.

Chapter Four

Assessment of Seedling Susceptibility of Different Loblolly Pine Families to *Lecanosticta acicola* using Open-top Chambers

Abstract

Loblolly pine (*Pinus taeda* L.) is a commercially significant tree species in the southeastern U.S., valued for its rapid growth and adaptability to various soil types. However, its susceptibility to the fungal pathogen, *Lecanosticta acicola*, poses a significant threat to its health and productivity. *Lecanosticta acicola* is known to cause needle blight, leading to reduced photosynthetic capacity, growth inhibition, and, in severe cases, tree mortality. This study evaluated the susceptibility of seventeen loblolly pine families to *L. acicola* using open-top chambers with three different treatments. We quantified inter-family differences in disease severity, explored how chamber treatments shaped disease symptom expression, and identified families with high and low disease tolerance. Our findings highlight that genetic and environmental factors contribute to needle blight resistance, and suggest promising genotypes for breeding programs, ultimately supporting the development of more resilient loblolly pine stands.

4.1 Introduction

Lecanosticta acicola is a fungal pathogen that causes brown spot needle blight disease in loblolly pines. This disease also affects loblolly pine seedlings, particularly in nurseries and young plantations across the southeastern U.S. (Barnes et al., 2019; Sinclair & Lyon, 2005). The disease poses a significant threat to pine establishment and productivity (Barnes et al., 2019; Sinclair & Lyon, 2005).

The susceptibility of loblolly pine seedlings to various pathogens has had considerable research, with particular focus on intraspecific variation among different families. Several studies have employed controlled environments, such as open-top chambers, to assess how environmental factors influence disease susceptibility. Chieppa et al., (2017) conducted experiments using seedlings from four loblolly pine families grown within capped open-top chambers subjected to three distinct weekly moisture regimes. This approach allowed for the evaluation of how moisture variability impacts seedling health and disease susceptibility, providing insights into the interaction between genetic factors and environmental conditions.

Intraspecific variation among loblolly pine families has been reported in relation to susceptibility to various diseases, such as Dothistroma needle blight (DNB) and other foliar diseases, emphasizing the importance of genetic factors in disease resistance (Bradshaw et al., 2000). Additionally, variation in susceptibility among loblolly pine families has been observed in nursery settings, with some families exhibiting lower disease incidence, possibly due to inherent genetic resistance (Cordell et al., 1989).

The use of open-top chambers has proven to be effective in isolating and studying genetic and environmental factors thereby providing valuable insights into how these factors may influence disease susceptibility in loblolly pine seedlings. Considering the economic importance of loblolly pines to the southern forestry industry, future research should continue to explore these dynamics to inform breeding and management strategies aimed at enhancing disease resistance in pine plantations. This study seeks to employ open-top chambers with different treatments to assess the susceptibility of seedlings of different loblolly pine families to *L. acicola.*

4.2 Materials and Methods

4.2.1 Study site and Open-top chambers

The study was conducted at the Atmospheric Deposition Site (approximately 0.02 km^2 in area), located approximately 5 km north of Auburn University Campus. The open-top chambers (OTC) were used as a relatively more controlled environment to replicate the experiment. The OTCs were 4.8 m high, 4.5 m in diameter with aluminum framed structures and chamber plastics attached to each OTC permit adequate airflow (Gilliland et al., 2012; Heagle et al., 1989). Before the study, the vegetation growing in each OTC was killed with a 3% solution of glyphosate. Once dead, the vegetation was cleared, and the ground was covered with landscape fabric to prevent further unwanted vegetation growth within the chambers. Eight chambers were used with inoculation treatments which were either bare ground (negative control), inoculation with infected needles, or inoculation with healthy needles (positive control).

4.2.2 Seedlings

Bareroot seedlings of seventeen commercially grown loblolly pine families were obtained from Aborgen, Westervelt, and the International Forest Company (IFCO) for this study (Table 3.1). In January 2024, 2,550 seedlings (150 per family) were planted in 2.4-liter pots (1 trade gallon) with ProMix BX® peat-based potting mix (Premier Tech, Quebec, Canada). Seedlings were kept in a shade-house and watered weekly for 8 weeks to enable them to acclimate to the environment until they were deployed into the chambers in March 2024. The pine families used for the study are shown in Chapter 3 (Table 3.1).

4.2.3 Inoculation

Eight chambers, and three treatment levels for the chambers: Infected, Positive control and Negative control treatments were used for this experiment. Four chambers were assigned for the infected treatment, and two chambers each for the two control treatments. The inoculum for the infected chambers was obtained by harvesting infected pine needles from diseased trees in Osko Forest. The trees were selected from unburned stands which had trees showing visible crown disease symptoms (> 2/3 disease rating). These trees were felled with a chain saw and the needles were manually ripped off and placed into sterile bags and labelled.

The inoculum for positive control (sterilized needles) treatment was obtained from a controlled-burned stand with relatively healthy/uninfected trees showing no disease symptoms. The trees were felled, and the needles were ripped off manually and placed into separate sterile bags and labelled. The bags were transported to the Forest Health Dynamics Lab, where the needles were sterilized under oven dry heat at 160 ºC for 2 hours, and then allowed to cool under a laminar flow chamber after which it was transported to the OTCs and spread cover the floor of the chambers. The two negative control (no needles) chambers did not have any inoculum at all. Seedlings were set on the bare ground in the chambers. In each chamber, 7 seedlings per family were randomly deployed for a total of 119 seedlings per chamber (Figure 4.1). The total number of seedlings used in the OTCs was 952. Optimum water content was maintained throughout the exposure period by watering them weekly and then increasing the watering regime to twice weekly during the summer period.

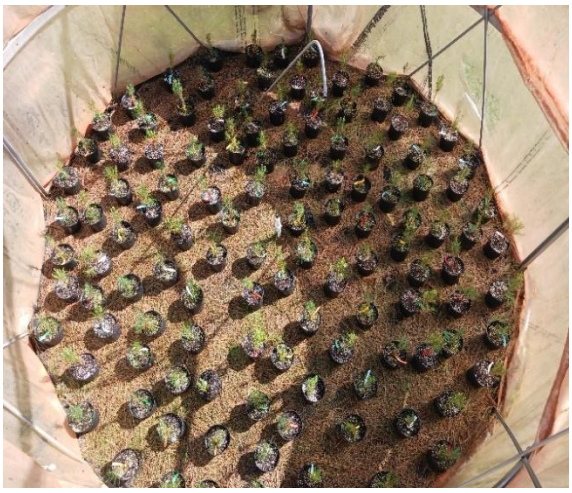

Figure 4.1 Seedlings deployed in Open-top chambers

4.2.3 Measurements

Root collar diameter (RCD) and height measurements were taken monthly and recorded for all seedlings throughout the study period using a digital caliper and a meter rule. Seedling RCD and height trajectories across families and treatments was used to distinguish lines that tolerate infection maintain near-normal growth from those that simply show low disease and normal growth (Eckhardt et al., 2016; Walkinshaw and Barnett, 1998).

Relative water content was assessed on two randomly selected seedlings per family per chamber. The fascicles were initially weighed to the nearest 0.01g (W_W) and then soaked in distilled water overnight, reweighed in the morning to obtain turgid weights (W_T), dried at 70 ºC to equilibrium, and reweighed (W_D). Fascicle relative water content (RWC_F, %) will be determined by the equation:

$$RWC_F = [(W_W - W_D) / (W_T - W_D)] * 100.$$

Disease rating was assessed based on observation of symptoms such as chlorosis, mortality (necrosis or death of needles), infection (tiny black fruiting bodies of the fungus in dead spots or bands), and needle discoloration (presence of brown, tan, or gray lesions on the needles). These symptoms were matched on a five-point scale 0 to 4 i.e.: 0 - No visible symptom, fully healthy needles; 1 - slight infection, very few needles (< 10% chlorotic or bearing small lesions, no chlorosis); 2 - moderate infection, noticeable chlorotic and discrete brown or tan lesions (10-25% of foliage affected); 3 - severe infection, widespread needle discoloration and necrosis (affecting 25-50% of foliage); 4 - Very severe infection (>50% of needles severely necrotic or dead).

4.2.4 Statistical analysis

The main effects of inoculation treatments on the height and disease rating of the seedlings were analyzed by one-way analysis of variance (Pro GLM, SAS Inc., Cary, NC, USA). Prior to analysis, each dependent variable was checked using Levene statistic test to check for the assumption of equal variances before ANOVA was performed. Differences in disease symptoms of seedlings between chamber treatments were examined. Post Hoc test using Tukey's adjustment for differences in least square means and Bonferroni's correction test for multiple comparisons was used to control Type 1 error due to multiple testing. Differences between means were considered significant at p-values <0.05.

4.3 Results

To evaluate the influence of the different chamber treatments on seedling performance, disease rating, height and root collar diameter measurements were assessed. Kruskal-Wallis tests followed by Dunn's pairwise comparisons were used to assess the treatment effects, and family means were ranked within each chamber to examine family-specific responses.

4.3.1 Chamber treatment effects on disease rating of seedlings

Significant differences in disease severity were detected among the chamber treatments ($\chi^2 = 32.54$, $p < 0.001$). Seedlings in the infected chambers displayed the highest mean disease ratings, significantly greater than those in both positive control ($Z = 5.67$, $p < 0.001$) and negative control ($Z = 3.36$, $p = 0.002$) chambers. The contrast between the two control treatments was marginal ($Z = 2.23$, $p = 0.078$), which suggests minimal background disease pressure in the absence of infected inoculum (Figure 4.2).

Within the infected chambers, the lowest disease rating was observed in families F13 (Mean = 0.197), followed closely by F14 (0.218) and F17 (0.225), suggesting moderate resistance. Conversely, family F3 had the highest disease severity (0.380), indicating high susceptibility under inoculum pressure. Among control chambers, family F13 again showed the lowest disease in the negative control (0.0579) and maintained low values in the positive control chamber (0.0672), reflecting consistent performance across treatments.

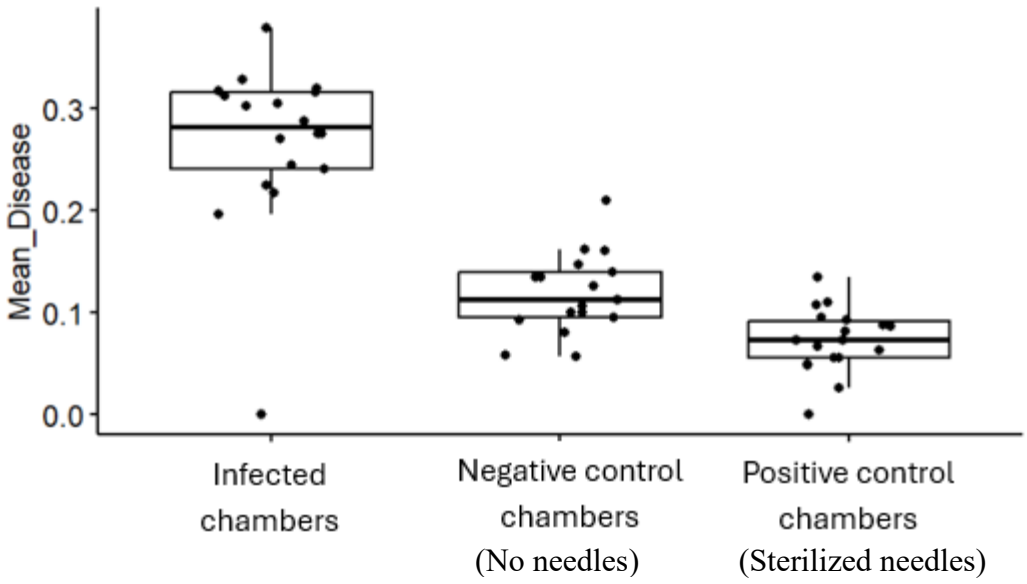

Figure 4.2 Comparison of mean disease rating across the various chamber treatments

4.3.2 Seedling height response across treatment chambers

Although mean seedling height varied among the various treatments (Figure 4.3), the Kruskal-Wallis test was not statistically significant ($\chi^2 = 5.08$, $p = 0.079$). A weak trend suggested slightly lower height in the infected group compared to the negative control (Dunn, $p = 0.076$), but no difference was found between the positive and the negative control groups. Within each chamber, families F4 (62.2 cm), F8 (62.0 cm), and F2 (60.7 cm) ranked highest in height under infected needle conditions, suggesting robust growth in height despite pathogen presence. In the negative control, family F8 (58.4 cm) and F2 (57.2 cm) again ranked high, supporting their consistent growth performance. In the positive control chambers, the top four families by height were F18 (64.2 cm), F3 (60.3 cm), and F4, F6 (57.6 cm), highlighting variability in growth performance depending on exposure environment.

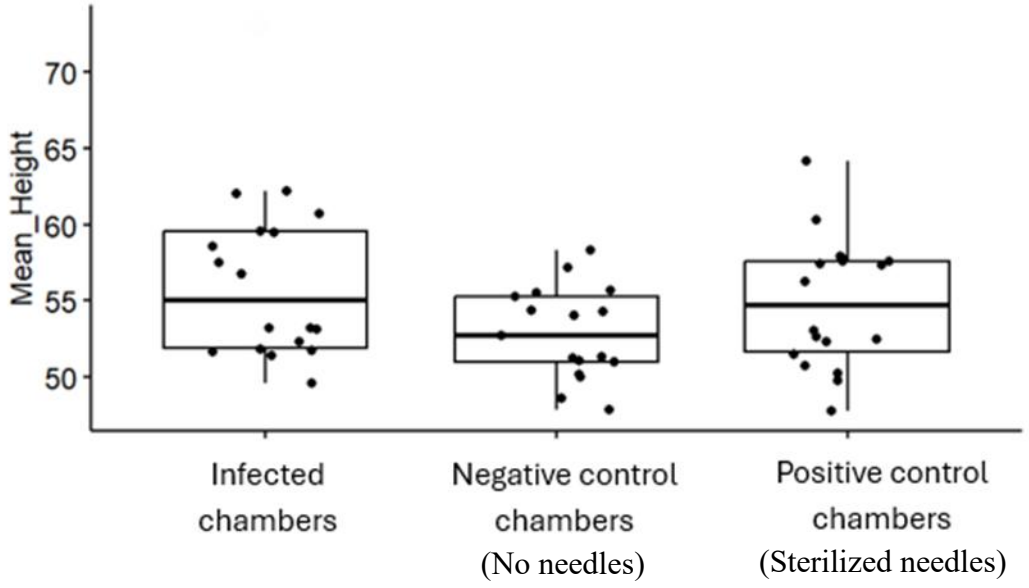

Figure 4.3 Comparison of mean height across treatment chambers

4.3.3 Root collar diameter (RCD) variation across treatment chambers

Root collar diameter did not vary significantly across chambers ($\chi^2 = 0.998$, $p = 0.61$), and all pairwise comparisons were non-significant ($p > 0.36$). However, within chambers, distinct patterns emerged (Figure 4.4). Under the infected chambers, families F4 (9.46 mm), F5 (9.24 mm), and F8 (8.97 mm) showed the highest average RCD values, indicating potentially strong structural development despite foliar stress. In the negative control chambers, families F8 (8.61 mm), F5 (8.48 mm), and F2 (8.21 mm) ranked highest in RCD, paralleling their height performance. Notably, family F2 performed consistently well across all chambers, maintaining a high height and RCD while demonstrating moderate disease resistance. In contrast, family F3, which had the weakest disease performance under the infected chambers (0.380), also ranked low in growth metrics, suggesting an increased susceptibility. Family F13 demonstrated low disease across all chambers and moderate to low growth, suggesting stable resistance with conservative growth strategy.

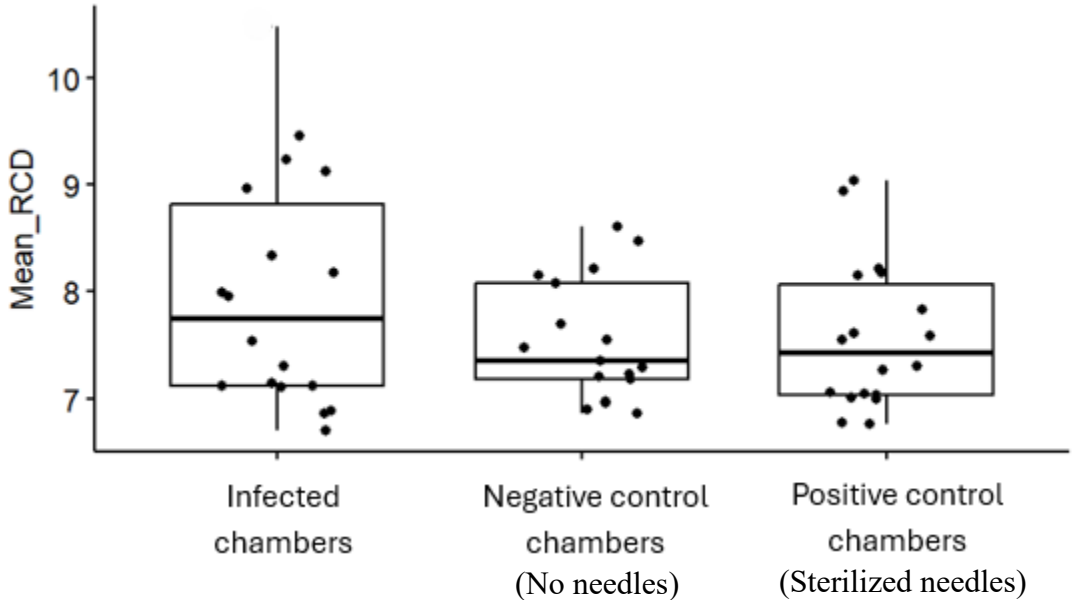

Figure 4.4 Comparison of mean root collar diameter across treatment chambers

4.3.4 Comparison of family performance across infected chambers based on disease severity, height, and RCD

The comparative summary of seedling performance under the infected chamber treatment, ranked according to mean disease severity, height, and root collar diameter (RCD) showed that families F13, F14, and F17 exhibited the lowest mean disease severity, suggesting higher tolerance to *Lecanosticta acicola*. Among them, F13 had the best disease ranking (1st), although it ranked low in height (15th) and moderately in RCD. Conversely, F4, F2, and F3 showed superior growth traits; F4 ranked 1st in height and had the highest mean RCD (9.46) but was ranked 5th in disease resistance. F3 had the poorest disease ranking (17th) despite favorable height and RCD. This highlights a trade-off between disease resistance and growth traits in some families, with few families, such as F2 and F4, demonstrating a desirable balance of moderate disease resistance and superior growth performance (Table 4.1).

Table 4.1 Summary of family rankings across infected chambers based on disease severity, height, and RCD

Family	Mean Disease	Disease Rank	Mean Height (cm)	Height Rank	Mean RCD (mm)
F13	0.197	1	51.7	15	7.12
F14	0.218	2	53.2	10	7.11
F17	0.225	3	51.8	13	7.14
F2	0.241	4	60.7	3	8.18
F4	0.245	5	62.2	1	9.46
F5	0.271	6	59.5	5	9.24
F7	0.275	7	51.7	14	9.13
F12	0.276	8	53.1	11	6.89
F10	0.288	9	52.3	12	7.12
F1	0.303	10	56.8	8	7.54
F16	0.305	11	51.4	16	7.31
F6	0.313	12	57.5	7	7.96
F11	0.317	13	53.2	9	6.86
F9	0.317	14	58.5	6	7.99
F15	0.32	15	49.5	17	6.7
F8	0.329	16	62	2	8.97
F3	0.38	17	59.5	4	8.34

4.3.5 Comparison of family performance across negative control chambers based on disease severity, height, and RCD

The comparative performance of seedlings in the negative control chambers with rankings based on mean disease severity, height, and root collar diameter (RCD), revealed that families F13 and F9 exhibited the lowest disease severity (both ranked 1st and 2nd, respectively), suggesting a strong baseline resistance to disease even in the absence of pathogen pressure. Family, F8 attained the greatest mean height (58.4 cm) and highest RCD (8.61 mm), though it ranked 10th in disease resistance. Families such as F2 and F5 combined relatively strong disease performance (ranked 7th and 5th) with robust growth traits, placing them among the most balanced performers. In contrast, F10 and F17 were among the lowest in height and

RCD, with F17 maintaining a high disease resistance rank. Overall, the table reveals variation in baseline growth and health traits among families, useful for identifying genotypes with both inherent vigor and disease resilience under non-inoculated conditions (Table 4.2).

Table 4.2 Summary family rankings across negative control chambers based on disease severity, height, and RCD

Family	Mean Disease	Disease Rank	Mean Height (cm)	Height Rank	Mean RCD (mm)
F13	0.0579	1	51.2	11	7.21
F9	0.0579	2	52.7	9	7.47
F17	0.0813	3	48.6	16	6.9
F4	0.0932	4	55.3	5	8.15
F5	0.0952	5	55.7	3	8.48
F12	0.1	6	50.1	14	6.97
F2	0.101	7	57.2	2	8.21
F7	0.107	8	51	12	6.96
F14	0.113	9	50.9	13	7.29
F8	0.126	10	58.4	1	8.61
F1	0.134	11	55.5	4	7.7
F3	0.134	12	54.3	6	8.08
F10	0.14	13	47.9	17	6.86
F15	0.147	14	54	8	7.36
F11	0.161	15	51.3	10	7.23
F16	0.162	16	50	15	7.54
F6	0.21	17	54.3	7	7.18

4.3.6 Comparison of family performance across positive control chambers based on disease severity, height, and RCD

The comparison of seedling performance across the positive control chambers showed that Family F16 had the lowest disease severity (ranked 1st), though it ranked low in height (16th), suggesting strong disease resistance but limited growth. Similarly, families F14 and F15 ranked highly in disease resistance but were also among the shortest. In contrast, family F3 ranked last in disease resistance but achieved the highest mean height (60.3 cm) and largest

RCD (9.04 mm), indicating a potential trade-off between growth and disease tolerance. Several families such as F2, F4, and F8 demonstrated a favorable balance, combining moderate to high disease resistance with strong growth performance. This variation highlights key genetic differences in growth and health traits under non-infected, but controlled, environmental exposure (Table 4.3).

Table 4.3 Summary of family rankings across the positive control chambers based on disease severity, height, and RCD

Family	Mean Disease	Disease Rank	Mean Height(cm)	Height Rank	Mean RCD (mm)
F16	0.0259	1	49.7	16	7.03
F14	0.048	2	50.7	14	6.77
F2	0.05	3	56.3	8	7.55
F15	0.056	4	50.2	15	7
F17	0.056	5	47.7	17	6.76
F10	0.064	6	52.4	11	7.31
F13	0.0672	7	52.6	10	7.61
F7	0.0738	8	51.5	13	7.06
F8	0.0738	9	57.9	2	8.21
F4	0.0813	10	57.6	5	8.18
F6	0.0873	11	57.6	4	7.58
F9	0.088	12	57.3	7	7.84
F1	0.0932	13	57.7	3	7.27
F5	0.0957	14	57.4	6	8.15
F11	0.108	15	53.1	9	7.01
F12	0.11	16	52.3	12	7.04
F3	0.134	17	60.3	1	9.04

4.3.7 Variation in relative water content across chambers

Two-way ANOVA test was conducted to determine the effects of chamber treatments and seedling families on the relative water content. Chamber treatments and family variation did

not have any significant effect on the change in the relative water content of the seedlings across all families ($p = 0.315$; $p = 0.975$ respectively) (Table 4.4).

Table 4.4 Two-way ANOVA relationship between treatments and family effects on RWC change

Source	Sum of squares	df	F-statistic	p-value
Treatment	1494.16	2	1.17	0.315
Family	4226.22	16	0.41	0.975
Residual	52861.18	83		

Df: Degree of freedom

4.4 Discussion

The susceptibility of loblolly pine seedlings to *Lecanosticta acicola* is strongly modulated by ambient environmental stressors. Open top chamber experiments have long been used in studies such as in examining how atmospheric pollutants influence pine physiology and disease susceptibility. By employing open-top chambers to maintain uniform environmental conditions, we minimized external variability and sharpened family level effects (Olszyk, Tingey, & McMichael, 1980). Unlike many prior surveys that focused on testing the susceptibilities of multiple species (Aldrich & McCarty, 2019; Davis & Thompson, 2018), this experiment uniquely targets only loblolly pine families under open-top chambers (with three different treatments). Our findings pointed out that regardless of the treatment used, seedling height increased by approximately 2.00 cm, month by month. This could be explained by the fact that the seedlings were watered consistently throughout the period and increasing the watering regime during the summer when the environment was predominantly dry. Also, relative water content change across the different treatment chambers did not vary significantly ($p = 0.315$) suggesting that the seedlings were well hydrated during the exposure period.

Families with reduced symptom expression may harbor structural or physiological defenses such as thicker cuticular layers or elevated phenolic compound production that merit targeted biochemical and anatomical analyses (Barnes et al., 2019). Our findings suggest that selecting seedlings from these three families (F13, F14, F8) could promise an approximately 40-50% reduction in disease severity compared to the bottom three low performing families (F3, F8, F15). Moreover, our findings show a significant genotype and environmental interaction: the expression of resistance traits depended on both genetic background and microclimatic factors within the chambers (Zhang et al., 1994). In conclusion, exploring these dynamics is critical for predicting loblolly pine resilience to future BSNB outbreaks and for guiding selection in breeding programs aimed at enhancing durable resistance. Also, seedlings from less tolerant families can be incorporated into early detection-based studies and operations in the future. Susceptible families develop visible symptoms more rapidly and at lower inoculum levels than tolerant genotypes. By deploying these families in sentinel plots or alongside spore-trap networks, managers can detect initial pathogen incursions or emerging more aggressive strains sooner than would be possible using only tolerant stock.

Chapter Five

Detection of *Lecanosticta acicola* Spore Load Using Spore Traps

Abstract

Brown spot needle blight (BSNB) is a significant foliar disease affecting pine species, with *Lecanosticta acicola* recognized as the primary causal agent. The disease is historically found throughout the southeastern U.S. from Virginia through Alabama, Florida and west to Louisiana where warm, humid summers sustain multiple infection cycles. Knowledge of the epidemiology and climatic variables that affect its spread will be essential to understand and improve management of the disease. Monitoring *L. acicola* spore dispersal using spore traps has revealed that rainfall, temperature, and relative humidity (RH) independently drive inoculum pressure throughout the sporulation season (March to November). This study used 20 spore traps deployed on 5 BSNB-infected study plots from March to November, to assess the spore load in the plots and how climatic variable affect the spread of the spores. Our mixed-effects models showed that each 10 mm of monthly rainfall increases mean spore counts by ~17%, a 5 °C rise in temperature boosts count by ~19%, and a 5% relative humidity increment nearly doubles spore counts (101%). Poisson incidence-rate ratios (IRR= 1.02-1.26) confirm these effects after accounting for modest between plot heterogeneity (variance = 0.016, SD = 0.13). The peak for spore abundance occurred in July and then it fell in the subsequent months, with November having the lowest spore count. Our results will be useful for managers and landowners to find the best strategies for controlling the disease.

Keywords: brown spot needle blight, foliar pathogen, spore trap

5.1 Introduction

Brown spot needle blight (BSNB), caused by *Lecanosticta acicola* (Thüm.) Syd. & P. Syd., has emerged as a serious constraint on pine health and productivity across North America, Europe and parts of Asia and South America. The pathogen now threatens more than 50 *Pinus* species, causing growth loss, premature needle cast, and under epidemic pressure, plantation failure (van der Nest et al., 2019). Recent interceptions in previously unaffected regions and its listing on multiple quarantine schedules underscore the need for robust surveillance strategies. Disease development hinges on the production and aerial dissemination of conidia from acervuli on infected needles. Conidial release is strongly modulated by moisture and temperature: peaks occur during warm, wet periods, with rainfall events acting as the primary trigger for mass discharge and subsequent wind or splash-borne spread (Wyka et al., 2018c).

In the Atlantic coastal pine stands of northern Spain, daily spore loads recorded with volumetric samplers surged from early autumn, and generalized additive models identified maximum temperature and cumulative precipitation as the best predictors of airborne inoculum (Mesanza et al., 2021b). Because foliar symptoms can remain latent for months, measuring the flux of spores in the forest atmosphere is pivotal for early warning and for parameterizing epidemiological models. Spore traps, which draw a constant air flow across an adhesive surface or tape, remain the essential tool of forest aerobiology; recent innovations include automated image recognition, on-trap DNA extraction, and networked samplers that stream near-real-time data to decision dashboards (West & Kimber, 2015). These advances shorten the feedback loop

between inoculum detection and management action, enabling fungicide timing, targeted silvicultural interventions and quarantine enforcement.

Additionally, combining spore trapping data with spatiotemporal modeling methodologies enhances our understanding of temporal spore release patterns and environmental conditions that favor pathogen establishment, thus informing strategies to mitigate detrimental effects on forest health and biodiversity (Wyka et al., 2018c). Such an integrated approach also fosters deeper knowledge of the pathogen's life cycle, especially its adaptive responses to environmental fluctuations, supporting the development of targeted interventions aimed at increasing forest resilience against invasive pathogens. Moreover, utilizing multi-dimensional data analysis and predictive modeling frameworks can uncover intricate host-pathogen dynamics, identifying critical thresholds and feedback mechanisms that influence host susceptibility. This knowledge is pivotal for developing evidence-based conservation strategies and promoting ecosystem stability amidst biotic invasions (van der Nest et al., 2019).

Furthermore, the application of advanced statistical techniques and machine learning algorithms in analyzing spatiotemporal infection patterns enhances predictive accuracy, enabling timely anticipation of outbreaks and initiative-taking management actions. These methodological advancements not only provide nuanced insights into epidemiological trends associated with *L. acicola* but also empower forest managers and researchers to make informed decisions regarding resource allocation and ecological restoration practices, safeguarding biodiversity, and forest health (West & Kimber, 2015; Mesanza et al., 2021b).

This study therefore focuses on quantifying *L. acicola* spore load using spore traps deployed across representative pine stands and determining how climatic factors affect spore load and distribution. The resulting framework will contribute to initiative-taking surveillance networks capable of mitigating the expanding footprint of *L. acicola* in commercial and natural pine ecosystems.

5.2 Materials and Methods

5.2.1 Spore Trap Construction

Twenty spore traps were deployed in March 2024. Each trap was positioned at the center of every subplot. The spore traps were about 1.8m tall and pegged into the ground inclined at an angle of 45º. The free end of the rod is bent downwards, and hole was drilled through it, where a rope was looped through it to enable a motor to be suspended from it. The motors were about 25 inches in length with a 1.3mm gauge to which two plastic slides per trap were fastened. A plastic disposable cup was looped through the rope to cover the motor and to shield it from excess rain (Figure 5.1). Microscope slides (plastic) were coated with petroleum jelly (Vaseline®) and labelled with specific numbers for easy identification and matching with plots. A battery-powered rotating motor was tied with a rope to hang on the metal rods of the trap.

Figure 5.1 Picture of spore trap deployed in the field

5.2.2 Spore trap deployment

The experiment was set up in Cullman county (Osko Forest) (Chapter 2, Table 2.1). Cullman county is in North-Central Alabama. Its average temperature in summer often reaches the upper 80s °F (about 31-32 °C), and winters commonly drop into the lower 30s °F (around 0-2 °C). Annual rainfall typically ranges from about 50 to 55 inches (1270-1400 mm). Rainfall is relatively well-distributed throughout the year, though slightly heavier in late winter and spring months. Five research plots were set up with each plot having four subplots based on Dunn (1999), comprised of one central plot and three sub-plots identical to it. The subplots were located 120 feet from the central plot and at bearings of 120º, 240º, and 360º. Each plot covers an area of approximately 2.3 acres (Chapter 2, Figure 2.1). This privately owned forest consisted of mostly loblolly pines and a few hard woods. This site has moderate presence of brown spot needle blight with around 20-30% of trees showing symptoms of the disease. The

slides in the spore traps were replaced weekly and stored in a sterile slide box and transported to the Forest Health Dynamics Laboratory for analysis. The rechargeable batteries in the motors were also replaced weekly to ensure continuous rotation of the motors for effective spore trapping. The sampling period was from March to November 2024.

5.2.3 Spore slide examination

Spore slides were examined under a compound microscope at 100× magnification. Lactophenol cotton blue dye was used to enhance the contrast. To obtain a more accurate spore count, a grid slide was placed beneath the slide under the microscope. Conidia were identified based on their morphological description as previously described by Jankovský et al., 2009. Other fungi recovered were identified using a manual by Barnett and Hunter (1998).

5.2.4 Weather data

Weather data available online (http://www.weatherspark.com) obtained from the nearest weather stations to the study sites were used to determine the monthly averages for temperature, relative humidity and rainfall (Chapter 2, Table 2.2). To determine the effects of the weather factors on spore loads, the data was incorporated into the model and analyzed (Boateng and Lewis, 2015).

5.2.5 Statistical analysis

The data collected from all twenty traps during the study period was used for statistical analysis using JMP Pro11.2.1. Spore counts from the two slides of each trap were averaged. Mean counts for every bi-weekly period were calculated on all plots. To determine the overall spore released, spore counts were averaged per month and per plot and transformed to fit the assumptions of Analysis of variance (ANOVA) (Boateng and Lewis, 2015). Also, two complementary models (i.e. Poisson regression Generalized Linear Model and Linear Mixed-

effects Model) were used to quantify the independent effects of rainfall (mm), temperature (ºC) and relative humidity on *L. acicola* spore counts.

5.3 Results

5.3.1 Patterns of spore dispersal

The spore-trap system effectively captured *Lecanosticta acicola* conidia across all five plots, and throughout the sampling period. Spores were first recovered during the third week of March (16-29 March) (Table 5.1), confirming that dispersal had begun soon after the traps were deployed. Counts rose steadily and reached their peak within the period of 7 to 28 July, with plot 11 having an average of 23.9 spores, plots 10 and 14 recorded the lowest overall means 13.0 and 8.7 spores respectively (Table 5.2). After July, spore numbers declined toward the close of the sampling season. Statistical analysis showed no significant variation in monthly spore totals among the plots ($p = 0.672$). Spores recovered from plots 12 and 13 were 198 and 180 respectively with a mean by month count of 22 and 20 respectively (Table 5.2). The number of spores released fell sharply after July, and the subsequent months had low counts with the least being in November (spore count = 5) (Figure 5.2). Negative binomial GLM test showed that there was no significant variation in monthly spore totals among the plots ($p = 0.672$) (Table 5.3).

Table 5.1 Summary table showing total monthly spore count by plot

Month	Total spores	Mean per plot
March	112	22.4
April	147	29.4
May	159	31.8
June	47	9.4
July	260	52.0
August	23	4.6
September	19	3.8
October	16	3.2
November	5	1.0

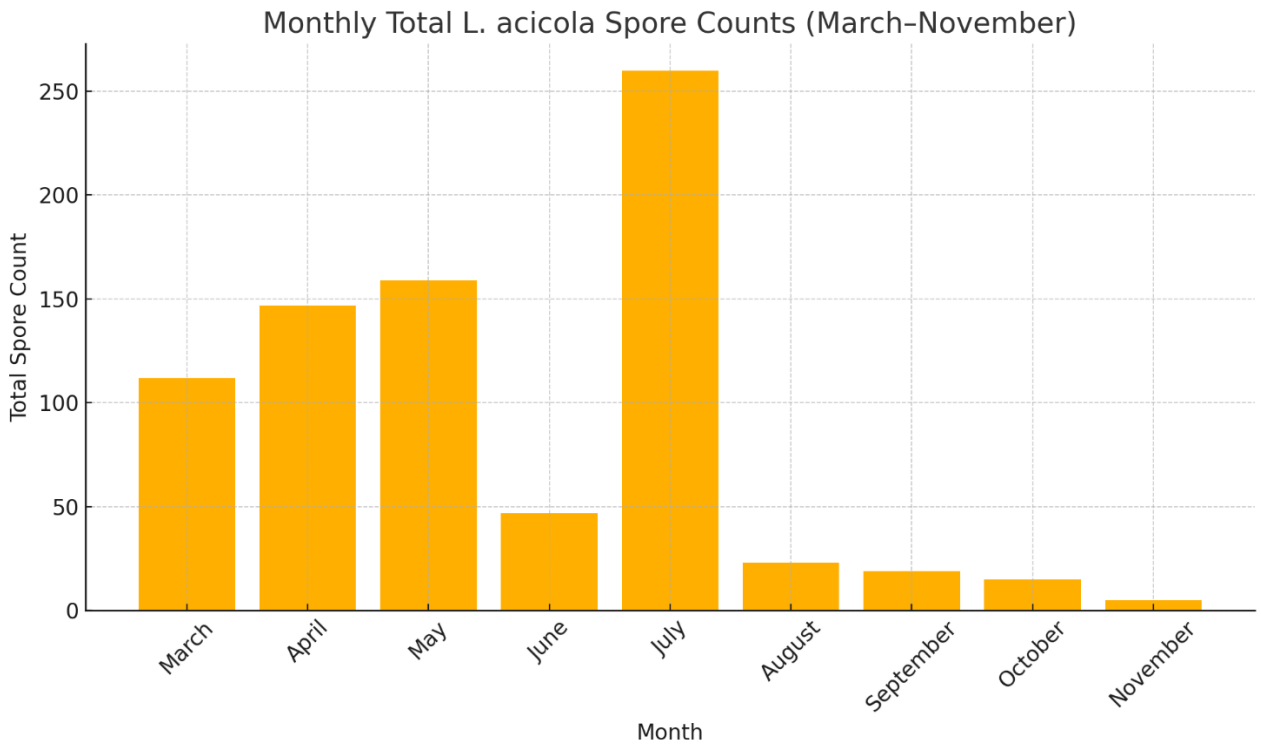

Figure 5.2 Monthly distribution of *L. acicola* spores across the various plots

Table 5.2 Summary table showing cumulative spore count by plot from March to November

Plot	Total count	Mean per month	Rank
BS 11	215	23.90	1
BS 12	198	22.00	2
BS 13	180	20.00	3
BS 14	117	13.00	4
BS 10	78	8.70	5

Table 5.3 Statistical test result for across plot variation in spore count

Test	Statistic	Df*	p-value
Negative-binomial GLM	Likelihood ratio = 2.35	4	0.672
Kruskal-Wallis (non-parametric test)	H = 1.92	4	0.750

*Df: Degrees of freedom

5.3.2 Effects of climatic variables on spore dispersal

The Cullman county weather data (Chapter 2, Table 2.2) from March to November was used to determine the effects of climatic variables on spore abundance and release. There was a positive association found between cumulative rainfall and spore count in the month of July (IRR =1.017, $p = 0.001$) (Table 5.4). The data further showed a significant relationship ($p < 0.001$) between the expected spore count, temperature and relative humidity. For every 1ºC rise in temperature and every 1% increase in relative humidity, there was a corresponding 3.7% and 5.2% increase in the spore count respectively.

Table 5.4 Summary table for Poisson regression model of climatic variables with spore count

Predictor	Incident-rate ratio†	95% CI*	p-value
Rainfall (mm)	1.017	1.008 – 1.027	0.001
Temperature (ºC)	1.037	1.019 – 1.056	< 0.001
Relative humidity (%)	1.225	1.103 – 1.427	< 0.001
Intercept	0.000		

†IRR: Incident-rate ratio = exp(β), values > 1 implies positive association, *CI: Confidence interval.

The linear mixed effect model showed a modest but non-negligible random-effect by plot variation (variance = 0.016, SD = 0.13), indicating that the little difference in baseline disease pressure was not enough to dominate the overall variability of the experiment (Table 5.5).

Table 5.5 Descriptive statistics for linear mixed-effect model of climatic variable with spore count

Predictor	β (log-scale)*	Std. Error**	Z value	P value
Rainfall (mm)	0.016	0.007	2.32	0.021
Temperature (ºC)	0.035	0.012	2.88	0.004
Humidity (%)	0.183	0.064	2.87	0.004
Intercept	-14.85	4.47	-3.33	0.001

*β(log-scale): β- coefficient represents the estimated change in the dependent variable for a unit change in the predictor variable, Std Error: Standard Error.

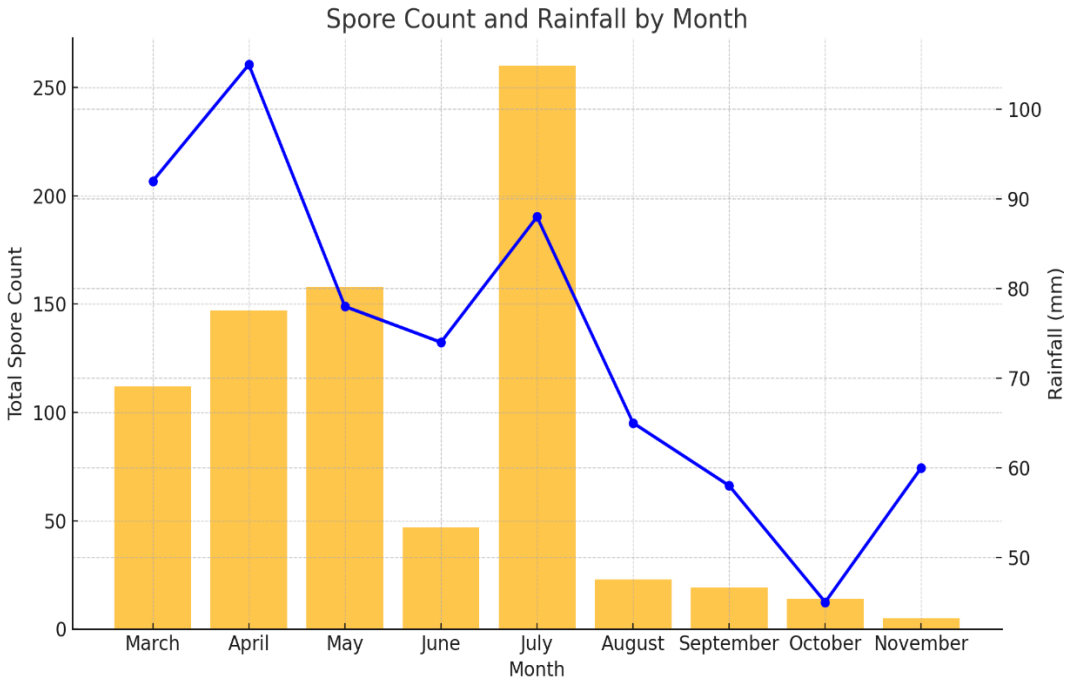

Figure 5.3 Relationship between Spore count vs Rainfall

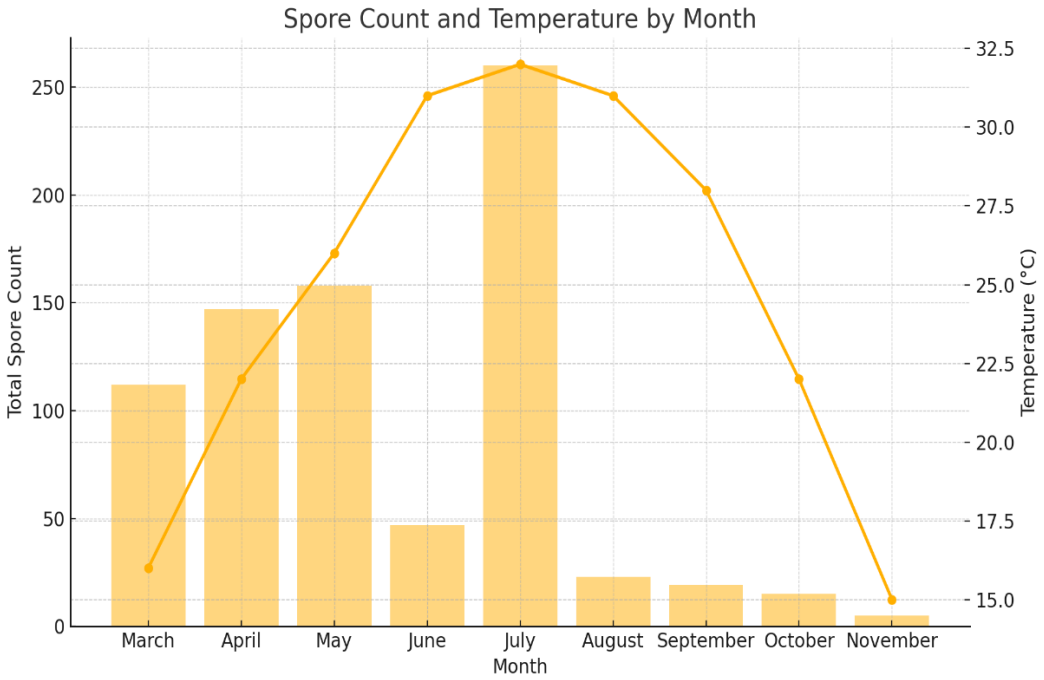

Figure 5.4 Relationship between Spore count vs Temperature

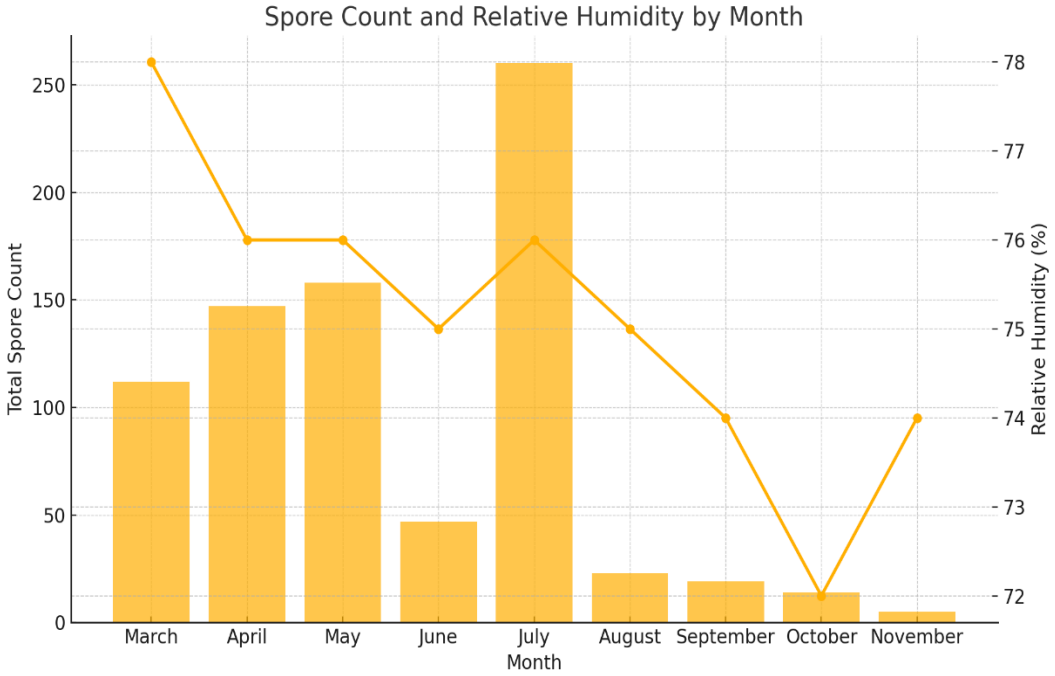

Figure 5.5 Relationship between Spore count vs Relative humidity

5.4 Discussion

Spore trap monitoring has become indispensable for mapping *Lecanosticta acicola* dispersal and forecasting BSNB epidemics. Long-term surveys in Spain's Basque Country, for example, deployed 16 traps over three years, revealing how trap location and sampling duration shape our view of regional spore dynamics (Martínez et al., 2020). Yet passive impact traps have sometimes failed to capture the pathogen's airborne sexual spores, suggesting that conidial splash dispersal and environmental wash-out can limit trap efficiency (González & Pérez, 2018).

Our analyses demonstrate that the key climatic factors of rainfall, temperature, and relative humidity (RH) are each robust, independent drivers of *L. acicola* spore release (Figures

5.3, 5.4, 5.5). In the mixed effects framework, every 10 mm increment in monthly precipitation elevated the geometric mean spore count by 17%, suggesting that rain splash and needle wetness directly facilitate conidial release and dispersal (Sinclair & Lyon, 2005). Likewise, a moderate 5 °C rise in mean air temperature boosted spore abundance by approximately19 %, consistent with laboratory data showing optimal conidial germination at 20-30 °C (Barnes et al., 2019). The most dramatic effect arose from relative humidity where a mere 5% increase doubled spore numbers (101%), underscoring the pathogen's reliance on sustained humid conditions to form and eject acervuli (Wyka et al., 2018c). Poisson regression corroborated these patterns with incidence rate ratios (IRR = 1.02-1.26 per unit), confirming that each variable exerts an additive influence on inoculum pressure over the March to November trapping season. The concordance between mixed-effects estimates and IRRs highlights the stability of these relationships even after accounting for plot-level heterogeneity (variance = 0.016, SD = 0.13).

Conidial release in *L. acicola* is facilitated by a mucilaginous matrix; raindrop impact physically ejects spores and creates splash dispersal, so rainfall events are routinely highlighted as the main "switch" for epidemics (Mesanza et al., 2021b). The positive rainfall coefficient here aligns with classic slide-trap studies in the U.S. Lake States, where Skilling & Nicholls (1974) recorded the bulk of conidial showers during wet periods between May and September (Wyka et al., 2018b). Notably, our March rainfall (91 mm) coincided with only moderate counts, while July peaks occurred under less humid but wet conditions (94 mm). This supports field observations that very heavy, persistent rain can wash spores from the air column faster than they are liberated, producing a non-linear response once a saturation threshold is crossed.

Daily maximum temperature emerged as the second-strongest predictor. A recent risk model for Atlantic-coast plantations likewise found higher *L. acicola* spore counts under warmer days, with significant effects above 25 °C (García-García et al., 2025). While laboratory work on central-European isolates places the sporulation optimum at 15-20 °C and > 90% relative humidity (Dvořák et al. 2012), southeastern U.S. field data, including our 31-32 °C July maximum (Figure 5.4) suggests that southern genotypes or local microclimates extend that thermal window. This regional plasticity is important for forecasting disease under climate-warming scenarios.

The results show relative humidity as an amplifying but not merely a permissive factor. Relative humidity above roughly 75% is generally cited as the threshold for conidial development and germination (Agrios, 2005). Our models indicate that once that threshold is met, incremental rises in RH sharply elevate airborne inoculum (IRR ≈ 1.26 per 1% RH). The biology is two-fold: (i) high RH keeps acervular mucilage hydrated, facilitating discharge, and (ii) wet needles prolong germ tube viability, increasing the odds of infection between successive showers. Field guides on needle blights similarly warn that outbreaks can initiate any time there is a coincidence of high RH and spores, even outside the classic spring window. As spore traps evolve from passive collectors to components of integrated surveillance networks, their strategic deployment alongside environmental data will sharpen early-warning systems and improve BSNB management.

5.5 Conclusion

In conclusion, spore traps remain an indispensable tool for understanding the dispersal dynamics of *L. acicola*. The choice of trap type, placement, and environmental considerations critically influence the quality and reliability of spore detection data. While active traps like rotating-arm samplers have demonstrated high efficacy, passive traps may require optimization to improve their effectiveness. Integrating spore trapping with molecular detection techniques and environmental data can significantly advance disease prediction and management strategies. Future research should focus on refining trap designs and deployment strategies to maximize detection sensitivity and accuracy in diverse ecological contexts.

Chapter Six

Conclusion and Recommendations

6.1 Conclusion

Brown spot needle blight is no longer a minor seedling disease of longleaf pine but an emerging threat to mature loblolly plantations across the southeast. Combining genetics, climate-smart silviculture, targeted fungicides, and real-time spore monitoring can shift management from reactive salvage to proactive suppression. Strategic research, especially into host resistance mechanisms and microbiome-based biocontrol, will provide the next generation of low-input solutions that keep loblolly pine a cornerstone of the southern forestry economy.

6.2 Recommendations

Establishing a coordinated, international research agenda is essential for unraveling how geography, host ecology and local climate shape pathogen diversity, spore movement and infection dynamics. Such programs should couple harmonized surveillance (standardized spore-trapping networks and rapid diagnostic protocols) with advanced epidemiological modelling to forecast shifts in disease spread under future climate scenarios. Parallel efforts must accelerate the development of resistant pine germplasm: pinpointing genetic markers for resistance and resilience will greatly streamline selective breeding and molecular breeding pipelines.

Deeper insights into host-pathogen interactions including population genetic structure, host preference and virulence determinants will refine early warning systems and guide outbreak response. Long-term management of *L. acicola* demands an integrated strategy that blends early detection, adaptive silviculture and cross-border collaboration. Because climate

change is likely to amplify both incidence and severity, control plans must be explicitly climate-resilient. Emerging technologies such as remote sensing for canopy health, high-throughput molecular diagnostics for pathogen detection can shorten the interval between incursion and intervention. Finally, sustained partnerships among researchers, policymakers, and industry, coupled with targeted training programs for forest managers, are critical to safeguarding global pine resources against this pathogen.

References

Agrios, G. N. (2005). Plant Pathology (5th ed.). Academic Press.

Alexopoulos, C. J., Mims, C. W., & Blackwell, M. (1996). Introductory Mycology (4th ed.). John Wiley & Sons. ISBN: 9780471522294.

Badger, P. C., & Stephenson, C. D. (1989). A Review of Wood Energy in The Southeastern United States. https://doi.org_10.2172_5333442.

Baker, James B.; Langdon, O. Gordon. (1990). *Pinus taeda* L. loblolly pine. In: Burns, Russell M.; Honkala, Barbara H., technical coordinators. Silvics of North America. Volume 1. Conifers. Agric. Handb. 654. Washington, DC: U.S. Department of Agriculture, Forest Service: 497-512.

Barnard, E. L., & Blakeslee, G. M. (1980). Brown spot needle blight, and its impact on southern pines. Forest Pathology, 12(3), 145–152.

Barnes I., Crous P. W., Wingfield B. D., & Wingfield M. J. (2004). Multigene phylogenies reveal that red band needle blight of Pinus is caused by two distinct species of Dothistroma, *D. septosporum* and *D. pini*. Studies in Mycology 50, 551–565.

Barnes, I., Crous, P. W., Wingfield, B. D., & Wingfield, M. J. (2008). *Lecanosticta acicola* sp. nov., the causal agent of brown spot needle blight of pine. Mycologia, 100(6), 925–934.

Barnes, I., Fourie, G., Wingfield, M. J., Harrington, T. C., McNew, D. L., Lombard, L., & Crous, P. W. (2019). *Lecanosticta acicola*: A growing threat to expanding global pine plantations. Molecular Plant Pathology, 20(9), 1327–1364. https://doi.org/10.1111/mpp.12853.

Barnes, I., van der Nest, A., Grove, T., Joubert, L., Paap, T., Wingfield, M. J., & Wingfield, B. D. (2016). Endophytes of pine needles: Out of sight, out of mind? Fungal Ecology, 20, 51–59.

Barnett, H. L., & Hunter, B. B. (1998). Illustrated Genera of Imperfect Fungi (4th ed.). APS Press. ISBN: 9780890541920.

Boateng, K., and Lewis K. J. (2015). Spore dispersal by *Dothistroma septorum* in northwest British Columbia. Phytopathology 105:69-79.

Bradshaw, R. E., Ganley, R. J., Jones, W. T., & Dyer, P. S. (2000). Intraspecific variation in susceptibility to Dothistroma needle blight. New Zealand Journal of Forestry Science, 30(1/2), 187-197.

Brender, Ernst V.; Belanger, Roger P.; Malac, Barry F. (1981). Loblolly pine. In: Choices in silviculture for American forests. Washington, DC: Society of American Foresters: 37-45.

Brown, R., Priest, E., Naglik, R. J., Richardson, P. J. (2021). Fungal Toxins and Host Immune Responses, Frontiers in Microbiology, 2021.

Carey, J. H. (1992). *Pinus taeda* (loblolly pine). In Fire Effects Information System. U.S. Department of Agriculture, Forest Service, Rocky Mountain Research Station.

Cech, T. A., & Klepzig, K. D. (2001). Fern-pine rust *Coleosporium pinetorum*. In R. A. Windham & R. C. McDonald (Eds.), Forest pathology: State of the art (pp. 145–156). APS Press.

Cherubini, P., Battipaglia, G & Innes, J. L. (2021). Tree Vitality and Forest Health: “Can Tree-Ring Stable Isotopes Be Used as Indicators?”. Current Forestry Reports, 2021.

Chieppa, J., Eckhardt, L., & Chappelka, A. (2017). Simulated Summer Rainfall Variability Effects on Loblolly Pine (Pinus taeda) Seedling Physiology and Susceptibility to Root-Infecting Ophiostomatoid Fungi. Forests, 8(4), 104. https://doi.org/10.3390/f8040104.

Cordell, C. E., Filer, T. H., Anderson, R. L., & Maffei, H. M. (1989). Forest nursery pests. USDA Forest Service Agriculture Handbook No. 680.

Crous, P. W., Wingfield, M. J., Burgess, T. I., Hardy, G. E. S., & Crane, C. (2019). Fungal pathogens of trees. Microbiology Spectrum, 7(2), 1–31.

Crous, P. W., Wingfield, M. J., Burgess, T. I., Hardy, G. E., & Frean, S. (2015). Fungal Planet description sheets: 320–370. Persoonia, 34, 167–266. https://doi.org/10.3767/003158515X688433.

Demidko, A. D., Sultson, S., Mikhaylov, P., & Verkhovets, S. (2021). Influence of Weather Conditions and Climate Oscillations on The Pine Looper *Bupalus piniaria* (L.) Outbreaks in The Forest-Steppe of The West Siberian Plain, Forests, 2021.

Deng, S., Li, P., Li, Y., Ran, Z., Peng, Y., Yang, S., He, H., Zhou, K., Yu, J. (2021). "Alleviating Cd Translocation and Accumulation in Soil–rice Systems: Combination of Foliar Spraying of Nano-Si or Nano-Se and Soil Application of Nano-humus", Soil Use and Management, 2021.

Desprez-Loustau, M. L., Robin, C., Reynaud, G., Deque, M., Badeau, V., Piou, D., Husson, C., & Marçais, B. (2007). Simulating the effects of a climate-change scenario on the geographical range and activity of forest-pathogenic fungi. Canadian Journal of Plant Pathology, 29(2), 101–120. https://doi.org/10.1080/07060660709507450.

Devkota, K., Kamvar, Z. N., Cregg, B. M., & Cannon, J. R. (2019). Intraspecific response of *Pinus taeda* L. to *Grosmannia huntii* and *Leptographium* spp.: implications for family selection. Forest Pathology, 49(3), e12578.

Dobbertin, M. (2006). Tree Growth as Indicator of Tree Vitality and of Tree Reaction to Environmental Stress: A Review, European Journal of Forest Research, 2006.

Drenkhan, R., Riit, T., Adamson, K., Hanso, M. (2016). The earliest samples of *Hymenoscyphus albidus* vs *H. fraxineus* in Estonian mycological herbaria. Mycological Progress, 15, 835-844.

Durán, A., Gryzenhout, M., Slippers, B., Ahumada, R., Rotella, A., Flores, F., ... & Wingfield, M. J. (2008). *Phytophthora pinifolia* sp. nov. associated with a serious needle disease of *Pinus radiata* in Chile. Plant Pathology, 57(4), 715–727. https://doi.org/10.1111/j.1365-3059.2008.01856.

Dvořák, M., Vítová, Š., & Jarošová, J. (2012). Sporulation patterns of *Lecanosticta acicola* isolates under controlled conditions. Forest Pathology, 42(4), 255–263. https://doi.org/10.1111/j.1439-0329.2011.00747.

Eckhardt, L. G., et al. (2016). Growth impacts of brown spot needle blight on loblolly pine seedlings under controlled inoculation. Forest Pathology, 46, 257–266.

Erwin, D. C., & Ribeiro, O. K. (1996). Phytophthora diseases worldwide. APS Press.

Food and Agricultural Organization of the United Nations (2016). Forestry for a low-carbon future: Integrating Forests and Wood Products in Climate Change Strategies (FAO Forestry Paper 177). Food and Agriculture Organization of the United Nations. http://www.fao.org/3/a-i5857e.

Food and Agriculture Organization of the United Nations. (2001). Planted forests in the United States of America: Past, present and future. FAO.

Fisher, T. (2022). Loblolly, Pine of the Piedmont. Atlanta History Center. https://www.atlantahistorycenter.com/blog/loblolly-pine-of-the-piedmont.

Gao, R., Wang, Z., Wang, H., Hao, Y., & Shi, J. (2019). Relationship Between Pine Wilt Disease Outbreaks and Climatic Variables in The Three Gorges Reservoir Region, Forests, 2019.

García-García, D., Mesanza, N., Raposo, R., Pascual, M. T., Barrena, I., Urkola, A., Berano, N., & Iturritxa, E. (2025). Risk prediction of *Lecanosticta acicola* spore abundance in Atlantic climate regions. Agricultural and Forest Meteorology, 362, Article 110360. https://doi.org/10.1016/j.agrformet.2024.110360.

Geils, B. W., Hummer, K. E., & Hunt, R. S. (2010). White pines, Ribes, and blister rust: a review and synthesis. USDA Forest Service General Technical Report RMRS-GTR-206. https://www.fs.usda.gov/treesearch/pubs/34129.

Gibson, I. A. S. (1995). Rust disease of forest trees. In S. B. Mathur (Ed.), The Rust Fungi: Biology, Structure and Systematics (pp. 225–246). Science Publishers.

Gilliland, N.J.; Chappelka, A.H.; Muntifering, R.B.; Booker, F.L.; Ditchkoff, S.S. (2012). Gibson Digestive utilization of ozone-exposed forage by rabbits (*Oryctolagus cuniculus*). Environ. Pollut., 163, 281–286.

González, A., & Pérez, M. (2018). Evaluating passive spore-trap efficiency for needle-blight pathogens. Mycological Research, 122(9), 769–777. https://doi.org/10.1016/j.mycres.2018.04.009.

Goswami, R. S., & Pereira, O. C. (2011). Epidemiology and management of *Coleosporium* needle rusts in North American pine plantations. Forest Pathology, 41(2), 164–176. https://doi.org/10.1111/j.1439-0329.2010.00693.

Hansen, E. M., & Lewis, K. J. (1997). Compendium of Conifer Diseases. American Phytopathological Society (APS Press). https://apsjournals.apsnet.org/loi/phyto.

Hansen, E. M., and Goheen, D. J. (2000). White Pine Blister Rust and Brown Spot Needle Blight: A Model for Disease Interventions. Phytopathology, 90(6), 624-627.

Hansen, E. M., Reeser, P. W., & Sutton, W. (2012). *Phytophthora* beyond agriculture. Annual Review of Phytopathology, 50, 359–378. https://doi.org/10.1146/annurev-phyto-081211-173915.

Harrington, T. C., McNew, D. L., & Vidaver, A. K. (2010). Population structure of *Lophodermium* spp. causing needle cast in pines. Mycologia, 102(4), 937–948. https://doi.org/10.3852/09-207.

Hartman, J. (2018). Spruce problems: Rhizosphaera needle cast and other issues. University of Kentucky Cooperative Extension Service.http://plantpathology.ca.uky.edu/files/ppfs-or-w-20.

Heagle, A.S.; Philbeck, R.B.; Ferrell, R.E.; Heck, W.W. Design and performance of a large field exposure chamber to measure effects of air quality on plants. J. Environ. Qual. 1989, 18, 361–368.

Hennon, P. E., Shaw, C. G., & Hansen, E. M. (2007). Disease and Insect Resistance in Forest Trees. USDA Forest Service, Pacific Northwest Research Station.

Huang, C.-L., Yang, D.-M., & Tsui, P.-T. (1995). Severe damage to pine plantations caused by *Lecanosticta acicola* in southeastern China. Plant Disease, 79(7), 641–648.

Huber, L., & Gillespie, T. J. (1992). Modeling Leaf Wetness in Relation to Plant Disease Epidemiology. Annual Review of Phytopathology, 30, 553–577. https://doi.org/10.1146/annurev.py.30.090192.003005.

Hyde, K. D., Norphanphoun, C., Maharachchikumbura, S. S. N., Bhat, D. J., Jones, E. B. G., Bundhun, D., ... & Hongsanan, S. (2016). Refined families of Sordariomycetes. Fungal Diversity, 80(1), 321–344.

Ioos, R., Fabre, B., Saurat, C., Fourrier, C., Frey, P., & Marçais, B. (2010). Development, comparison, and validation of real time and conventional PCR tools for the detection of the fungal pathogens causing brown spot and red band needle blights of pine. Phytopathology, 100(1), 105–114. https://doi.org/10.1094/PHYTO-100-1-0105.

Jackson RB, Schlesinger WH (2004). Curbing the U.S. carbon deficit. Proc. Natl. Acad. Sci. USA 101: 15827-15829.

Jacobi, W. R., & Tisserat, N. (2011). Detecting and managing spruce needle casts and needle blights. Colorado State University Extension Fact Sheet No. 2.909.

Jankovský, L., & Palovčíková, D. (2003). Brown spot needle blight of pines in the Czech Republic. Journal of Forest Science, 49(3), 101–106.

Jankovský, L., Palovčíková, D., Dvořák, M., & Tomšovský, M. (2009). Records of brown spot needle blight related to Lecanosticta acicola in the Czech Republic. Plant Protection Science, 45(1), 16–18. https://doi.org/10.17221/39/2008-PPS.

Janoušek, J., Laas, M., Drenkhan, R., Adamson, K., and Dämmrich, F. (2016). Genetic diversity and mating system of *Lecanosticta acicola* in Estonia. Fungal Biology, 120(1), 131-141.

Janoušek, J., Tomšovský, M., and Hlásková, K. (2014). *Lecanosticta acicola* on pine trees: detection of teleomorph and molecular variability of the pathogen. Forest Pathology, 44(4), 303-313.

Jarecki, W., and Bobrecka-Jamro, W. D. (2014). "Influence of Initial Dose of Nitrogen and Foliar Nutrition on LAI Index and Infection of Fungal Pathogens of Two Morphotypes of Field Bean", Progress in Plant Protection, 2014.

Jayanthi, H. L. (2001). Interaction of *Fusarium oxysporum* and *Lecanosticta acicola* on loblolly pine needles. Mycological Research, 105(9), 1002–1007. https://doi.org/10.1017/S095375620100399X.

Jones, P. D., & Smith, A. B. (2021). The influence of genetic diversity on disease resistance in loblolly pine. Forest Genetics, 28(3), 201–210. https://doi.org/10.1007/s11295-021-01512-1.

Kais, A. J. (1971). Sporulation and dispersal of *Lecanosticta acicola* and its relation to brown spot needle blight of pine. Canadian Journal of Botany, 49(4), 653-659.

Kaufert, F. (1935). Some morphological aspects of fungi. Mycologia 27(2), 224–232.

Kelley, W. D., & Williams, J. C. (2019). Longleaf pine regeneration and management: Controlling brown spot needle blight. Alabama Cooperative Extension System.

Kinloch, B. B., Sniezko, R. A., Dupper, G. E., & Vogler, D. R. (2003). Genetic resistance to white pine blister rust in sugar pine: Evidence for major gene resistance. Phytopathology, 93(5), 574–578. https://doi.org/10.1094/PHYTO.2003.93.5.574.

Kinloch, B. B., & Stonecipher, R. W. (1969). Genetic variation in susceptibility to fusiform rust in seedlings from a wild population of loblolly pine. Phytopathology, 59(9), 1246–1255.

Lavallée, A., Hamelin, R. C., & Lachance, D. (2019). Identification of fungi associated with eastern white pine needle diseases in Québec, Canada. Canadian Journal of Forest Research, 49(12), 1483–1493. https://doi.org/10.1139/cjfr-2019-0161.

Lazarević, J., & Menkis, A. (2020). Fungal diversity in the phyllosphere of *Pinus heldreichii* H. Christ, An endemic and high-altitude pine of the Mediterranean region. Diversity, 12(5), 172. https://doi.org/10.3390/d12050172.

Liechty, O. L., Luckow, R. K., & Guldin, M. J., (2005). Soil Chemistry and Nutrient Regimes Following 17-21 Years of Shortleaf Pine-bluestem Restoration in The Ouachita Mountains of Arkansas, Forest Ecology and Management, 204, 345-357.

Liu, F., Bonthond, G., Groenewald, J. Z., Cai, L., Crous, P. W. (2019). Sporocadaceae, a family of coelomycetous fungi with appendage-bearing conidia. Studies in Mycology, 92, 287–415.

Maharachchikumbura, S. S. N., Hyde, K. D., Groenewald, J. Z., Xu, J. C., & Crous, P. W. (2014). *Pestalotiopsis* revisited. Studies in Mycology, 79, 121–186.

Maloy, O. C. (1997). White pine blister rust control in North America: a case history. Annual Review of Phytopathology, 35(1), 87–109. https://doi.org/10.1146/annurev.phyto.35.1.87.

Martínez, J. R., Eguizábal, R., & González, E. (2020). Longitudinal spore-trap monitoring of *Lecanosticta acicola* in pine plantations. Plant Disease, 104(7), 1812–1820. https://doi.org/10.1094/PDIS-11-19-2456-RE.

McDonald, B. A., and Linde, C. (2002). Pathogen population genetics, evolutionary potential, and durable resistance. Annual Review of Phytopathology, 40(1), 349-379.

McKeand, S. E., Jokela, E. J., & Huber, D. A. (2003). Performance of genetically improved loblolly pine: growth, survival, and fusiform rust resistance. Forest Ecology and Management, 177(1–3), 135–144.

Mesanza, N., Solla, A., Díaz-Sala, C., and Fernández, M. (2021a). The sexual state of *Lecanosticta acicola* in a natural *Pinus radiata* forest in northern Spain. Forest Pathology, 51(3), e12694.

Mesanza, N., García García, D., Raposo, E. R., et al. (2021b). Weather variables associated with spore dispersal of *Lecanosticta acicola* causing pine needle blight in northern Spain. Plants, 10(12), 2788.

Miller, J. D., & Thompson, S. (2023). The interaction of environmental stressors and pathogens in loblolly pine seedlings. Forest Pathology, 53(1), e12678. https://doi.org/10.1111/efp.12678.

Munck, I. A., Bennett, M., & Livingston, W. H. (2016). Factors influencing white pine needle damage in New England, USA. Forest Pathology, 46(2), 129–137. https://doi.org/10.1111/efp.12232.

Muñoz-Adalia, E. J., Sanz-Ros, A. V., Flores-Pacheco, J. A., Hantula, J., Diez, J. J., & Vainio, E. J. (2017). Sydowia polyspora dominates fungal communities carried by two Tomicus species in pine plantations threatened by *Fusarium circinatum*. Forests, 8(5), 127. https://doi.org/10.3390/f8050127.

Nilsson, R. H., Tedersoo, L., & Lindahl, B. (2012). Pinned reviews and resources: The importance of taxonomic revision in fungal community analyses. Fungal Ecology, 5(1), 10–13.

Nottingham, A., Montero-Sanchez, M., Slot, M., Hubert, A., Szczygieł, H., Velasquez, E., & Meir, P. (2023). Seedling Growth Declines in Warmed Tropical Forest Soils, BIOTROPICA, 2023.

Olszyk, D. M., Tingey, D. T., & McMichael, B. L. (1980). Field evaluation of open-top chambers for atmospheric pollution research. Atmospheric Environment, 14(7), 933–936. https://doi.org/10.1016/0004-6981(80)90206-1.

Ostry, M. E., LaMadeleine, L. A., & Mielke, M. E. (2012). White pine needle damage: A new disease complex. USDA Forest Service, Forest Health Protection Report. https://www.fs.usda.gov/Internet/FSE_DOCUMENTS/stelprdb5369733.

Palmer, M. A., Stewart, E. L., & Wingfield, M. J. (1987). Variation among isolates of *Sphaeropsis sapinea* in the north central United States. Phytopathology, 77(7), 944–948.

Pandit, K., Smith, A. J., Quesada, T., Villari, C., & Johnson, J. D. (2020). "Association of Recent Incidence of Foliar Disease in Pine Species in The Southeastern United States with Tree and Climate Variables", FORESTS, 2020.

Peterson, L. E., & Kent, D. J. (2010). *Alternaria alternata* colonization of *Lecanosticta acicola* lesions on *Pinus palustris* needles. Forest Pathology, 40(2), 82–90. https://doi.org/10.1111/j.1439-0329.2009.00631.

Petrini, O. (1991). Fungal endophytes of tree leaves. Mycological Research, 95(6), 641–649. https://doi.org/10.1016/S0953-7562(09)80730-1.

Phillips, A. J. L., Alves, A., Abdollahzadeh, J., Slippers, B., Wingfield, M. J., Groenewald, J. Z., & Crous, P. W. (2013). The Botryosphaeriaceae: Genera and species known from culture. Studies in Mycology, 76, 51–167.

Prasolova, N., Xu, Z., & Lundkvist, K. (2005). Genetic Variation in Foliar Nutrient Concentration in Relation to Foliar Carbon Isotope Composition and Tree Growth with Clones of The F1 Hybrid Between Slash Pine and Caribbean Pine, Forest Ecology and Management, 2005.

Pscheidt, J. W. (1992). Pine (*Pinus* spp.) Lophodermium needle cast. In C. T. Ingerson (Ed.), Pacific Northwest Plant Disease Management Handbook (pp. 1–5). Oregon State University Extension.

Purdy, L. H. (1978). *Fusarium solani* as an endophyte of American pines. Plant Disease Reporter, 62(2), 110–113.

Reeser, P. W., Sutton, W., Hansen, E. M., Remigi, P., & Adams, G. C. (2013). *Phytophthora pluvialis* sp. nov., a new species that causes red needle cast of Pinus radiata in New Zealand. Mycologia, 105(5), 1010–1026. https://doi.org/10.3852/12-240.

Schmidt, A., & Roling, P. (1984). The Occurrence of *Hendersonia* species in pine needles with brown spot needle blight. Forest Pathology, 14(3), 149–156. https://doi.org/10.1111/j.1439-0329.1984.tb00419.

Schoch, C. L., Robbertse, B., Robert, V., Vu, D., Cardinali, G., Irinyi, L., ... & Hyde, K. D. (2014). Finding needles in haystacks: Linking scientific names, reference specimens, and molecular data for Fungi. Database, 2014. https://doi.org/10.1093/database/bau06.

Schoch, C. L., Seifert, K. A., Huhndorf, S., Robert, V., Spouge, J. L., Levesque, C. A., Chen, W., & Fungal Barcoding Consortium. (2012). Nuclear ribosomal internal transcribed spacer (ITS) region as a universal DNA barcode marker for Fungi. Proceedings of the National Academy of Sciences of the United States of America, 109(16), 6241–6246. https://doi.org/10.1073/pnas.1117018109.

Siggers, J. (1939). Brown spot needle blight of pine. Journal of Forestry, 37(1), 47-53.

Siggers, P. V. (1944). The brown spot needle blight of pine seedlings (U.S. Department of Agriculture Technical Bulletin No. 870). U.S. Department of Agriculture.

Sinclair, W. A., & Lyon, H. H. (2005). Diseases of Trees and Shrubs (2nd ed.). Cornell University Press. ISBN: 9780801443718.

Skilling, D. D., and Nicholls, T. H. (1974). Dispersal of *Lecanosticta acicola* conidia in relation to brown spot needle blight of pines. Canadian Journal of Botany, 52(3), 559-563.

Smith, C. S., & Peterson, R. K. (2017a). Host water status as a determinant of foliar pathogen virulence. Phytopathology, 107, 563-572.

Smith, A. B., & Peterson, R. L. (2017b). Characterization of *Hendersonia* spp. associated with pine needle blight. Mycologia, 109(2), 235–245. https://doi.org/10.1080/00275514.2017.1297845.

Smith, D. R., & Stanosz, G. R. (2006). A species-specific PCR assay for detection of *Diplodia pinea* and *D. scrobiculata* in dead red and jack pines with collar rot symptoms. Plant Disease, 90(3), 307–313. https://doi.org/10.1094/PD-90-0307.

Smith, J. A., & Green, T. (2020). Evaluating the susceptibility of loblolly pine families to *Lecanosticta acicola* in field trials. Journal of Forestry Research, 31(2), 145–156. https://doi.org/10.1007/s11676-019-01005-4.

Smith, J. A., Couper, D. T., & Wingfield, M. J. (2010). Impact of plantation monoculture on pine disease prevalence: A global assessment. Forest Pathology, 40(1), 10–21.

Smith, R. N. (2015). Pathology of coniferous species: Recent advances and perspectives. Journal of Forestry Studies, 45(2), 123–135.

Smith, R. N., & Jones, D. A. (2020). Advances in molecular identification of conifer foliar pathogens. Forest Health and Protection, 32(1), 50–62.

Smith, W. B., Miles, P. D., Vissage, J. S., & Pugh, S. A. (2001). Forest resources of the United States, 1997. Gen. Tech. Rep. NC-219. St. Paul, MN: U.S. Department of Agriculture, Forest Service, North Central Research Station.

Spaulding, P. (1922). Blister rust of white pine. USDA Bulletin No. 957.

Stenström, E., & Ihrmark, K. (2005). Identification of *Lophodermium seditiosum* and *L. pinastri* in Swedish forest nurseries using species-specific PCR primers from the ribosomal ITS region. Forest Pathology, 35(3), 163–172. https://doi.org/10.1111/j.1439-0329.2005.00398.

Stone, J. K., & Roberts, S. (2002). Global review of needle cast disease complexes of pines and spruces. Forest Pathology, 32(5), 293–308. https://doi.org/10.1046/j.1439-0329.2002.00285.

Sykes, R. W., Isik, F., Li, B., Kadla, J. F., & Chang, H.-M. (2003). Genetic variation of juvenile wood properties in a loblolly pine progeny test. Canadian Journal of Forest Research, 33(12), 2417–2422.

Tanaka, K., Endo, M., Hirayama, K., & Sato, T. (2011). Phylogeny and taxonomy of the family Sporocadaceae, with a focus on Pestalotiopsis species in Japan. Mycoscience, 52(1), 1–22.

Thomma, B. P. H. J. (2003). *Alternaria* spp.: From general saprophyte to specific parasite. Molecular Plant Pathology, 4(4), 225–236. https://doi.org/10.1046/j.1364-3703.2003.00184.

U.S. Department of Agriculture, Forest Service. (2012). Resources Planning Act Assessment of Forest and Range Lands: Fiscal Year 2010 Assessment Report (RPA-FIA-2010). Washington, DC: U.S. Government Publishing Office.

U.S. Forest Service & Alabama Forestry Commission. (2022). Alabama forest health highlights 2022 (Publication FHP-AL-22). U.S. Department of Agriculture, Forest Service.

van der Nest, A., Wingfield, M. J., Janoušek, J., & Barnes, I. (2019). *Lecanosticta acicola*: A growing threat to expanding global pine forests and plantations. Molecular Plant Pathology, 20(10), 1327–1364.

van der Nest, A., Wingfield, M. J., Janoušek, J., & Barnes, I. (2019). *Lecanosticta acicola*: A growing threat to expanding global pine forests and plantations. Molecular Plant Pathology, 20(10), 1327–1364. https://doi.org/10.1111/mpp.12854.

Wahlenberg, W. G. (1960). Loblolly pine, its use, ecology, regeneration, protection, growth, and management. Durham, NC: Duke University, School of Forestry. 603 p.

Wakeley, P. C. (1970). Brown spot needle blight of pines: life history of *Scirrhia acicola* and symptom development in Pinus palustris. Phytopathology, 60(4), 413–417.

Walkinshaw, C. H., & Barnett, J. P. (1998). Genetic variation in loblolly pine response to *Scirrhia acicola*. Plant Disease, 82, 89–93.

Watanabe, T. (2010). Pictorial Atlas of Soil and Seed Fungi: Morphologies of Cultured Fungi and Key to Species (3rd ed.). CRC Press. ISBN: 9781420042813.

Wear, D. N. (1996). Forest management and timber production in the U.S South. SCFER Working Paper 82. Research Triangle Park, NC: Southeastern center for Forest Economics Research: 40 p.

Wear, D. N. (1996). The southern timber production region. In R. W. Haynes, G. L. Johnson, & R. P. Vlosky (Eds.), Southern Forest Resource Assessment (pp. 1–18). Asheville, NC: U.S. Department of Agriculture, Forest Service, Southern Research Station.

Webber, J. F., & Flentje, N. (2008). *Dothistroma* needle blight: biology, epidemiology and management. Fungal Biology Reviews, 22(3), 160–188. https://doi.org/10.1016/j.fbr.2008.06.002.

West, J. S., & Kimber, R. B. E. (2015). Innovations in air sampling to detect plant pathogens. Annals of Applied Biology, 166(1), 4–17. https://doi.org/10.1111/aab.12191.

White, T. J., Bruns, T., Lee, S., & Taylor, J. (1990). Amplification and direct sequencing of fungal ribosomal RNA genes for phylogenetics. In M. A. Innis, D. H. Gelfand, J. J. Sninsky, & T. J. White (Eds.), PCR Protocols: A Guide to Methods and Applications (pp. 315–322). Academic Press. https://doi.org/10.1016/B978-0-12-372181-5.50042-1.

Wingfield, M. J., Slippers, B., Roux, J., & Wingfield, B. D. (2015). Global spread of diaporthalean fungi: Implications for Agriculture and Forestry. Phytopathology, 105(7), 889–898.

Wingfield, M. J., Slippers, B., Wingfield, B. D. (2009). Global movement of forest trees and pathogens: Drivers, impacts and management. Forest Ecology and Management, 257(5), 2009–2015.

Worf, G. L. (2002). Rhizosphaera needle cast of spruce. Plant Disease Diagnostic Clinic Factsheet. University of Wisconsin Extension. https://pddc.wisc.edu.

Wyka, A. S., Munck, A. I., Brazee, J. N., & Broders, K., (2018a)., Response of Eastern White Pine and Associated Foliar, Blister Rust, Canker and Root Rot Pathogens to Climate Change, Forest Ecology and Management, 2018.

Wyka, S. A., et al. (2018b). Climatic influences *L. acicola* spore dispersal. Phytopathology, 108, 374 383.

Wyka, S. A., McIntire, C. D., Smith, C., Munck, I., Rock, B. N., Asbjornsen, H., & Broders, K. D. (2018c). Effect of climatic variables on abundance and dispersal of *Lecanosticta acicola* spores and impact of defoliation on eastern white pine. Phytopathology, 108(4), 374–383. https://doi.org/10.1094/PHYTO-02-17-0065-R.

Zellner, Z., Frantz, J., Leisner, S., (2011). "Silicon Delays Tobacco Ringspot Virus Systemic Symptoms in *Nicotiana tabacum*", JOURNAL OF PLANT PHYSIOLOGY, 2011.

Zambino, P. J., & Kinloch, B. B. (2007). White pine blister rust in North America: Past and prognosis. Phytopathology, 97(12), 1522–1527. https://doi.org/10.1094/PHYTO-97-12-1522.

Zhang, J., Guo, S., & Hyde, K. D. (2012). Morphological and molecular evidence for several distinct *Pestalotiopsis* species in China. Persoonia, 28, 126–140.

Zhang, S., Lyons, D. B., & Peterson, G. W. (1994). Genotype-environment interactions in pine seedling disease resistance under controlled conditions. Forest Science, 40(3), 517–526. PMID: 15107424.

Appendices

Appendix A

Figure 1. Flowchart followed for morphological identification of fungi

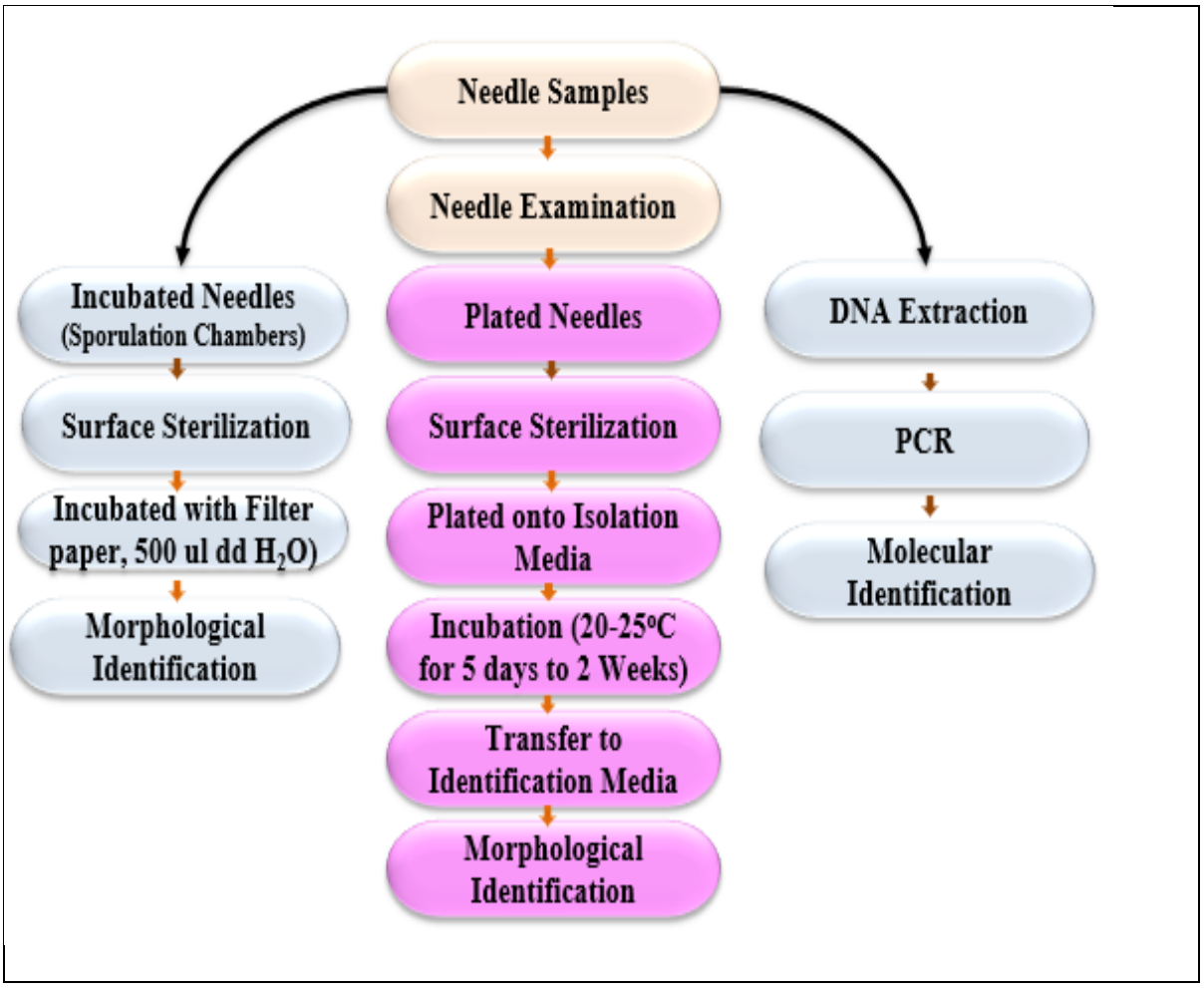

Procedure followed for DNA Extraction

The following procedure was used for all needle samples collected for the study.

1. Grind fresh needle samples with liquid nitrogen and transfer them into prelabelled PCR tubes

2. Add 500µL of CD1 solution to each sample
3. Vortex for 3 minutes
4. Place the tube in a centrifuge (ensure they are arranged symmetrically) and spin for 2 minutes
5. Take 350 - 400µL of the supernatant into prelabelled corresponding tubes
6. Add 200µL of CD2 solution
7. Vortex briefly and centrifuge for 2 minutes
8. Transfer the supernatant, without touching the pellets, into new tubes
9. Add 500µL of Buffer APP solution and vortex for 5 seconds
10. Transfer 600µL of the resulting solution into spin column tubes
11. Centrifuge for 1 minute
12. Separate from the filter tubes and pour out the liquid
13. Repeat Step 10
14. Put the filter tubes into new collection tubes and add 650L of AW1 solution and centrifuge for 1 minute
15. Discard the solution in the collection tubes and add 650µL of AW2 solution into the filter tubes
16. Centrifuge for 1 minute and discard the solution in the collection tube
17. Centrifuge again for 2 minutes
18. Take the filter out and put them into new tubes
19. Add 75µL of Buffer EB solution into the filter tubes
20. Centrifuge for 1 minute and discard the filter tubes leaving the DNA in the collection tubes

Procedure followed for PCR

1. Obtain DNA samples from freezer and thaw them on ice
2. Label PCR tubes with sample ID on the worksheet
3. Label Mix Tube (2 mL) and place in ice
4. Prepare a PCR mix befitting the number of samples, a negative control and 1 extra mix per 20 samples
5. Ensure PCR Mix is well mixed
6. Distribute 23 µL of PCR Mix in each sample tube
7. Add 2 µL of each sample to the labeled tubes
8. If not working on a thermocycler with a heated lid, add 4 µL of mineral oil to ensure that the sample volume does not evaporate
9. Set up PCR machine with the desired program

Procedure followed for Gel Electrophoresis

1. Tape gel tray on both ends ensuring that it is well sealed, place comb in the gel plate
2. Prepare a 2% gel (2.0g of agarose to 100ml of 1X TAE buffer)
3. Microwave the solution in 30 seconds interval until gel is completely molten
4. Wait for it to cool down until it is safe to handle
5. Add 10 µL of GelRed®(10,000X) to agar
6. Mix properly until gel staining dye is dissolved by swirling the flask, pour out the solution into the gel plate
7. Wait until it is solidified

8. Remove tape from the plate and place gel in electrophoresis tray with the wells close to the negative side (black)
9. Fill the tray with 1X TAE to cover the gel and remove the comb
10. Prepare samples, controls and ladder to be loaded
11. Load the samples into the wells in the gel, and record the order of placement on the worksheet
12. Place the lid on the tray and connect the cables to the corresponding terminals
13. Plug the other end of the wires into the electrophoresis power supply. Plug the red wire into the red outlet and black wire into the black outlet directly below it
14. Turn on the power supply machine. Set the voltage to 80V and check after 30 minutes, while ensuring that the dye does not run over
15. Turn off the power and take out the gel block; visualize bands using a transilluminator machine and record the results.

Appendix B

Brown Spot Needle Blight Symptomatology and various expressions of *Lecanosticta acicola* conidia

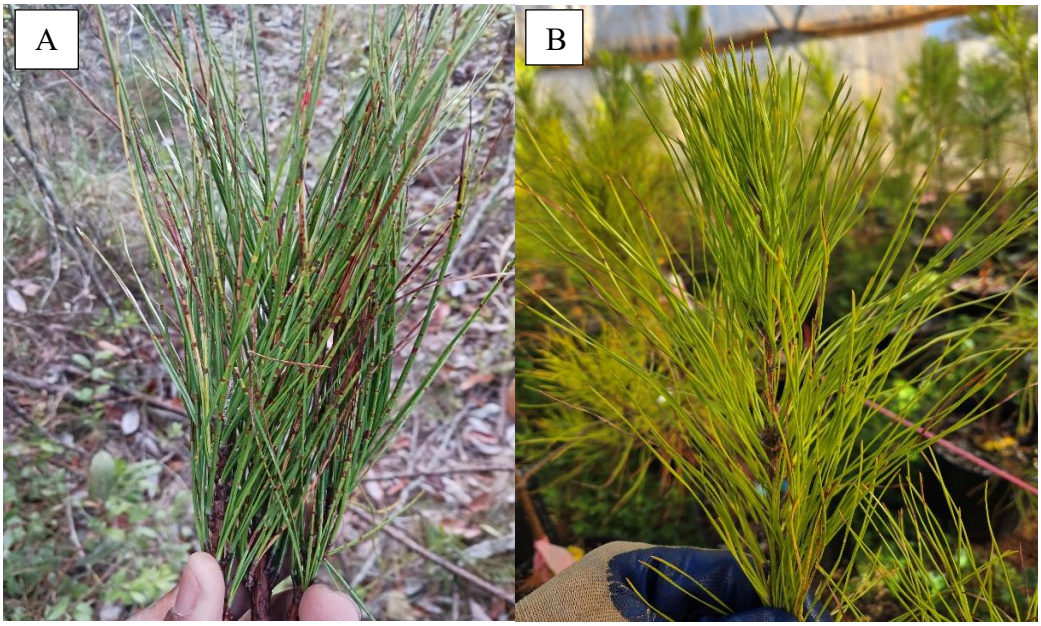

Figure 2. Disease symptoms in (A) mature branch and (B) seedling, showing multiple irregular brown spots surrounded by a yellow halo, with some needle tips being necrotic.

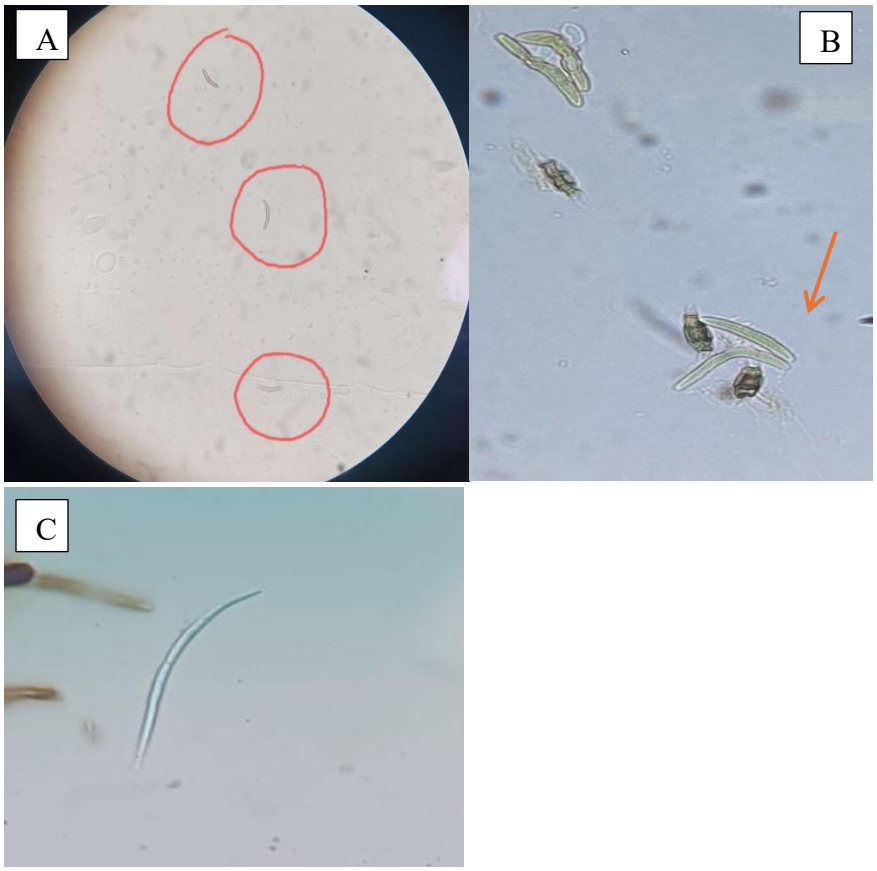

Figure 3. Reproductive structures showing microscopic banana-shaped conidia recovered from (A) spore trap slide (B) sporulation chambers and (C) culture plates